MicroRNA Release in Acute Myocardial Infarction

Thesis presented for the degree of
Doctor of Philosophy in Cardiovascular Medicine
at the University of Oxford

Dr Sam Dawkins

BSc (Hons) MBBS MRCP (Lon)

Department of Cardiovascular Medicine
and Trinity College, University of Oxford

Supervisor: Professor Keith Channon

1 Table of contents

2 List of Figures

3 List of Tables

4 Acknowledgements

I am grateful to the British Heart Foundation Centre of Research Excellence in Oxford for funding this work through their Clinical Research Training Fellowship programme. I would like to thank my supervisor, Professor Keith Channon, for his support and advice throughout this work. His energy, enthusiasm and thoughtful advice during our regular meetings and, more impressively, in the early hours of the morning in the cath lab, have been inspirational. Dr Nicola Smart has been an invaluable second supervisor, offering another point of view, particularly for the basic science aspects of the work.

The transition from clinician to scientist is challenging and I would like to thank Dr Janet Digby for taking me under her wing, like so many others before me, and training me in the ways of the basic science lab with kindness and good humour. I would like to thank Dr Grant Belgard for his statistics and bioinformatics expertise, Dr Gillian Douglas and the Channon Lab Group for their constructive input and practical help in the lab and Dr Mark Sheehan for his ethical oversight.

Research on acutely unwell patients is challenging and requires the involvement of a large number of people. All those involved, including the nurses, radiographers, physiologists, Patient Advocates, OxAMI fellows, interventional cardiologists, the teams from the Acute Vascular Imaging Centre (AVIC), the Oxford Centre for Clinical Magnetic Resonance (OCMR) and, of course, the patients have been key players in this work and I am grateful to them all for their enthusiasm and support.

Finally, I would like to thank my family for their ongoing and unquestioning support since I first decided to become a doctor at the age of seven. It has been rather a long investment, but their patience is paying off!

5 Abstract

Coronary heart disease (CHD) is the single biggest cause of death in the United Kingdom[1]. Primary percutaneous coronary intervention (primary PCI) has transformed the early treatment of acute myocardial infarction (MI), improving outcome by rapidly re-opening the occluded coronary artery, with a larger mortality benefit and reduced risk compared with thrombolysis[2–4]. Despite these advances, and even with the optimal treatment, some patients still sustain substantial myocardial damage leading to mortality and morbidity. MicroRNAs (miRs) are short non-coding RNAs with a role in regulating protein synthesis. Some miRs are cardiospecific, can be detected in plasma after a myocardial infarction and show promise as biomarkers and insights into the mechanisms of myocardial injury[5].

In this work, as part of the Oxford Acute MI (OxAMI) Programme, a cohort of patients recruited at the time of ST elevation MI underwent detailed clinical and microRNA analysis at the time of myocardial infarction. This work was validated using separate discovery and validation cohorts. The source of detected miRs was further analysed in an *in-vitro* endothelial cell culture model and by measuring miRs released into the venous drainage of the heart, the coronary sinus.

In the Discovery Cohort, miRs previously shown to be increased in myocardial infarction (e.g. *miR-1, -133a, -499*) were detectible in plasma after myocardial infarction, and this was confirmed in the validation cohort. Other miRs with a similar relationship were also identified (e.g. *miR-30a, -378a, 125b*). Microvascular obstruction was found to be associated with increased infarct size and also with release of microRNAs correlating with infarct size suggesting a link between microvascular obstruction and myocardial necrosis. Analysis of paired coronary

artery and coronary sinus samples showed that these miRs increased down the myocardial gradient, suggesting myocardial release.

The culmination of this work was to use the experimental findings from circulating plasma, cultured endothelial cells and coronary sinus experiments to design a microRNA panel using a blood sample taken six hours after admission to use in a regression model which was more predictive of final infarct size than troponin alone.

6 Background: Myocardial infarction

6.1 Introduction

Acute ST elevation myocardial infarction (STEMI) remains a major cause of death and the leading cause of chronic heart failure in the UK[1]. Primary percutaneous coronary intervention (primary PCI) has transformed the early treatment of myocardial infarction, reducing mortality and morbidity by rapidly re-opening the occluded coronary artery, with major efforts in healthcare policy and guidelines aimed at minimising delays in patient pathways and 'door to balloon' times[2–4]. However, prompt restoration of vessel patency does not necessarily lead to effective myocardial reperfusion. Indeed, apparently similar patients with good angiographic primary PCI results often experience very different outcomes in myocardial salvage and final infarct size[6]. This effect is partly driven by ischaemia reperfusion injury, a major component of which is endothelial dysfunction in the downstream coronary circulation which leads to microvascular obstruction, manifest as the 'no-reflow' phenomenon after primary PCI.

In patients with STEMI the emphasis is on rapidly restoring the patency of the epicardial coronary artery and this strategy, whether it is achieved with thrombolysis or primary percutaneous coronary intervention, improves patient outcome[7–9]. However, even with a patent epicardial coronary artery, between 7% and 65% of patients have significant microvascular obstruction depending on patient group and the criteria used for its assessment[10]. Although major advances have been made in the treatment of acute myocardial infarction in recent decades, limited progress has been made in treating microvascular obstruction. This is important because these patients have an increased risk of cardiovascular events both acutely and in the

longer term[11,12]. In one series, patients with normal microvascular function patients had a ten year cardiac mortality of 5% whereas in patients where it was impaired it was 31%[13].

6.2 Historical Context of Myocardial Infarction

Coronary thrombosis as a cause of myocardial infarction was first recognised as an entity in the 19th century, based on animal studies and post mortem findings[14]. The advent of the electrocardiogram (ECG) in 1902 by Einthoven provided a tool to aid diagnosis of arrhythmias which had previously been diagnosed by palpating the apex beat. The changes in the ECG waveform seen with myocardial ischaemia were described by Oppenheimer and Rothschild in 1917[15].

The first myocardial infarction case series was published by Joseph Wearn, a pathologist from the Brigham Hospital in Boston, Massachusetts, in 1923. He described 19 patients with the condition, and concluded that it was most likely caused by 'thrombus in an atherosclerotic left anterior descending coronary artery mostly affecting fifty-year-old male patients, with sudden chest pain in the heart region'. The episode could be associated with breathlessness and examination usually revealed 'signs of the failing circulation, such as pale and cold skin, lung crackles, enlarged heart, pericardial rub and irregular rhythm', a description that would not seem out of place in a contemporary medical textbook[16,17].

Although confidence in diagnosis grew, there was little progress in the management of AMI, with analgesia being the mainstay of treatment. As an indication of the rate of progress, the decision to allow patients to spend some of their convalescence in a bed rather than a chair, was hailed as a major development[18].

The Coronary Care Unit (CCU) was a British invention proposed in 1961 by Desmond Julian, an Edinburgh medical registrar. He felt that specialist wards should be developed that had the equipment and expertise to care for AMI patients. The subsequent invention of central monitoring and the defibrillator allowed ventricular arrhythmias to be diagnosed and treated safely and effectively, provided they were identified early. Over the following five years, Coronary Care Units became the standard of care for AMI patients and early AMI mortality fell by half (from 30% to 15%) largely due to the early recognition and treatment of ventricular arrhythmias[14,19].

Streptokinase was first isolated from the bacterium *beta haemolytic streptococcus* in 1933. It was shown to convert tissue plasminogen into the fibrinolytic enzyme plasmin. The first therapeutic use for this drug was for the treatment of complicated empyema in 1951 and in 1958 the first study of fibrinolysis with streptokinase for thrombolysis in acute myocardial infarction was carried out[20,21]. The GISSI trial randomised 11,806 patients to receive streptokinase or standard clinical care. 30-day mortality in the streptokinase group was 13% compared with 10.7% in the control group[9].

Although the benefits of aspirin for the secondary prevention of cardiovascular disease were well known, it was not until the ISIS-2 trial in 1988 that the use of aspirin in AMI was rigorously tested. The study was a 2x2 randomised controlled trial comparing aspirin, streptokinase, aspirin and streptokinase or placebo. Aspirin was found to reduce absolute vascular mortality at five weeks from 11.8% to 9.4%, and streptokinase demonstrated a similar benefit when compared with placebo. The effect of aspirin and streptokinase was additive; in this group mortality fell from 13.2% to 8%[22]. Similar benefits were seen at ten year follow up[23].

Although thrombolysis reduced mortality in AMI patients, the therapy did have several disadvantages. The major risk associated with thrombolysis is bleeding, with minor bleeding seen in 3-4% of patients and major bleeding (including haemorrhagic stroke) seen in 1.2% of patients[9,24]. Additionally, thrombolysis fails to restore coronary flow in 20-50% of patients depending on the agent[25].

As the pharmacological management of AMI was developing, a revolution was occurring in coronary intervention. Coronary angiography had been developed in the 1950s by Mason Sones and the femoral approach using the Seldinger technique was developed by Melvin Judkins in 1967. The first balloon angioplasty was carried out to an iliac artery stenosis in 1963. These developments in peripheral intervention paved the way for Andreas Gruentzig to carry out the first coronary angioplasty in a 37-year-old with unstable angina in 1977. This technique was subsequently used for patients where thrombolysis did not achieve reperfusion, so called 'rescue' percutaneous coronary intervention (PCI)[26].

Over subsequent years, balloon angioplasty was used to treat patients with AMI as the primary therapy, rather than only those patients who had failed thrombolysis. Primary angioplasty was shown to reduce in-hospital mortality to 2.6% compared with 6.5% in patients receiving thrombolysis[27]. This benefit was even greater in higher risk patients, such as older patients and those with anterior MI (10.4% vs. 2%, thrombolysis vs. primary PCI respectively). Another major benefit of balloon angioplasty was that patients were not exposed to the bleeding risk seen with thrombolysis.

The first coronary stent was implanted in 1986 and since then every aspect of the technology has evolved, from the stent delivery system to drug coating and the alloys used[28]. In the 1990s, coronary stents were starting to be used in the early treatment of patients with AMI and

primary angioplasty with stents started to be carried out in preference to balloon angioplasty alone. Although there was no significant mortality benefit from stenting compared with balloon angioplasty, there was a reduced risk of revascularisation in the six months post-MI (17% vs 7.7%)[29].

The importance of rapid reperfusion was demonstrated in the early thrombolysis trials; with 65 lives saved for every 1000 treated if thrombolysis was initiated within one hour of symptom onset compared with 9 lives saved for patients treated between 12 and 24 hours of symptom onset[2]. This phenomenon is also seen in the modern primary PCI era. Mortality increases with longer door to balloon time, with 3% mortality for patients treated within 90 minutes of arriving at hospital, versus 7.4% for patients waiting longer than 150 minutes[30].

6.3 Contemporary Management of Myocardial Infarction

The current standard of care for the management of acute ST elevation myocardial infarction is primary PCI. In the UK in 2015, 98.5% of patients receiving reperfusion therapy for STEMI underwent primary PCI compared with 2% ten years ago when the standard of care was thrombolysis[31]. With efficient patient pathways, this treatment can be started within a few minutes of hospital arrival. In Oxford last year, >90% of patients presenting with ST elevation myocardial infarction underwent primary PCI within 90 minutes of hospital arrival, and median time to from hospital arrival to reperfusion (the 'door-to-balloon' time) was 25 minutes.

Huge progress has been made in the diagnosis and treatment of AMI over the last century. From being an almost universally fatal condition in the early 20th century it now has a 30-day mortality of less than 5% and most AMI patients will have a hospital day of three days or less. To identify

how to improve outcomes further still, it is important to be able to accurately quantify outcome beyond the hard endpoint of mortality.

The diagnosis of ST elevation myocardial infarction is made on the basis of clinical and ECG evidence. Diagnosing and classifying the other acute coronary syndromes, such as unstable angina and non-ST elevation MI can be more difficult as clinical features are variable and the ECG may be normal. Myocardial injury leads to the release of structural proteins into the circulation which can be measured, and these can be used to aid diagnosis and predict outcome. In the late twentieth century, the MB isozyme of creatine kinase (CK-MB) was the standard test for diagnosing non-ST elevation myocardial infarction. Serum CK-MB peaks 6-12 hours after MI and falls back to baseline after 36-48 hours. It is a muscle specific, rather than cardiac muscle specific, so is less helpful where co-existing skeletal muscle injury is present.

Troponin

Troponin is present in cardiomyocytes in three isoforms: troponin-I, -T and -C. Troponin-I is the most cardiospecific of the three isoforms and is now widely used for the diagnosis of acute coronary syndromes. It is detectable 3-6 hours after MI and peaks after approximately 24 hours. It falls to baseline after up to two weeks which makes it helpful for detecting late-presenting MIs but it can be difficult to distinguish residual troponin detection from an index MI from a further event.

Troponin is useful for predicting infarct size. In patients with STEMI, troponin-I at 72 hours correlates well with infarct size at 5 and 30 days with correlation coefficient of >0.70[32]. Higher troponin levels also are associated with increased risk of adverse events, with patients in the upper tertile in this study having almost double the risk than those in the lower tertile (42% vs 23%).

Infarct size

Left ventricular (LV) function is commonly assessed soon after myocardial function using transthoracic echocardiography. This information is used to direct drug and device therapy and to diagnose the complications of MI such as LV thrombus and mitral regurgitation. On a practical level, it is also used to determine the length of time a patient should not drive. LV function can also be used to make predictions about prognosis; patients with severe LV impairment have a higher six-month mortality compared with patients with good left ventricular function (11% vs. 0.7%)[33].

Infarct size can be measured using cardiac magnetic resonance imaging (MRI). This is achieved using the contrast agent gadolinium which is injected into a peripheral vein and after 10-15 minutes the MRI images are acquired. Areas with late gadolinium enhancement (LGE) correspond to scar and using image analysis software this can be quantified into grams of scar tissue, which can then be expressed as a percentage of left ventricular mass. There is a strong correlation between infarct size and outcome. Six-month event rate (mortality, hospital admission with heart failure) is less than 10% where infarct size is less than 10% of total LV volume and is over 70% where infarct size is over 25%[34]. There is also a strong correlation between delayed primary PCI treatment and infarct size[35].

Although infarct size provides useful prognostic information it does not really measure the 'success' of the primary PCI procedure. For example, if a patient occluded a small distal vessel and all myocardium beyond the occlusion was irreversibly damaged, the patient may have had a small infarct but this does not indicate a successful procedure as all myocardium downstream of the occlusion (the 'area at risk') was damaged, and primary PCI did not 'save' any myocardium. Conversely, a patient with a proximally occluded vessel with a substantial area at risk who has a

similar infarct size gained more benefit from the procedure as it would be anticipated that with a large area at risk, the infarct size would be larger. Measuring area at risk soon after myocardial infarction, which appears as myocardial oedema on MRI, and then infarct size at six months (late gadolinium enhancement) allows the calculation of the Salvage Index (*Salvage Index = (Myocardial oedema-Infarct size) ÷ Myocardial oedema*) which not only gives a more meaningful indication of procedural success, but also is more predictive of outcome than infarct size alone[36].

6.4 Microvascular Dysfunction

Among interventional cardiologists, it is well known that two patients who occlude the same vessel and undergo reperfusion in the same timeframe may have very different outcomes. Although the contemporary management of myocardial infarction focuses on restoring patency of the epicardial coronary arteries, the function of the microvascular bed is also important. Impairment of microvascular function is associated with worse outcome, and this is another predictor of salvage index. In a study which assessed microvascular function at the end of primary PCI, those with preserved microvascular function had a higher salvage index compared with patients with microvascular obstruction[37]. Microvascular function is also linked with outcome; patients with microvascular obstruction identified on cardiac MRI have an increased risk of cardiovascular events both acutely and in the longer term[11,12].

In order to be able to offer targeted therapy, and also to carry out research to understand more about the underlying pathology, microvascular dysfunction first needs to be identified and quantified. The coronary microvasculature cannot be directly imaged *in vivo* and multiple invasive and non-invasive techniques have been developed for its diagnosis and quantification:

1. <u>In-vitro</u>

The gold standard for identifying and measuring microvascular obstruction in the laboratory setting is Thioflavin-S staining[38]; it stains intact endothelium and therefore well perfused myocardial tissue fluoresces in ultraviolet light. In infarcted tissue, the endothelium is damaged and hypointense areas are seen. In vivo, cardiac MRI can be used to identify microvascular obstruction and areas of hypoenhancement soon after contrast injection correlate with hypointense areas identified by thioflavin staining (Figure 1)[39].

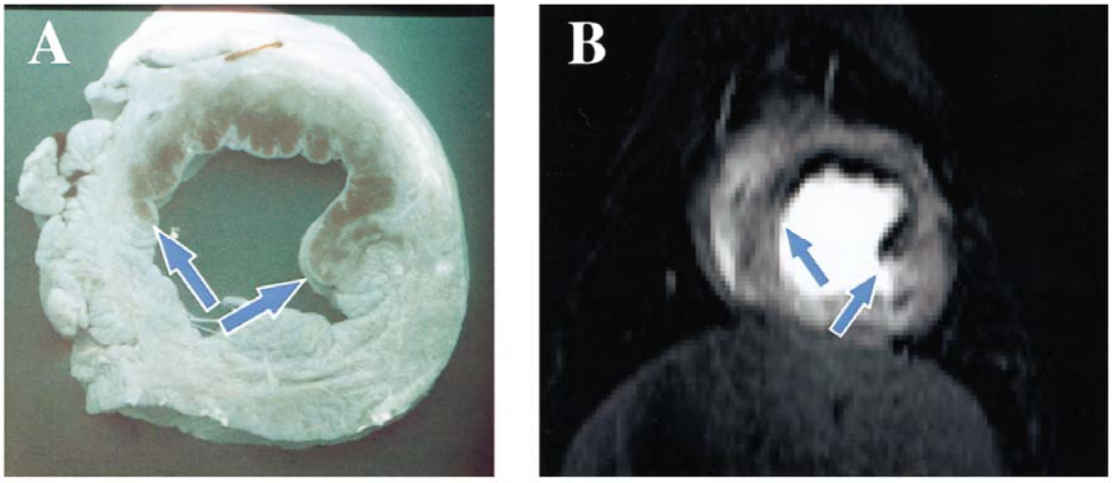

Figure 1: Relationship between histological and CMR methods for assessing microvascular obstruction shown in a canine model of ischaemia-reperfusion.
Panel A shows the thioflavin stained section; microvascular obstruction is present in the brown area between the arrows. B shows the corresponding CMR image. Reprinted from Rochitte C et al[39].

2. Cardiac MRI

Cardiac MRI is now commonly used in the days following myocardial infarction to provide an accurate assessment of left ventricular function, oedema and microvascular function. A bolus of gadolinium contrast agent is injected and images are acquired 3-5 minutes later. Areas of hypoenhancement are seen where contrast has not reached some areas of the myocardium. These areas correlate well with in-vitro thioflavin-S staining (Figure 1) and are

expressed as grams of myocardial tissue affected. In patients with acute myocardial infarction, those with MRI evidence of microvascular obstruction have an increased risk of further adverse cardiovascular events, even controlling for infarct size[11].

3. Fluoroscopy

Coronary blood flow can be described using the Thrombolysis in Myocardial Infarction (TIMI) score, which is a visual assessment of the appearance of contrast flow on angiography. No coronary flow is TIMI=0, and TIMI=3 indicates that coronary flow is the same in the culprit artery as in other vessels. If TIMI score is ≤3 in the absence of thrombus, dissection or stenosis then no-reflow is present. A limitation of the TIMI score is that it TIMI=3 flow defines a non-culprit vessel as having 'normal' flow (which may not be the case). This method is a blunt tool for assessing microvascular function and there is also significant interobserver variability which limits its usefulness for the quantitative assessment of microvascular function.

The TIMI myocardial perfusion grade (TPMG) is a more quantitative measure of coronary flow[40]. The assessor counts the number of recorded angiographic frames from the moment dye fills the culprit vessel proximally, until contrast is seen entering a distal anatomical landmark vessel. Assuming there is no stenosis, dissection or thrombus, a higher TIMI frame count (i.e. the time taken for contrast to pass through the vessel is longer) suggests impaired coronary microvascular blood flow.

The Myocardial Blush Grade (MBG) assesses contrast opacification of the myocardium in the infarct related territory as a measure of microvascular function[41]. MBG=0 is reported when contrast fails to enter the microvasculature. MBG=1 describes contrast seen slowly entering the microvasculature but failing to exit. Contrast is still present 30 seconds later. MBG=2

means dye is seen entering and clearing the microvasculature but this is delayed. Dye washout takes more than three cardiac cycles. MBG=3 describes normal contrast appearance entering and exiting the microvasculature. i.e. there is a ground glass appearance (blush) of the myocardium which then is cleared within three cardiac cycles. Even when TIMI=3 flow is restored to the culprit vessel after ST elevation MI, MBG=3 is only present in one third of patients[42]. Both MBG and TPFG predict left ventricular function, arrhythmias and mortality post-MI[43].

4. Coronary physiology

The objective assessment of epicardial coronary stenosis is possible using a specialised coronary guide wire with a pressure and temperature sensor at the tip. At maximal hyperaemia, coronary artery pressure has a linear relationship with flow and so a pressure drop between proximal coronary (P_A) and distal coronary artery (P_D) implies a fall in coronary blood flow in the epicardial artery[44]. A healthy artery has minimal resistance so P_D/P_A, also known as the Fractional Flow Reserve (FFR), should be close to 1. An FFR of less than 0.80 has been shown to correlate with worse outcome which is improved after treatment with percutaneous coronary intervention[45]. This value is therefore used as the clinical cut-off value for treatment of angiographically moderate lesions with PCI. Severe or critical lesions are generally treated pragmatically without FFR measurement.

FFR provides an objective measurement of epicardial stenoses but does not assess microvascular function. Coronary Flow Reserve (CFR) is a measurement of the increase in coronary flow with hyperaemia. This is measured using the same coronary guide wire; a bolus of room temperature saline is rapidly injected into the coronary artery at rest and at adenosine-induced hyperaemia[46,47]. The time taken (the transit time, T_{mn}) for the bolus of

saline to transit the coronary artery is then measured. The ratio between T_{mn} at rest and hyperaemia is the CFR.

The Index of Microvascular Resistance (IMR) is an independent measure of coronary microvascular function which, unlike CFR, is unaffected by epicardial coronary stenoses. It is calculated using the equation $IMR = P_d \times T_{mn}$.

Many different approaches have been used in an attempt to prevent or treat impairment of microvascular function, including mechanical thrombus removal, the use of filters to reduce downstream embolisation of thrombus debris, intracoronary administration of antiplatelet agents, vasodilators and thrombolytic agents, all with limited success[48]. No therapy has been shown to be effective in a randomised controlled trial.

6.5 Conclusions

There has been a revolution in our understanding of myocardial infarction over the last century, from a condition that was usually diagnosed post-mortem with no effective treatments to one that can be diagnosed in the community with rapid effective treatment administered through well organised national networks. While this has had a dramatic impact on patient outcome, there is a pressing need to develop effective treatments for microvascular obstruction, a condition which affects a substantial number of the primary PCI population leading to reduced myocardial salvage, left ventricular impairment and worse outcome. Understanding more about the biology of the condition will aid this process and may identify new therapeutic targets.

7 Background: MicroRNAs

7.1 Introduction

MicroRNAs (miRs) are small non-coding RNAs that regulate gene expression by binding to specific messenger RNAs where they block the ribosome, inhibiting translation, and may also promote mRNA degradation[49]. Most human protein coding genes have at least one miR binding site which suggests that miRs play a key role in the regulation of protein synthesis[50]. Increasing evidence supports the role of miRs in many different pathological processes, including cancer, infection and cardiovascular disease.

MicroRNAs are readily detectable in the plasma, and many have tissue- or disease-specific expression. Extracellular miRs are either protein bound or transported in microvesicles, and are therefore very stable and resistant to degradation during sampling, processing and storage. They have been shown to be resistant to multiple freeze-thaw cycles and prolonged incubation at room temperature, which makes them potentially useful biomarkers[51].

More exciting is their use for potential new therapies. Once the base sequence of a miR is known, a synthetic miR can be produced to, for example, augment the effect of the miR that offers a protective effect. Conversely, a synthetic miR can be produced that is complementary to a miR shown to have a deleterious effect – an 'antagomiR'. This technology has successfully been used to create an antagomiR to *miR-122* which has a role in hepatitis C (HCV). In a recent phase II trial, this antagomiR reduced viral RNA levels, and in some patients HCV RNA became undetectable and this effect extended beyond the end of active therapy[52].

With such specificity and stability, microRNAs offer the clinician and scientist the opportunity to gain new insights into biology of many different diseases, and the potential for the discovery of novel biomarkers and therapies.

7.2 Nomenclature

Since the first miR was discovered, they were named according to their function, for example the miR *lin-4* inhibits the synthesis of the protein *lin-14* and *let-7* inhibits the *lethal-7* gene, both of which are important for the regulation of development in the roundworm[53]. MiRs discovered since 2003 have been named according to a convention, with the format *hsa-miR-499-3p*[54]. The initial 'hsa' refers to the species homo sapiens. 499 is the identifying number, which are allocated in order of discovery. The suffix -3p or -5p describes which arm of the miR precursor the miR was derived from. Where a miR is discovered that has a very similar sequence to a known miR, they may be given the same number with the suffix -a and -b. The suffix * indicates the passenger strand (see 7.4 MicroRNA Biology).

Many miRs are highly conserved between species, or conserved with a minor base sequence difference. Where a new miR is identified in one species, and there is a known miR with the same sequence in another species, they are allocated the same number. Experimentally validated databases, such as miRviewer, are available that catalogue miR conservation between species[55].

7.3 Historical Context

In 1993, the Ambros lab in Harvard discovered that a short mRNA, *lin-4*, had an effect on *lin-14* which is a protein essential for the normal development of the *Caenorrhabditis Elegans*

roundworm[53]. It might be expected that the presence of a mRNA might lead to an increase in protein transcription. However, the presence of lin-*4* resulted in decreased *lin-14* expression. They then noticed that *lin-4* had antisense complementarity the 3' untranslated region of the *lin-14* protein and the group hypothesised that base pairing may result in some kind of translational repression. Although the name came later, *lin-4* was the first microRNA. Seven years later, the second microRNA was discovered, when the *let-7* mRNA was found to repress the *lin-14*, lin-41, lin-28 and *lin-4*2 genes and, for the first time, it was shown that some microRNAs where conserved between species[56].

The first link between microRNAs and disease, an association between chronic lymphocytic leukaemia (CLL) and loss of *miR-15* and *miR-16*, was identified in 2002[57]. In addition, patients with CLL and some other malignancies also had deletions in the 13q14 chromosome, which was also the site of the genes encoding *miR-1*5 and *miR-1*6. A microarray study in 2006 demonstrated the increased expression of *miR-1*95 in a mouse model of cardiac hypertrophy, and its functional significance was proved when overexpression was shown to cause hypertrophy and subsequent dilated cardiomyopathy[58].

Initial miR research so far focused on tissue expression of microRNAs. However, in 2008, the presence of circulating microRNAs in serum was shown for the first time, with ~100 different miRs identified in human serum samples[59]. Some circulating miRs were detectible in specific disease states, such as *miR-499* which was shown to be specific to myocardial tissue, and was detectable in increased concentrations in the plasma of patients who had suffered a myocardial infarction[60].

Parallel advances in RNA interference technology allowed the design and manufacture of synthetic miRs and miR antagonists (antagomiRs), raising the possibility of using this new

technology to design a new class of disease therapy. The intravenous administration of certain antagomiRs was shown to be feasible and long-lasting, and resulted in a reduction in tissue levels of the corresponding microRNA[61].

To date, over 2500 mature human miRs have been discovered and for many of these in vitro and in vivo studies have been carried out to explore their functions[62,63]. It has become clear that the early view of a single miR regulating a single gene in isolation is over-simplistic. MiRs are more likely to work in complex networks and pathways regulating many different biological processes and diseases. Advances in deep sequencing, target prediction and statistical modelling are helping increase understanding in these complex areas.

7.4 MicroRNA Biology

Precursor miRs are cleaved by the RNAse III enzyme Drosha in the nucleus (Figure 2). This ~70 nucleotide pre-miRNA is then transported into the cell cytoplasm by the nuclear pore transporter Exportin. The final processing of the hairpin pre-miRNA is carried out by the Dicer enzyme which removes the head of the hairpin and the passenger strand, to leave a single strand of miRNA which is around 20 bases long. This mature miR can then bind to the mRNA it regulates, blocking the ribosome and inhibiting translation.

The majority of microRNAs are encoded from the non-coding intron regions of a DNA strand, frequently with the mRNA they regulate. The miRNA transcription process is initiated by RNA Polymerase II, starting at a defined promoter region. The resulting RNA strand is a miRNA precursor called primary miRNA which is several thousand kilobases long, with a 5' cap and a poly-A tail. A single pri-miRNA contains a number of hairpin structures (between 1 and 6), and each will become a single miRNA. The pri-miRNA is processed to an approximately 70 nucleotide

pre-miRNA by the RNAse III enzyme Drosha which shortens the poly-A tail and separates the individual hairpin miRNA precursors. This is transported from the cell nucleus by the nuclear pore transporter Exportin into the cytoplasm.

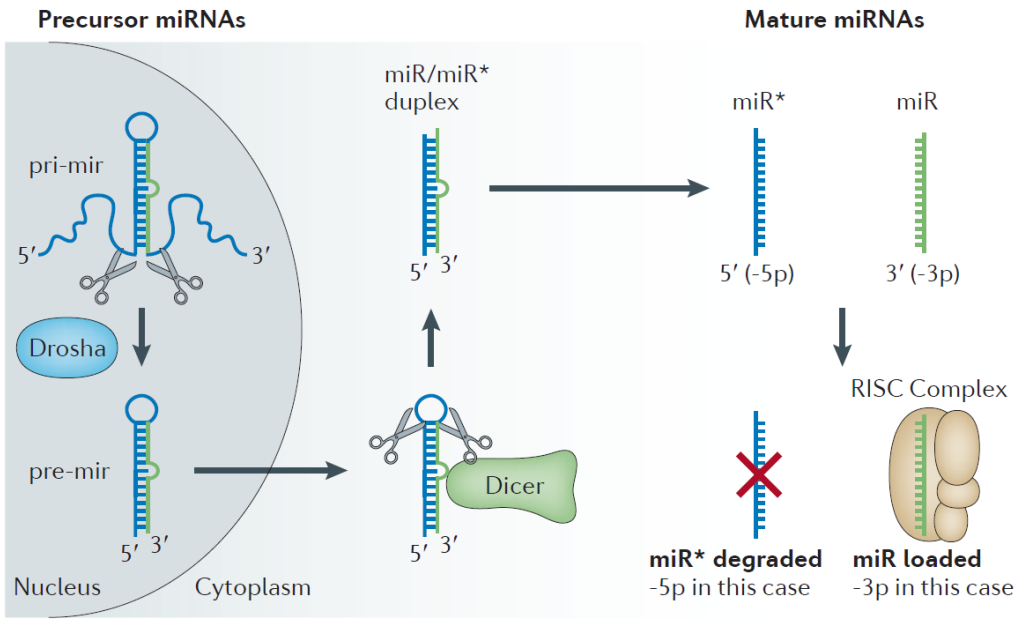

Figure 2: MicroRNA biogenesis.
Primary miRs are processed to pre-miRs in the nucleus before being transported to the cytoplasm via the nuclear pore transporter Exportin. Here the stem-loop is removed by Dicer to leave the miR and the passenger strand (miR*), which is subsequently degraded. The miR is then loaded onto the RNA Induced Silencing Complex (RISC). From Pritchard et al. (2012). Nature Reviews. Genetics[64].

The hairpin pre-miRNA structure is processed further by Dicer, which removes the 'head' and one of the strands (the passenger strand, annotated with *) to leave a microRNA. The microRNA can then bind to the mRNA it regulates; this blocks the ribosome, inhibiting translation. The microRNA does not bind with complete complementarity in eukaryotes, which means a single microRNA can have multiple downstream targets.

Circulating extracellular miRs are remarkably stable and, despite the presence of ribonucleases in the circulation, appear to be very resistant to enzymatic degradation. The reason for this

stability relates to the extracellular miR carrier. So far, several different carrier methods have been identified:

1. Protein bound

   Over 90% of microRNAs are protein bound. At the time of this discovery, the prevailing opinion was that miRs were predominantly found in exosomes and microparticles. When exosomes and microparticles are removed from plasma samples, the miR concentration changes very little[65]. Ultracentrifugation shows that the particle size the majority of plasma miRs are associated with is between 50 and 100 kDa. As miRs are known to be bound to *argonaute* protein within the cell, it was hypothesised that this may be the carrier protein in the extracellular space[66]. Western blot analysis with an *anti-argonaute* monoclonal antibody confirmed that this was the case. In disease states where cell death is increased, levels of extracellular miRs are increased which may suggest that cellular release of some miRs is a by-product of apoptosis, and because they are so stable, they then persist in the extracellular space.

2. Extracellular vesicles

   Many different cell types are known to release extracellular vesicles which have a role in intracellular communication. In vitro studies with stimulated monocytes, platelets and endothelial cells have shown that released microparticles have a distinct microRNA signature, which differs depending on the type and severity of stimulation[67].

3. Cholesterol bound

   Bioanalyser analysis of HDL cholesterol has shown detectable RNA in the 20-40 nucleotide length range and subsequent qPCR detected multiple different miRs. The miR

signature changes depending on the disease state, for example *miR-223* is increased nearly 4000-fold in familial hypercholesterolaemia compared with controls[68].

7.5 MicroRNA Therapeutics

Knockout mouse models missing the either of the miR processing enzymes Drosha or Dicer, or the protein *argonaute-2*, are embryonically lethal, suggesting the importance of miRs for survival[69]. The first miR, *lin-4*, was identified through the use of a loss of function study in the roundworm[53]. Although this particular model is embryonically lethal, the deletion of other miRs frequently has little or no effect on the phenotype. There are several possible reasons for this effect: many single miRs are part of a family of miRs with close homology which may provide a degree of redundancy; the effects of miRs may be most marked in conditions of stress (e.g. inflammation, myocardial infarction), with a less important role in the steady state; finally, one mRNA may be regulated by multiple miRs, reducing the effect of losing a single miR.

Although transgenic animals have been helpful for identifying the roles of different miRs, there are many several other approaches that can be used to manipulating miR activity in vivo and in vitro. The approach that is likely to be most practical for miR therapeutics in the future is antagomiR technology where a synthetic oligonucleotide with a complementary base sequence to the miR of interest is designed. It forms a long-lasting bond with this miR which blocks the ribosome and inhibits protein synthesis. An antagomiR has a structural change such as a methyl, methoxyethyl or fluoro group at the 2' position on the sugar to increase stability. Another common technology is the locked nucleic acid (LNA) which uses a methylene bridge instead. Shorter sequences can be used with as few as 8-15 nucleotides but this could reduce specificity and lead to off-target effects.

An ideal antagomiR has several qualities: it has close (or perfect) complementary to the miR it regulates to minimise any inhibitory effect on off-target mRNA with a similar base sequence; it should be resistant to nuclease activity; and, when bound to a miR it should be stable. All of the different chemistries increase the melting temperature of the miR-antagomiR duplex, inhibiting dissociation and therefore prolonging inhibition.

7.6 MicroRNAs in Myocardial Infarction

MicroRNAs are key regulators of the many biological processes that are involved in myocardial infarction which can be deleterious, such as cell death, or protective, such as the promotion of cardiomyocyte proliferation[70,71]. A distinct group of microRNAs are detectible in human plasma after acute myocardial infarction, with some detectible even before troponin; these have been named the 'myomiRs'. They may be useful as new biomarkers for the diagnosis of myocardial infarction and they may also provide insight into the mechanisms involved in myocardial necrosis and provide new targets for treatment.

Several small studies have reported myomiR release in patients with coronary artery disease. For example, several muscle specific (*miR-133a*, *miR-499* and *miR-208a*) and endothelial derived (*mir-126* and *mir-92a*) miRs are released in acute coronary syndrome, and coronary sinus *miR-499* strongly correlates with troponin measurements[5]. *MiR-208b* is a myocardial miR which shows promise as a biomarker, with reported detection 1600 fold higher in AMI patients versus healthy controls. It may also be useful at discriminating AMI from other causes of a raised troponin, such as viral myocarditis and decompensated heart failure which can cause a diagnostic challenge; in these conditions *miR-208b* is only mildly elevated (3-30 fold)[72].

MicroRNAs can be highly cell and tissue specific. While there are cell specific miRs (e.g. *miR-126* is an endothelial miR), there may be a different miR signature in different locations (e.g. aortic endothelium vs coronary artery endothelium). This phenomenon was shown in tissue analyses from different locations in a patient undergoing heart-lung transplantation[73]. Some miRs were found to be expressed in all endothelial cell locations, but three miRs (*miR-20b, miR-99b, let-7b*) differed substantially between each location. Some miRs (*miR-99b, miR-512*) were relatively overexpressed in coronary endothelial cells, whereas others (*miR-379* and *-424*) were underexpressed.

MiR-208a and *-499* are highly specific for myocardial tissue and *miR-1* and *-133a* are muscle specific, found in both skeletal and cardiac muscle (Figure 3)[74]. An animal study showed that circulating levels of these miRs are increased after myocardial infarction induced by LAD ligation (Figure 4), with levels peaking at 3-6 hours.

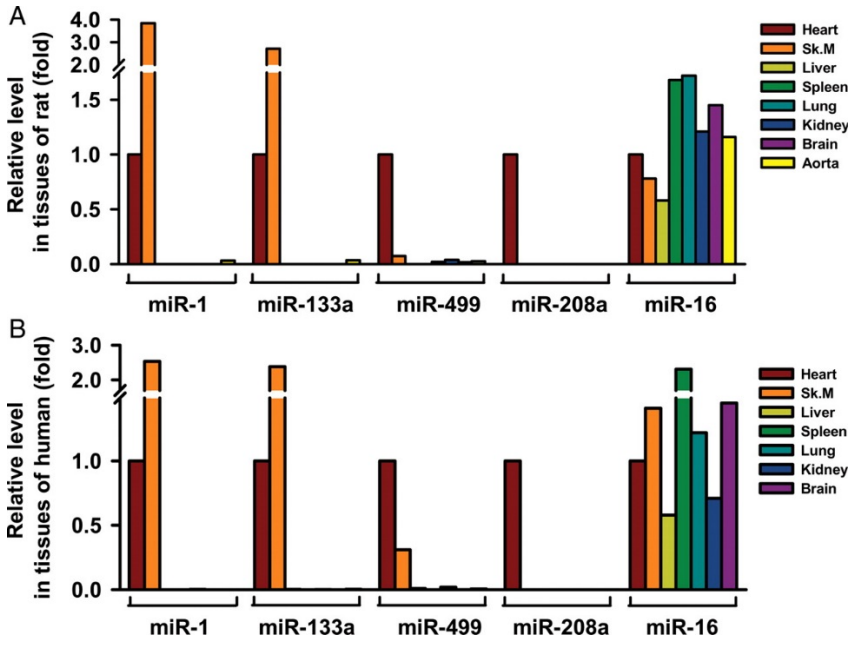

Figure 3: Tissue specific miR expression.
Panel A shows miR expression in rat tissue; B shows expression in human tissues (from Wang, G.-K. K. et al. (2010). European Heart Journal, 31(6), 659–666) [74].

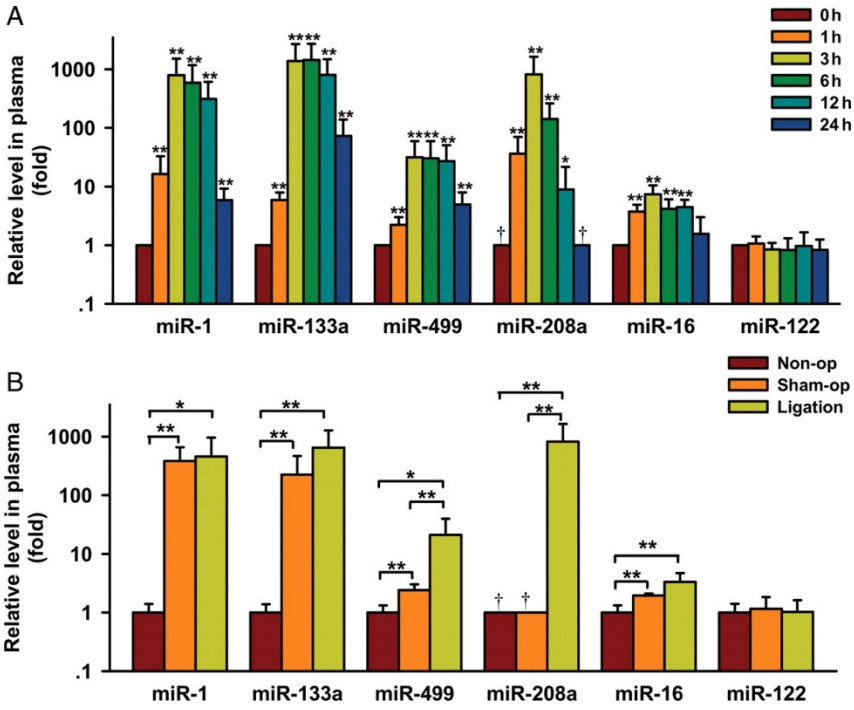

Figure 4: Plasma miR detection after myocardial infarction.
A: Detection of plasma myocardial miRs over 24 hours in an LAD ligation rat model of myocardial infarction. **B:** Circulating miRs 3 hours after LAD ligation in control, sham-operated and LAD ligated rats (from Wang, G.-K. K. et al. (2010). European Heart Journal, 31(6), 659–666)[74].

In addition to their potential usefulness as biomarkers, microRNAs may provide information on outcome after myocardial infarction. In a study of patients admitted to hospital with an acute coronary syndrome, elevated levels of miRs 133a and 208b were predictors of six-month mortality[75].

MiRs are not only detectable after acute myocardial infarction; specific miRs are associated with increased risk of future myocardial infarction. Over a ten year observation period, individuals from the Bruneck cohort expressing higher levels of endothelial *miR-126* had an increased risk of myocardial infarction, whereas those with higher levels of *miR-197* or *miR-223* had a lower risk[76].

MicroRNAs that are differentially expressed in myocardial infarction have been identified in two ways, which have different limitations. Animal models generally use LAD ligation and, although this causes distal ischaemia and infarction, this is a different mechanism from naturally occurring myocardial infarction which is usually initiated by atherosclerotic plaque rupture. Additionally, patterns of microRNA release may be different in humans. Human studies have catalogued the release of microRNAs after myocardial infarction, but in these 'real world' cases it is not possible to determine the precise timing of vessel occlusion and early microRNA signals may have resolved by the time the patient presents to hospital.

7.7 MicroRNA Analysis

The inherent stability of circulating microRNAs makes them an attractive target for research, and potentially useful as biomarkers. However, there are a number of important factors to consider in their sampling and processing to ensure accurate and reproducible measurements. The different blood components (erythrocytes, white blood cells, platelets) each have a unique miR

signature, with much higher detectible miR concentrations and an increased number of detected miRs when compared with plasma or serum samples (Table 1)[77]. For example, red blood cells have higher levels of *miR-16* and *miR-451*[78]. It is therefore important when analysing circulating miRs that samples are acellular, which can be achieved by centrifuging the sample once, and then centrifuging the supernatant a second time.

Sample number	Serum	Plasma	Platelets	RBCs	WBCs
1	185	200	341	454	374
2	156	164	288	477	391
3	194	201	285	450	397
4	240	212	301	421	359
5	195	161	309	471	395
6	123	123	280	457	374
MEDIAN	190	182	295	456	383

Table 1: The number of miRs detected (CT value ≤35) in samples taken from six healthy subjects.
RNA was extracted from 100µL of sample using the Qiagen miRNeasy kit, cDNA synthesis was carried out using the Exiqon MiRCURY LNA Universal RT kit and qPCR on Exiqon Human miR I & II panels[77].

Haemolysis can occur at multiple points throughout sample processing. It occurs most commonly at the time the sample is collected and can be related to the use of a narrow bore needle, or if aspiration is too aggressive. It is important to determine whether haemolysis has occurred because it changes the plasma miR profile, which may to skew miR analysis. Haemolysis can be assessed using spectrophotometry measuring oxyhaemoglobin absorbance, which has distinct peaks in haemolysed samples, but this can only be carried out on a sample before RNA isolation. In haemolysed samples, RBC specific miRs (e.g. *miR-16* and *-451*) are detectible in high concentrations. *MiR-23a* is found in serum and plasma and is not affected by haemolysis[78]. Measurement of *ΔmiR23a-miR-451* can be used to measure haemolysis in these samples and correlates well with spectrophotometry[79].

RNA Isolation

The most commonly used method for RNA isolation was developed in the 1950s. Phenol is added to the sample of interest; under acidic conditions, protein dissolves in the phenol, RNA is dissolved in the aqueous phase and DNA stays in the phenol-water interface. Chloroform is then added to remove and residual traces of DNA from the aqueous phase. The aqueous phase is then carefully removed with a pipette. This method was improved in 1979 with the addition of guanidinium thiocyanate (commonly known as TRIzol (*Ambien Technologies*)) which lowers the pH of the phenol-chloroform mixture and allows the RNA isolation to be carried out more quickly with fewer steps. A disadvantage of the original and the improved method is the difficulty of working with phenol and chloroform, both of which are noxious and need to be used in a fume cupboard.

The advent of silica column based RNA isolation in 1990 improved both the quality and ease of RNA isolation[80]. Under specific salt and buffer conditions, nucleic acids bind selectively to silica which can be mounted in a spin column designed to fit a microtube for centrifugation. After sample and protein precipitation the sample is applied to the silica column and centrifuged several times. The bound RNA can be washed and then eluted in nuclease-free water for subsequent reverse transcription.

A further important issue around using the TRIzol method is that RNAs with a low GC content are inefficiently isolated, especially when a small amount of starting material is used. This is of critical importance in miR research in biofluids as the amount of starting material is already at the limits of detection, and also because miRs have very variable GC content. This means that some miRs may not be detected in a sample due to a technical failure rather than for a biological reason. This phenomenon was only identified in 2012 and has led to the retraction of at least

one published journal article. The authors tested the TRIzol method against silica column extraction and found that miRs with a low GC content were isolated less efficiently using the TRIzol method[81].

Once microRNA has been isolated, it is reverse transcribed and measured using quantitative real-time PCR. The advantages of PCR over the other methods, such as microarray analysis and RNA-sequencing (RNA-seq), are that PCR allows microRNA detection at much lower concentration, the generation of data takes less than a day and this technique uses equipment found in most labs. It is cost-effective, reliable and, unlike RNA-seq, initial data analysis can be carried out without specialist bioinformatics input.

Normalisation

The isolation and analysis of microRNAs involves multiple steps and each step can potentially introduce technical variation which may then impact on the experimental result (Table 2). The aim of normalisation is to control for technical variation between samples unrelated to the condition being studied[64].

MicroRNA processing step	Potential sources of technical variation
Sample preparation	Haemolysis Presence of cell debris in sample Time between sample collection, processing and snap-freezing
RNA isolation	Input RNA amount RNAse contamination
Reverse transcription	Pipetting inaccuracies Variability in RT efficiency (more of an issue with microRNA due to short length and high C-G abundance)
Quantitative real-time PCR	Pipetting inaccuracies Variability between plates Run to run variation on PCR cycler

Table 2: Potential sources of technical variability when isolating and analysing microRNAs from biofluid samples.

When messenger RNA (mRNA) is being analysed, once RNA has been isolated from a sample, spectrophotometry (e.g. using a Bioanalyzer) is commonly used to measure the RNA concentration so a constant amount of RNA can be used for reverse transcription, which adjusts for differences in the efficiency of RNA isolation. While this is effective when analysing mRNA, or microRNA in tissue samples, microRNA levels in biofluid samples (such as serum or plasma) are too low for reliable detection and therefore other methods need to be used to control for inter-sample variation.

Spike-in Normalisation

A widely used method of normalisation is to spike in a known quantity of a synthetic non-mammalian microRNA at the RNA isolation stage. A microRNA from the worm *Caenorhabditis elegans* (*cel-miR-39*) is frequently used for this purpose. An advantage of this approach is that it controls for any differences in efficiency at each subsequent processing step. However, as the spike in RNA is bound to protein, lipid or exosome there may be unaccounted for variations in reaction kinetics extraction efficiency due to differing physical properties which may lead to ineffective normalisation. Spike-in normalisation is therefore not recommended as a robust normalisation strategy, however spike-in RNA and cDNA are useful for quality control, and can be used to test the efficiency of each stage of the microRNA analysis process.

Global Mean

Global mean (also known as $CT_{AVERAGE}$) normalisation is a mathematical method based on the assumption that overall microRNA expression will be similar between samples. For this method to be reliable, a large number of microRNAs need to be quantified in the same analysis, and the microRNAs being quantified are part of a large and unbiased panel. An unbiased panel would, for example, include microRNAs that are expected to be differentially expressed between

samples and also those that would be expected to be relatively stable. Global mean normalisation should not be used where the plate is designed only with microRNAs that are expected to differ between samples, as global mean normalisation in this setting may 'normalise out' any biological differences. In smaller panels, other methods of normalisation (such as reference gene normalisation) should be considered.

Global mean normalisation can be carried out using the following steps[82,83]:

1. Set a cut-off and exclude higher values

   At higher CT values (lower expression) qPCR is less reliable and therefore samples with a CT value above a selected cut-off are excluded from analysis.

2. Calculate the mean CT value of the remaining data

   A simple average is calculated using the remaining CT values.

3. Subtract the average CT value from all samples

   The CT average calculated in step 2 is now subtracted from all samples. The resulting normalised expression value can be used for data analysis. As with raw CT values, the scale is inverse: a smaller/more negative value equates to a higher absolute concentration. The normalised CT value will then be around zero but one unit is still one cycle.

Global mean normalisation has been shown to outperform other normalisation methods in large scale microRNA profiling studies by reducing technical variation and improving the detection of biological differences between samples[82].

Reference Gene Normalisation

Many microRNAs are stable between individuals and can therefore be used for normalisation; these are known as reference genes, reference microRNAs or housekeepers. As with global mean normalisation, higher CT values are first excluded. Then, rather than averaging all CT values, the CT value for the stable microRNA is then subtracted from all microRNAs to produce a

normalised expression value. If multiple reference microRNAs are used, then their CT values are averaged before subtraction from all microRNAs.

Many different microRNAs that have been used as stable reference genes and although some miRs appear to be stable between different patient groups, tissue types or pathologies, it is important to select and validate reference genes for the specific population and sample type being analysed.

A common strategy for identifying reference genes is to perform qPCR array analysis of a large number of microRNAs in a small number of samples. The microRNAs are then ranked according to their stability, and the most stable can then be used for normalisation in a much larger number of samples. Two software algorithms – *geNorm*[84] and *Normfinder*[85] – are commonly used to identify suitable reference genes.

8 Patient Recruitment

8.1 Introduction

The United Kingdom is a world leader in medical research in the critically ill, despite the inherent difficulties of carrying out research in this patient group. This has transformed the care we offer for many conditions, for example, the administration of intravenous steroids used to be the standard of care for patients with head injury; the MRC CRASH trial proved that patients who received steroid had an increased risk of death or severe disability and this work has since changed practice worldwide[86]. In the setting of out of hospital cardiac arrest, adrenaline is routinely given but its efficacy has never been tested with a randomised controlled trial; the Paramedic-2 trial aims to determine whether its use confers a survival benefit[87].

The Oxford Acute Myocardial Infarction (OxAMI) Study is a research programme investigating another challenging field – acute ST elevation myocardial infarction. The OxAMI Study is a prospective cohort study consisting of a number of substudies, each investigating a different aspect of MI biology, with each substudy operating using common standard operating procedures, case report forms (CRF) and administrative infrastructure.

Recent substudies have focused on aspects of cardiac MRI, including 'hyperacute' MRI at the time of MI, intracoronary imaging, coronary physiology and identifying novel biomarkers. Each patient recruited to the programme may be recruited to multiple substudies. The result is a rich bioresource of patients, comprehensively phenotyped with blood sampling from multiple sites, cardiac MRI and coronary physiology data. The recorded data can be used to answer many different biological questions both prospectively and retrospectively.

8.2 Methods

Study Design

Patient recruitment for this thesis was carried out as a substudy (the 'MicroRNA substudy') of the Oxford Acute Myocardial Infarction (OxAMI) Programme. All stages of the study including patient recruitment, consent, data collection and data storage were governed by the OxAMI Standard Operating Procedures (SOPs) which were stored on a shared server and were also published in the relevant clinical areas. The protocol was approved by the National Research Ethics Service Committee South Central – Oxford (REC reference: 11/SC/0397).

Study Participants

Patients aged between 30 and 90 with who were undergoing primary percutaneous coronary intervention for ST elevation MI were eligible for enrolment if onset of pain was within 12 hours. Exclusion criteria included contraindications to MRI (claustrophobia, implanted metal) or coronary physiology assessment (reactive airways disease, coronary anatomy considerations), patients presenting with cardiogenic shock and those with previous myocardial infarction or cardiac surgery. A patient could be excluded from the study at the investigator's discretion if they would be unlikely to complete the study protocol, or where follow up would not be possible (e.g. a visiting foreign national not planning to stay in the UK).

The Clinical Pathway

The diagnosis of ST elevation myocardial infarction was usually made in the community by ambulance personnel. South Central Ambulance Service had the facility to electronically

transmit ECGs to the Coronary Care Unit team where they could be reviewed to confirm the diagnosis and activate the Primary PCI team. Where the diagnosis of STEMI was made in hospital (usually in the Emergency Department), the patient was reviewed by the on-call cardiology registrar who then activated the primary PCI team.

The Primary PCI team included a consultant cardiologist (the OxAMI Investigator), two nurses, a radiographer, a cardiac physiologist and the OxAMI Fellow. The facility to review ECGs before patients arrive in hospital allowed the team to be assembled before the patient had left the scene, which meant the primary PCI team were usually present and ready to operate before the patient arrived, minimising delay to treatment and reducing door-to-balloon time.

On arrival to the hospital, patients were transferred immediately to the cardiac catheterisation laboratory. Dual antiplatelet therapy was initiated prior to the procedure with aspirin and clopidogrel or aspirin and ticagrelor. Coronary angiography was carried via the radial or femoral artery. Heparin or bivalirudin was used as for anticoagulation during the procedure. Once the culprit lesion was identified, a guide wire was passed across the lesion and, at the operator's discretion, a microcatheter was used to aspirate any thrombus.

Once coronary flow was restored, the operator (also an OxAMI investigator) had a discussion with the patient explaining the OxAMI research programme, outlining the purpose of the research and the extra investigations that would be carried out. The patient was then asked whether they would offer their assent to participation. This conversation was witnessed by a Patient Advocate, who was a member of the catheterisation lab staff specially trained to provide ethical oversight of the assent process. Provided the patient agreed to participate and the advocate and the OxAMI investigator both felt that the patient had received an adequate explanation which was understood by the patient, they could then be recruited into the OxAMI

study. Oversight for this part of the protocol was provided by an ethicist from the University of Oxford.

If the patient offered assent, their details were entered into a Microsoft Access database which then generated a unique patient identification number and the patient assent CRF which was signed by the operator and the patient advocate.

Labelled microtubes for storing aliquots of plasma or serum were prepared in advance for each OxAMI patient ID to minimise the administrative time taken recruiting a new patient. They were labelled by OxAMI ID, site and time point (Table 3). It is important to note that where times are given they are after hospital admission, not after myocardial infarction. It is difficult to be precise about myocardial infarction time because both symptoms and recollection of symptoms are highly variable. The time of onset of chest pain according to the patient was recorded.

Label	Time point	Sample site
1.2	During primary PCI procedure, before stent deployment	Coronary artery, coronary aspirate (thrombus), peripheral vein
1.3	During primary PCI procedure, after stent deployment	Coronary artery, peripheral vein, coronary sinus
2.1	6 hours after admission	Peripheral vein
2.2	24 hours after admission	Peripheral vein
2.3	48 hours after admission	Peripheral vein

Table 3: Blood sample collection time points.
Blood samples were collected at six time points after admission with acute myocardial infarction. Samples at time points 1.2 and 1.3 were collected in the cath lab at a time when patients had central venous and arterial access, enabling multiple blood samples to be taken. From time point 2.1 onwards, peripheral venous samples were collected on the ward.

After assent, the samples for time point 1.2 were taken. The lesion was predilated with a standard angioplasty balloon, an appropriately sized stent was deployed across the lesion and this was postdilated in the usual fashion. At this point, the time point 1.3 samples were taken

from coronary artery, coronary sinus and peripheral vein. Blood gas analysis was also carried out on all of these samples, including measurement of acid-base status, oxygenation and lactate.

At the end of the procedure, patients were transferred to the coronary care unit where they received the standard clinical care for patients undergoing primary PCI, including ECG monitoring, regular ECGs, echocardiography, secondary prevention drug therapy and a consultation with the rehabilitation team. Further venous blood samples for time points 2.1, 2.2 and 2.3 were taken at 6, 24 and 48 hours respectively. Cardiac MRI was carried out 24-48 hours after the procedure. Patients were discharged from hospital when it was felt to be appropriate by the clinical team; the OxAMI study did not delay discharge as all patients stay in hospital for at least 48 hours after MI.

Data Collection and Sample Processing

Blood Sample Collection

Blood samples were collected from the coronary guide catheter using a standard 10mL syringe. The first 5ml of blood was discarded and then 12ml of blood was aspirated by the operator and passed to the OxAMI investigator for processing. Peripheral venous samples for time point 1.2 were collected from a newly sited peripheral venous cannula. If thrombus aspiration was carried out, this sample was separated in to thrombus material and blood, using a filter (Figure 5). For time point 1.3 and 2.1 the peripheral venous sample was collected from a venous sheath which had been sited for coronary sinus blood collection and the measurement of the right atrial pressure.

In the early part of the study, femoral venous access was used for coronary sinus sample collection. As our experience grew, the right cephalic vein was used. This was felt to be safer than the femoral approach after anticoagulation as direct pressure could more easily be applied in the event of post-procedure bleeding, and this approach removed the risk of retroperitoneal haematoma.

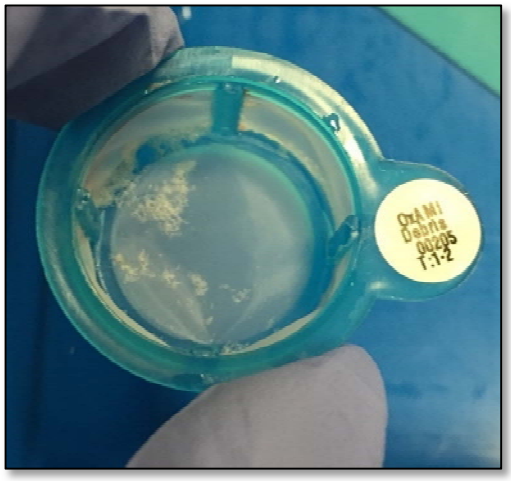

Figure 5: Platelet rich thrombus coronary artery aspirate from a patient at the time of primary PCI.
A microcatheter was used to aspirate thrombus from the culprit coronary artery. The aspirate was then filtered and rinsed with normal saline to reveal thrombotic debris.

A CASII or AL1 diagnostic catheter was used to intubate the coronary sinus with the image intensifier in the left anterior oblique position. Coronary sinus position was confirmed with a contrast injection and acquisition. Intubating the coronary sinus can be challenging due to anatomical variation between patients and the location of the Thebesian valve. Sometimes a coronary guidewire was used to provide stability. Aspirating blood from the coronary sinus is inherently difficult due to the low blood pressure at this site. Indeed, if blood is easy to aspirate, it is unlikely to be a true coronary sinus sample.

Blood gas analysis was carried out on all blood samples taken at time point 1.3. Measurements of pH, pO_2, pCO_2, lactate, base excess and electrolytes were all recorded both to contribute to the bioresource and to confirm the sample was a true coronary sinus sample. A sample was confirmed as true if the pO_2 of the coronary sinus sample was lower than the pO_2 of the venous sample.

Blood Processing

Once a blood sample was collected from the patient, it was transferred into two ethylenediaminetetraacetic acid (EDTA) and one serum separator (SST) tube (each containing 4-5mL whole blood) which were taken immediately to an adjoining laboratory for processing. The EDTA tubes were centrifuged at 1300g for 12 minutes to separate the plasma. The upper plasma layer was transferred to a new test tube and centrifuged at 2500g for 15 minutes to pellet platelet debris. This platelet poor plasma was stored in 220µL aliquots and frozen immediately to -80°C. One of these aliquots was subsequently used for miR analysis. The SST tubes were centrifuged at 2500g for 15 minutes and the serum was stored in aliquots in the same way.

Clinical blood samples were sent for analysis as would be done for a non-study patient after a myocardial infarction (e.g. full blood count, cholesterol, renal function) and these values were added to the study record retrospectively.

Aliquots of serum collected at 0, 6, 24 and 48 hours was used for troponin-I analysis. These samples were processed in batches by the local clinical biochemistry laboratory using an immunoassay technique on a Siemens Centaur XP analyser. The four troponin measurements were used to calculate an area-under-the-curve (AUC) measurement using the trapezoid rule (*Graphpad Prism version 6, La Jolla, CA USA*).

ECGs

Pre-hospital ECGs recorded by the ambulance crew were duplicated and added to the patient's research record. In-hospital 12-lead ECGs were recorded at the start of the procedure, the end of the procedure, 30 minutes after the procedure and 24 hours after admission. All ECGs were then scanned to the OxAMI server.

ECGs were analysed retrospectively using the image analysis software ImageJ (*National Institutes for Health, Bethesda, MA, USA*) to quantify ST elevation, which was measured 40ms after the end of the QRS complex. The correlation between ECG changes and final infarct size has been studied previously and various methods of quantification have been developed[88–90]. A large analysis of ECGs in the INFUSE-AMI trial showed that measuring ST resolution in the worst affected ECG lead (the 'maxST residual' method) showed the strongest correlation with final infarct size as measured by MRI, compared with various other more labour-intensive methods (e.g. summed ST resolution, summed residual ST elevation etc.)[88]. The maxST residual method was therefore used to analyse the pre-procedure and 30 minutes post-procedure ECG. As in the INFUSE-AMI analysis, ECGs in patients with LBBB, paced rhythm or ventricular rhythm were excluded from this particular analysis.

Cardiac MRI

Provided there were no contraindications, patients underwent a cardiac MRI scan within 48 hours of admission and six months later. The examinations were carried out using a 3 Tesla MRI scanner (*MAGNETOM TIM-Trio or MAGNETOM Verio, Siemens Healthcare, Erlangen, Germany*) using a spine coil and a 32 channel phased array coil.

By this stage, the patient had received patient information about the study and provided written consent. Before starting the scan, an MRI safety check questionnaire was completed and renal function was checked. Contrast was not administered if eGFR was less than 30 mL/min/1.73 m^2.

The scan was carried out under medical supervision with a minimum of three staff members present, all of whom had been trained in the safe evacuation of patients from the scanner. The supervising doctor was Advanced Life Support (ALS) certified and the other staff members were Immediate Life Support (ILS) trained as a minimum. Advanced resuscitation equipment including a defibrillator was available in the recovery area. Oxygen saturation and ECG were monitored throughout.

Left ventricular function, myocardial oedema and microvascular obstruction were quantified using Steady State Free Precession (SSFP), T2-weighted and late gadolinium enhancement (LGE) imaging. A gadolinium-based contrast agent (*Doltarem™ (gadoterate meglumine), Guerbet Groupe, Paris, France*) was administered at a dose of 0.1 mmol/Kg. Left ventricular volumes were measured using multiple slices in systole and diastole and left ventricular function was calculated using these measurements. Microvascular obstruction was assessed by manual delineation of the contrast-free areas and calculated as a percentage of left ventricular mass. All image analysis was carried out using cmr[42] (*Circle Cardiovascular Imaging, Calgary, Alberta, Canada*) by the local cardiac MRI core laboratory (*Acute Vascular Imaging Centre, University of Oxford*).

Six months after their initial presentation, patients were invited back to hospital to undergo a second cardiac MRI scan. A clinical review was carried out and a questionnaire was used to assess the patient's health and identify and document any interim hospital admissions. Prior to the scan, renal function was checked using a point-of-care analysis system to ensure the safety

of administering a gadolinium based contrast agent; if eGFR was <30 mL/min/1.73m, gadolinium was not administered.

Late gadolinium enhancement (LGE) imaging was used to determine final infarct size (scar). Left ventricular volumes and function were also assessed. Myocardial salvage index was calculated as the ratio between acute oedema (area at risk) measured at 48 hours and final infarct size measured at six months.

Data Storage

When a patient was identified as a suitable candidate for OxAMI, they were registered on the OxAMI patient database by NHS number. This process allocated the 'OxAMI number', a unique identifier used to label samples and clinical data throughout the study, and confirmed that the patient had not previously been recruited to the research programme. Patient identifiable information (e.g. name, address) was stored in a locked cabinet in a locked research office with an electronic access control system. This information was necessary for contacting patients for follow-up, but contact was only made after confirming with the general practitioner that this would be appropriate.

Server space was leased from the NHS for the OxAMI study (the 'OxAMI server') and this was hosted by the Oxford Health Informatics Service (OHIS). All OxAMI clinical and research data were stored on the OxAMI server indexed by OxAMI number. Access to the server was governed by a data access SOP. No patient identifiable data were stored on personal computers and any anonymised data were stored on an encrypted hard drive and individual data files were password protected.

8.3 Results

8.3.1 Patient recruitment

Clinical data for the entire OxAMI microRNA substudy is reported here. Recruited patients were allocated into Discovery and Validation Experiments and the baseline clinical data for these is reported in the Results section of the relevant chapter.

102 patients were recruited between June 2012 and March 2015. Time of presentation to hospital is shown in Figure 6. Baseline parameters are shown in Table 4.

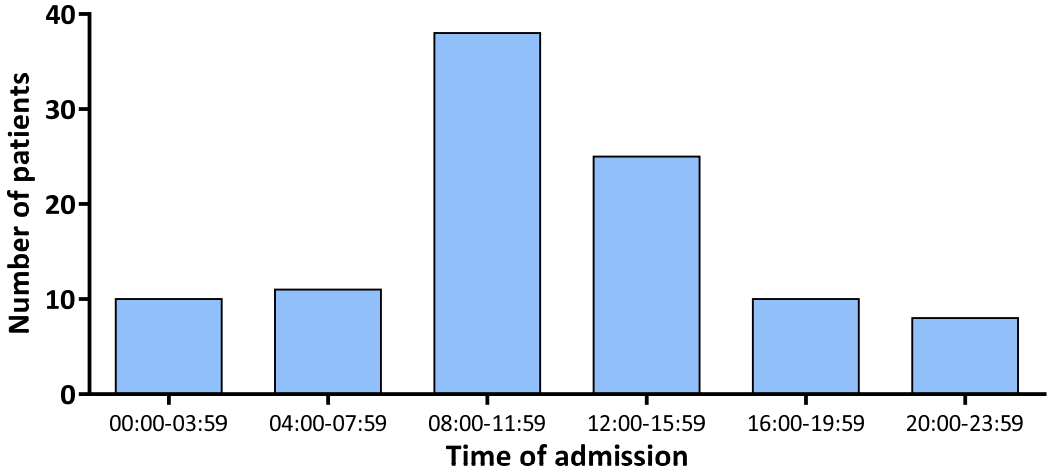

Figure 6: Time of admission of patients recruited to the OxAMI microRNA substudy.

Median follow up was 2.7 years (median 1,000 days, range 283-1,298). Outcomes were classified according to the Academic Research Consortium (ARC) criteria for endpoints in coronary stent trials[91]. No patients died during the study period. 4 patients (3.9%) reached an ARC endpoint with event-free survival in 96.1%. Two patients had a myocardial infarction in a different vessel (after 273 and 638 days respectively), one patient had target lesion revascularisation 184 days

after index procedure and one patient had subacute stent thrombosis 365 days after index procedure (after cessation of the second antiplatelet agent).

Gender n (%)	
Male	84 (82.4)
Female	18 (17.6)
TOTAL	102

Age	
Median	64
Range	31-90

Diabetes n (%)	
Oral medication	7 (6.9)
Insulin	2 (1.9)
New diagnosis	1 (1.0)
TOTAL	10 (9.8)

Smoking n (%)	
Current	35 (34.3)
Ex	33 (32.4)
Never	34 (33.3)

Creatinine (µmol/L)	
Median	74.5
Range	37.0-183.0

Culprit vessel n (%)	
LAD	50 (49.0)
Circumflex	11 (10.8)
RCA	41 (40.2)

Troponin-I (µg/L)	
Peak (median)	88.39
Peak (range)	0.63-1,689
AUC 0-48h (median)	2,507
AUC 0-48h (range)	21.7-28,946

Infarct size g (% LV)	
Median	14.9
Range	1.8-47.0

LV ejection fraction at 6 months %	
Median	55.3
Range	19.9-83.5

Total hospital stay (days)	
Median	2.4
Range	1.1.- 25.3

Table 4: Baseline patient characteristics for all patients recruited to the OxAMI microRNA substudy.
102 patients were recruited over 34 months. LAD=left anterior descending, RCA=Right coronary artery. Troponin-I was measured at four time points and a troponin-I area under the curve (AUC) was calculated using the trapezoid rule. Infarct size and ejection fraction were measured at the six month MRI scan. Infarct size was measured as late gadolinium enhancement.

8.3.2 Infarct Size and Troponin Release

The time-course of troponin release is shown in Figure 7. A Spearman rank-order correlation was carried out to assess the relationship between troponin release during the index admission and final infarct size at six months. This test was chosen as troponin release was not normally

distributed. This relationship was assessed with single troponin measurements (at 0, 6, 24 and 48 hours), peak troponin and troponin area under the curve (AUC) calculated using the trapezoid rule (AUC 0-6 hours and AUC 0-48 hours). There was a strong positive correlation between troponin release and final infarct size (Table 5). Scatter plots of these correlation relationships are shown in Figure 8. As the strongest correlation was between infarct size and 48-hour troponin-I (Table 5), linear regression was carried out which showed that 48-hour troponin could statistically significantly predict infarct size with adjusted an r^2 of 0.618 and $F(1,70)=116.07$, $p<0.0001$.

Troponin-I (µg/L)	Correlation coefficient (ρ)	Significance (p)
0 hours	0.55	<0.0001
6 hours	0.77	<0.0001
24 hours	0.79	<0.0001
48 hours	0.80	<0.0001
Peak troponin (0-48 hours)	0.79	<0.0001
AUC 0-6 hours	0.80	<0.0001
AUC 0-48 hours	0.84	<0.0001

Table 5: Spearman rank order correlation between troponin measurements and final infarct size.
Troponin was measured in µg/L. Peak troponin (0-48 hours) was the highest troponin measurement recorded over the first 48 hours. AUC = area under the curve of four troponin measurements in µg/L calculated using the trapezoid rule.

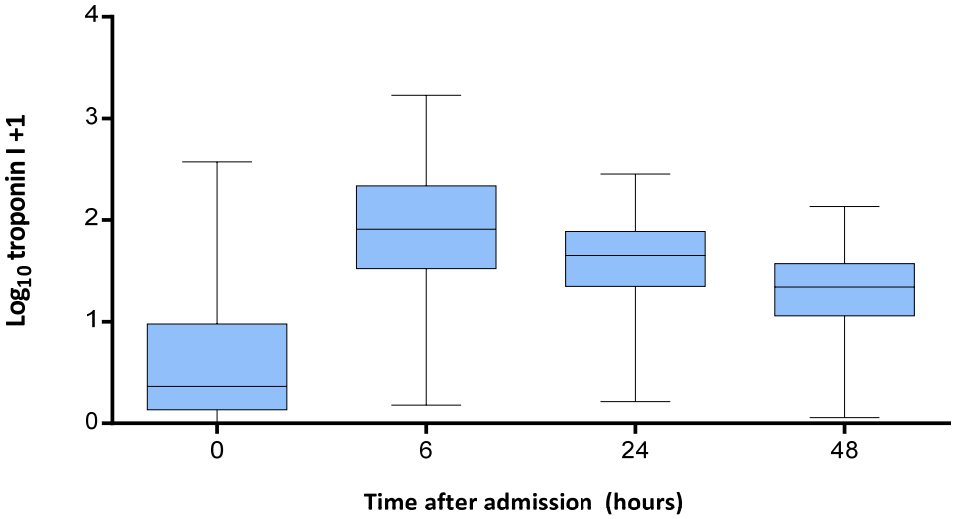

Figure 7: Troponin-I results for all patients measured 0, 6, 24 and 48 hours after admission (µg/L).
Troponin-I results underwent log transformation after which they were normally distributed. Box shows median and interquartile range, whiskers show range (n=102).

A

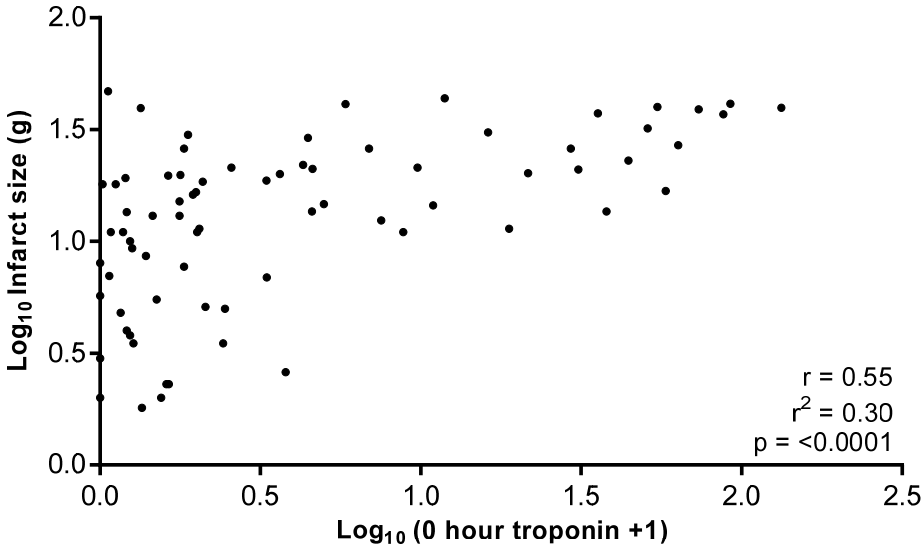

B

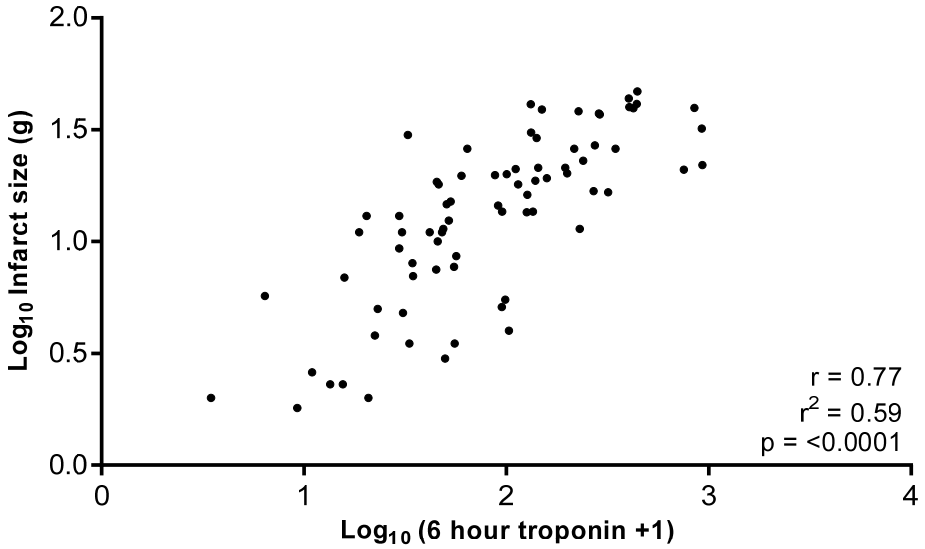
2.0
1.5
1.0
0.5
0.0
0
1
2
3
4
Log10 Infarct size (g)
Log10 (6 hour troponin +1)
r = 0.77
r2 = 0.59
p = <0.0001

C

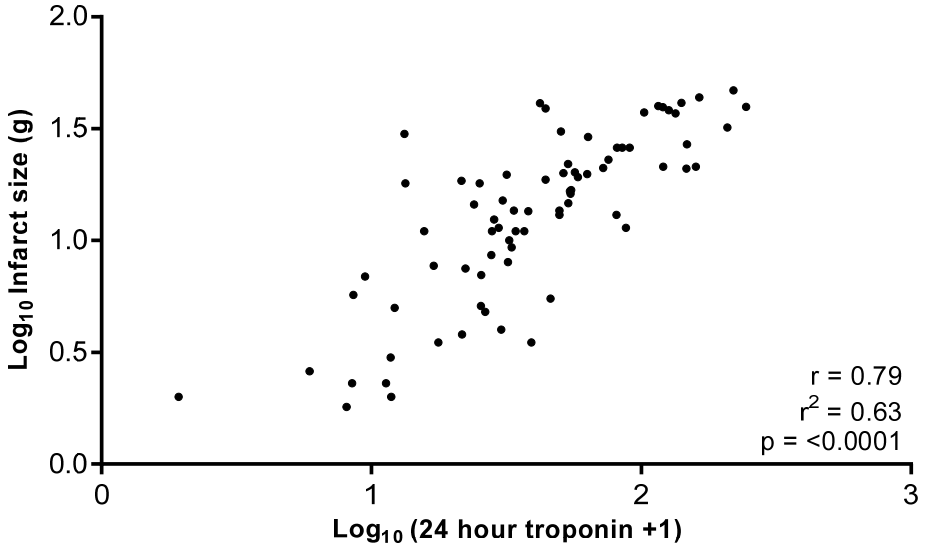
2.0
1.5
1.0
0.5
0.0
0
1
2
3
Log10 Infarct size (g)
Log10 (24 hour troponin +1)
r = 0.79
r2 = 0.63
p = <0.0001

D

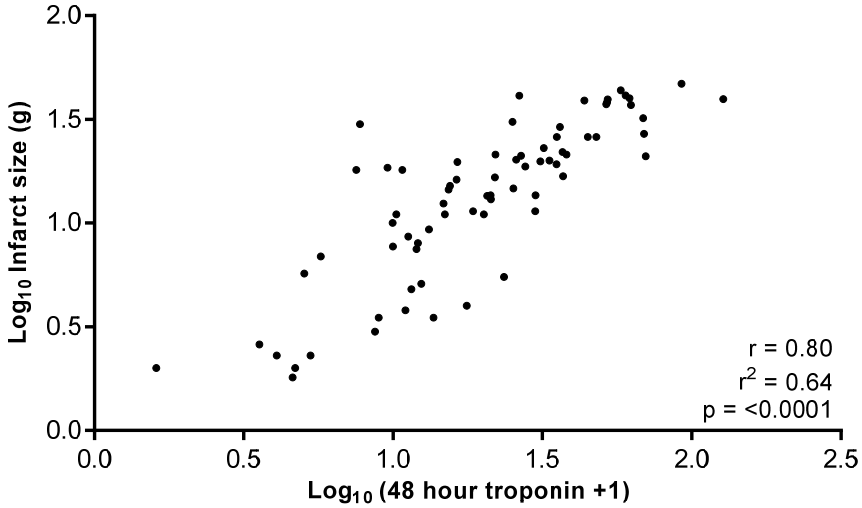
2.0
1.5
1.0
0.5
0.0
0.0
0.5
1.0
1.5
2.0
2.5
Log10 Infarct size (g)
Log10 (48 hour troponin +1)
r = 0.80
r2 = 0.64
p = <0.0001

E

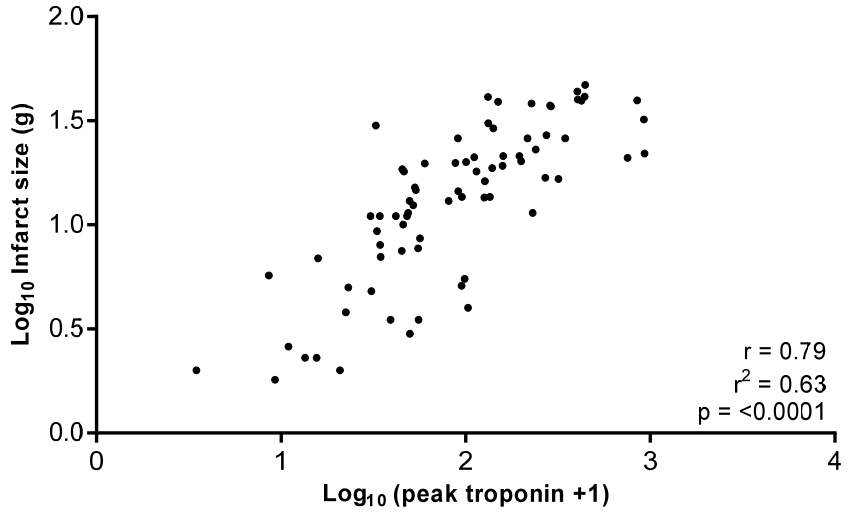

F

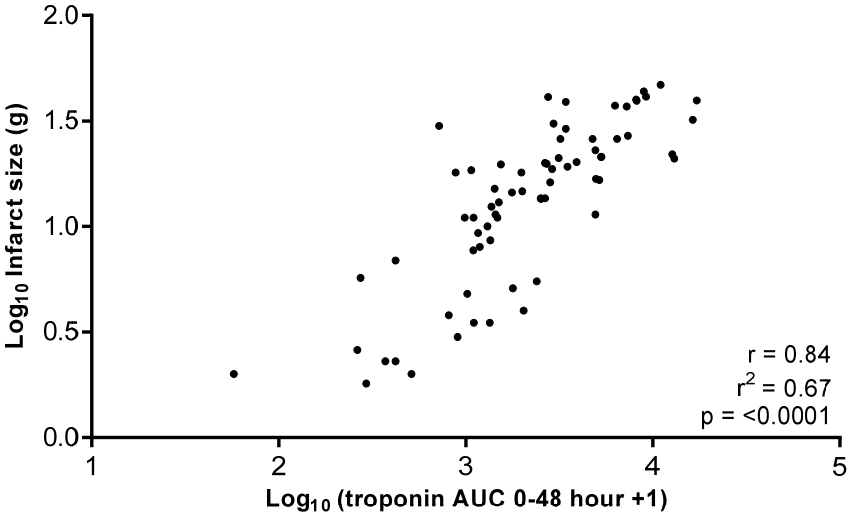

Figure 8: The relationship between infarct size and troponin-I release.
Different troponin measurements from single time points between 0 and 48 hours (panel A-D), peak troponin (E) and troponin area under the curve (0-48 hours) were used for correlation analysis with infarct size measured at a six-month MRI scan. As neither troponin measurements or infarct size were normally distributed, both were log transformed prior to analysis, after which they were normally distributed. All patients with four troponin measurements and a six month MRI scan were included (n=76).

8.3.3 Microvascular Obstruction

Microvascular obstruction, measured by cardiac MRI within 48 hours of myocardial infarction, and its relationships with troponin release and infarct size are shown in Figure 9 and Figure 10. Microvascular obstruction was defined as late hypoenhancement within hyperenhanced tissue on the late gadolinium images, and this was quantified in grams of tissue (an example image is shown in Figure 1, panel B). Patients with microvascular obstruction have increased peak troponin, and larger final infarct size.

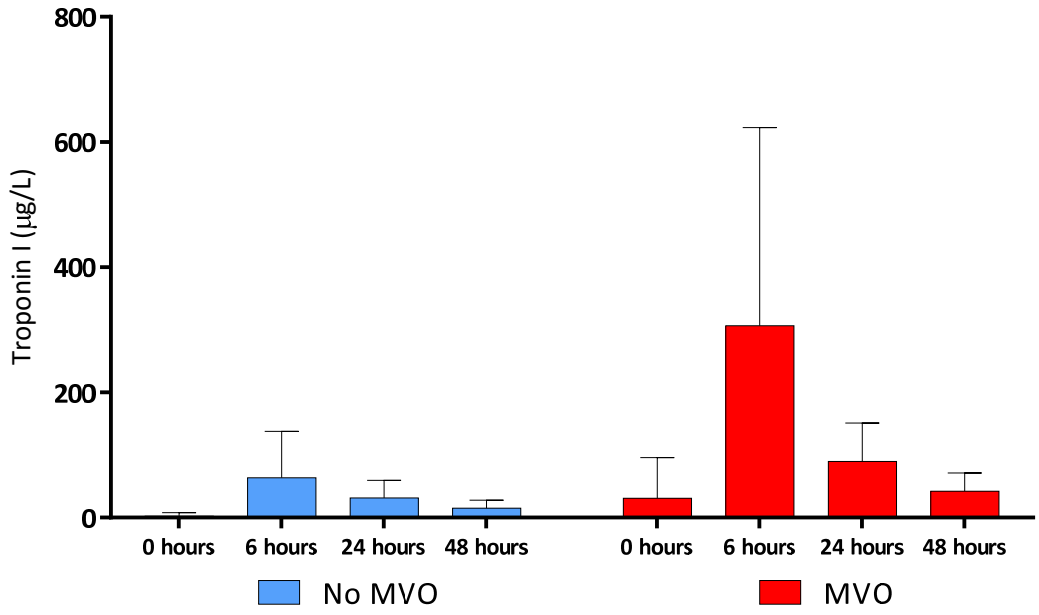

Figure 9: Troponin-I release and microvascular obstruction.
The troponin-I results at four time-points (0, 6, 24 and 48 hours) for all patients with no microvascular obstruction (shown in blue, n=49) and with microvascular obstruction (red, n=92) are shown. Bars show mean, error bars show standard deviation. Troponin-I was measured in µg/L. MVO=microvascular obstruction.

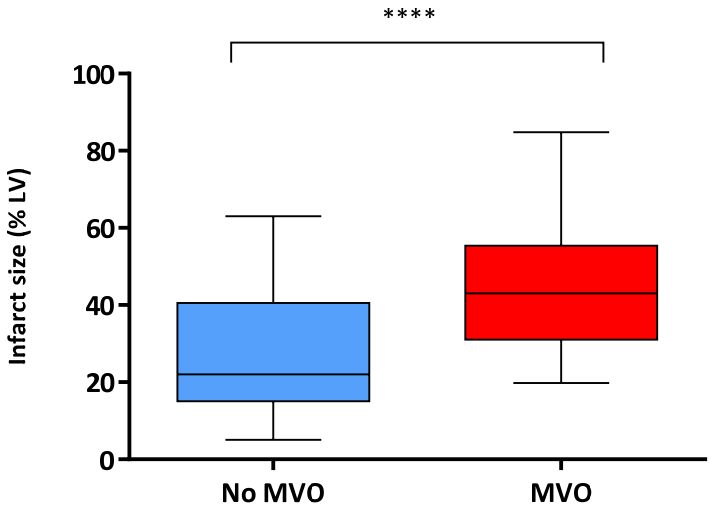

Figure 10: Microvascular obstruction and infarct size.
Infarct size measured at six-month cardiac MRI is shown in patients with MVO (in red, n=39) and without (blue, n=36). Box shows 25th-75th centiles, line represents median, whiskers represent range. A Mann-Witney test confirmed patients with MVO had larger infarcts than patients with no MVO (p=<0.0001). MVO=microvascular obstruction.

8.3.4 ECG Changes Predicting Outcome

ECG analysis was carried out on the post-procedure ECG, recorded a median of 93 minutes after hospital arrival. Patients were grouped by residual ST elevation in the worst affected lead, and shown with final infarct size measured at six months. Patients with more than 2mm of residual ST elevation had larger infarcts than those with less than 1mm or 1-2mm of residual ST elevation (Figure 11).

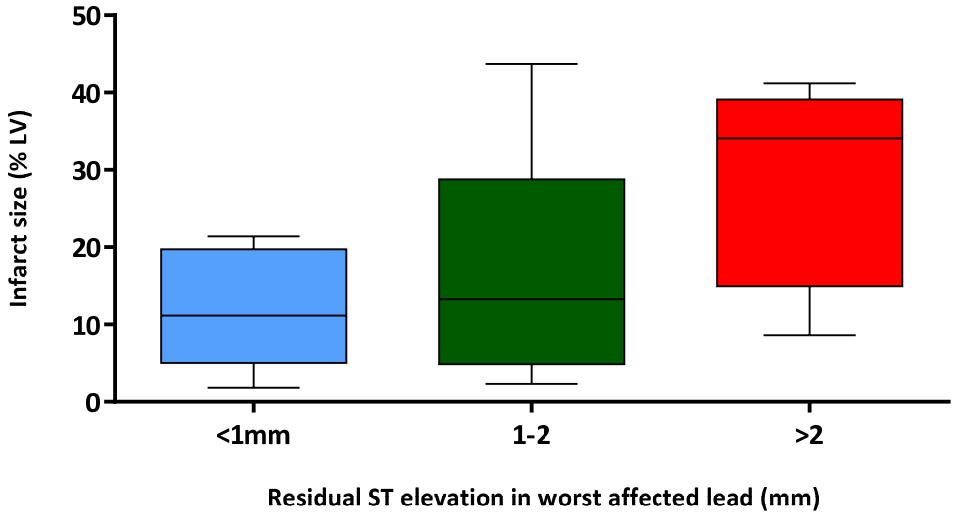

Figure 11: Post-procedure ECG prediction of final infarct size.
ECGs were recorded a median of 93 minutes after hospital arrival, were analysed retrospectively using ImageJ (National Institutes for Health, Bethesda, MA, USA) to measure residual ST elevation in the worst affected lead, which was measured 40ms after the end of the QRS complex. ECGs in patients with LBBB, paced rhythm or ventricular rhythm were excluded from this analysis. The results showed a statistically significant difference in ST elevation between the infarct size groups (Kruskal-Wallis, p=0.0081).

9 MicroRNA analysis

9.1 Introduction

MicroRNA analysis is challenging for a number of reasons. Firstly, abundance is low in plasma so detection can be difficult. Secondly, RNAses are ubiquitous and contamination can reduce the amount of RNA isolated. The magnitude of this effect can be variable between miRs leading to the experimental bias. For these reasons, before analysing the OxAMI samples, which were of high scientific value, it was important to be confident of the efficiency and reproducibility of each stage of the microRNA analysis process, from RNA isolation to quantitative RT-PCR, so that results were reliable and reproducible.

This chapter outlines the evolution of the microRNA analysis protocol, and the optimisation of each experimental stage. Initially, healthy control samples were used for this work and then surplus aliquots from the first OxAMI patients recruited. Once the protocol was finalised, analysis of the OxAMI samples could begin.

9.2 Overview

The process of microRNA analysis took approximately seven hours, from collecting the sample to generating quantitative data. Figure 12 outlines the steps involved.

First, the sample was collected from the patient and centrifuged. Cell and platelet debris have their own distinct microRNA signature so it was important to remove these from a plasma sample prior to analysis. Samples were then separated into aliquots and frozen at -80^{o}C. RNA

isolation was carried out to separate the RNA material from the sample. Reverse transcription was used to generate complementary DNA (cDNA) from the isolated microRNA, which was required for the next stage of the process; additionally, cDNA is more stable for long-term storage than RNA. Quantitative real-time PCR was then carried out for quantification of microRNAs and controls. These experimental steps are discussed in more detail later in this chapter (page 69). Prior to analysis, the quality of the sample and efficiency of isolation is assessed. The sample was also normalised. Once these steps are complete, statistical analysis can be carried out.

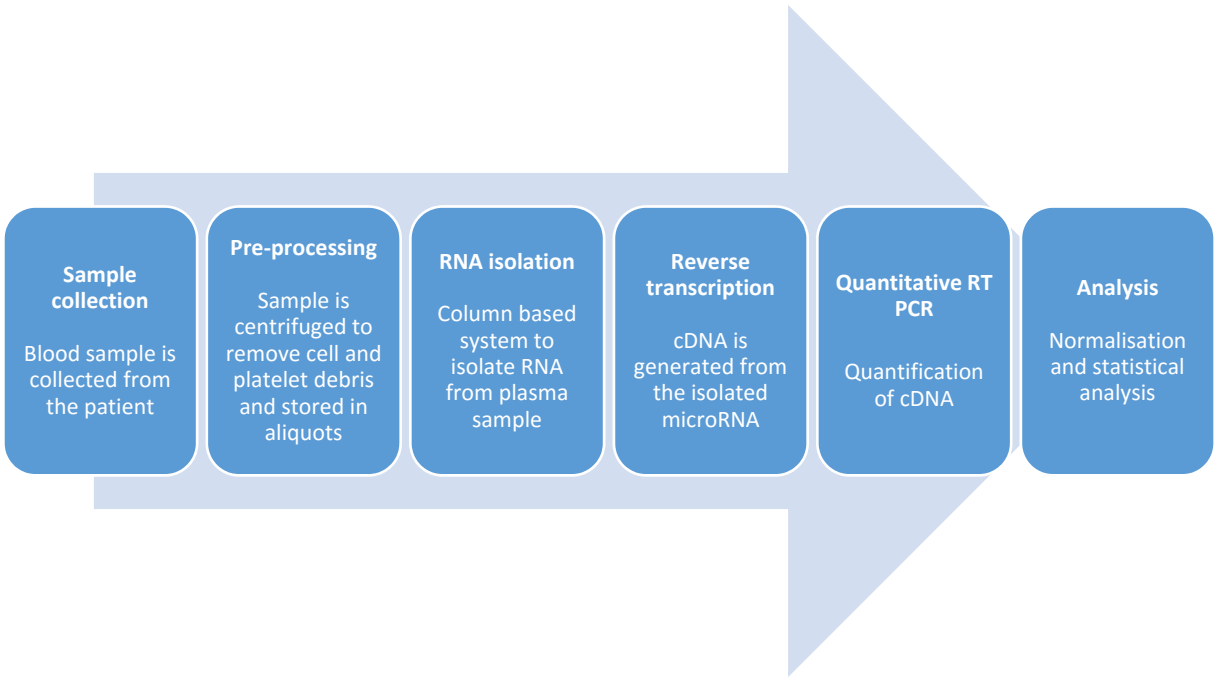

Figure 12: Overview of the microRNA processing protocol.

9.3 Sample and Data Management

Blood samples were collected and processed as described in the previous chapter (page 50). After processing, the aliquots from each patient were divided into two boxes and half of the aliquots for each time point and sample site were stored in separate boxes. The boxes were stored in -80^{o}C freezers, one in the laboratory and at a specialist sample storage facility offsite, to offer some protection in the event of a freezer failure.

The number of patients, sample sites and time points meant there was considerable risk of confusion while carrying out complex experimental protocols. For this reason, at the start of the experiment each aliquot to be analysed was given a unique four-digit identifier which was retained for the entire experiment. A spreadsheet was maintained to store the decode (Table 6). The number was allocated once the aliquot was checked for patient number, site and time point. Once the experiment was complete, the number was converted back to a patient ID, site and time point to allow analysis. This approach had the added benefit of blinding the investigator to the sample.

Additionally, each experiment was numbered and all data files generated (e.g. qPCR raw data) were named using a standardised naming convention, with date, experiment number and sample number. This ensured that experimental data were straightforward to locate and analyse at a later date.

Sample number	Patient ID	Time point	Site
1422	OxAMI01-00038	1.3	Coronary artery
1423	OxAMI01-00038	1.3	Coronary sinus
1424	OxAMI01-00039	1.3	Coronary artery
1425	OxAMI01-00039	1.3	Coronary sinus
1426	OxAMI01-00042	1.3	Coronary artery
1427	OxAMI01-00042	1.3	Coronary sinus

Table 6: Excerpt from the sample number spreadsheet.
Each sample was allocated a unique four-digit identifier to allow for rapid labelling and to reduce the risk of errors. The description of the time points is shown in Table 3 (page 49).

All experimental data were backed up live using an online file hosting service. Ten previous versions of every file were also stored so that unintentional errors and deletions could be easily restored. All experimental files were backed up onto a secure external hard disk weekly, and ten complete backups (i.e. ten weeks) were kept at all times. No identifiable patient data were stored on this system. On the occasions that identifiable patient data were used (e.g. to find a clinical blood result) these data were retrieved and analysed on an NHS computer and transferred to the OxAMI server in with patient identifiable data removed.

9.4 MicroRNA Controls

The next phase of experimentation concerned the design of the experimental protocol for microRNA analysis. There were multiple steps to this process and it was important to optimise each step. While many aspects of microRNA analysis are similar regardless of the source of microRNA (tissue, plasma, serum) because of the many variables in any experiment and the inherent difficulty in miR analysis, the efficiency and reproducibility of any technique needed to be re-assessed with each new experiment.

In messenger RNA work, the efficiency of RNA isolation can be assessed using a spectrophotometer to quantify the amount of RNA isolated. Unfortunately, the RNA concentration in microRNA analysis is below the level of detection for this technology so other methods need to be used. Therefore, multiple controls were used to confirm the efficiency of each step of microRNA isolation.

UniSP2, *UniSP4* and *UniSP5* are synthetic microRNAs which were spiked into plasma after lysis. They were added in reducing concentrations: 100, 10 and 1 fold respectively which allowed an assessment of the efficiency of RNA isolation over the full spectrum of miR concentration.

UniSP6 is a synthetic RNA which was added to the isolated RNA prior to reverse transcription to assess the reliability of this step. Another common spike-in control, *Cel-miR-39*, which is derived from the *Caenorhabditis elegans* roundworm, was also added at this stage. *UniSP3* is a synthetic cDNA which was added to the PCR master mix.

The above spike-in controls assessed the efficiency of each experimental step, but they do not provide information on the quality of the plasma sample. Many microRNAs are ubiquitous in human plasma and these were used as positive controls to confirm that these microRNAs in the plasma sample were not degraded (*miR-1*03 and *-191*).

9.5 Optimal Experimental Parameters

Silica column based RNA isolation was chosen for the practical benefits of working with silica columns rather than TRIzol and the large body of evidence confirming the efficiency and reproducibility of this method of RNA isolation[79,92].

In plasma samples, the amount of miR present is too small to be accurately measured. For this reason, a set volume of plasma, rather than an amount of RNA, was used for each analysis. The optimum plasma volume for RNA isolation was unknown. Therefore, RNA isolation, reverse transcription and PCR were carried out with different input plasma volumes to determine the optimum volume. It may be expected that an increased plasma volume would be associated with increased yield, but it is well known that with increasing RNA amount there may be

associated with an increased amount of RNA inhibitors and therefore, paradoxically, a smaller volume may provide a higher yield.

Figure 13 shows the effect of different input volumes on microRNA detection by PCR. At 50-100µL the ability to detect both spike in controls and ubiquitous human miRs was reduced and at 400µL it was likely that the presence of inhibitors has resulted in reduced microRNA detection. The optimum volume (dashed red line) was therefore 200µL.

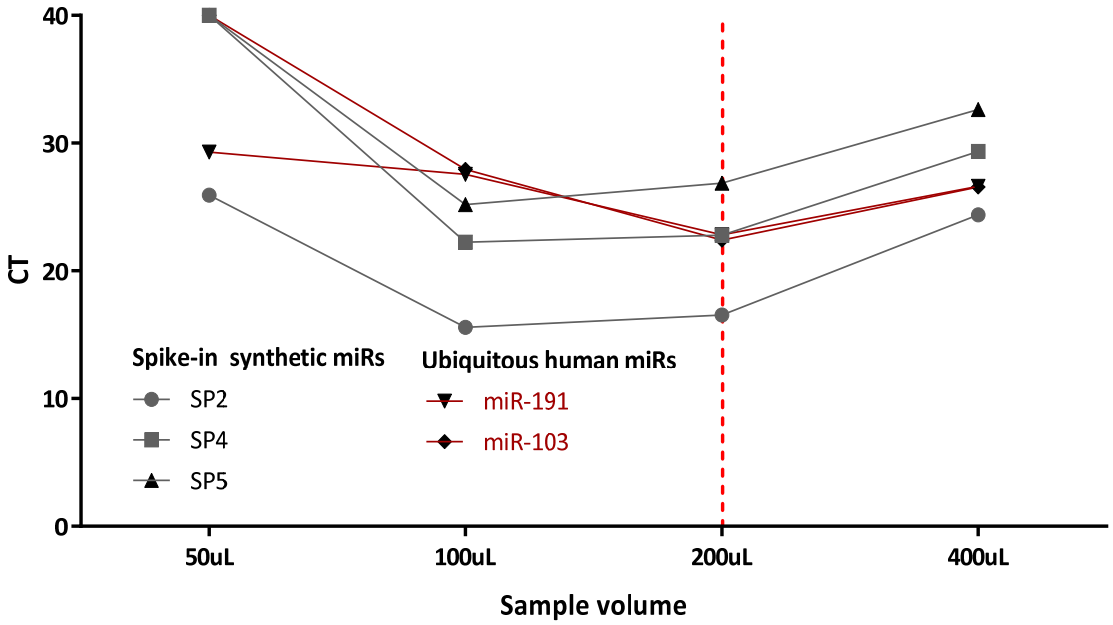

Figure 13: Determining the optimum sample volume in human plasma.
Different input volumes of platelet poor plasma (n=1 per sample volume tested) were used to determine the ideal sample volume. Levels of spike in miRs were measured (grey) and ubiquitous miRs (red). The optimum sample volume was confirmed as 200µL.

Biofluid samples contain very low concentrations of microRNA and there is therefore the risk of losing a significant amount of RNA during the isolation process. For this reason, many manufacturers recommend the use of a carrier protein such as *Bacteriophage MS2* or glycogen to increase yield and reduce experimental variation.

Figure 14 shows the effect of *MS2* carrier on spike-in and ubiquitous miRs detection. Where RNA isolation was carried out with *MS2* as carrier, RNA yield was improved (lower CT value) for both synthetic spike-in RNA and ubiquitous human miRs. Variation between duplicates was also reduced. Therefore, as *MS2* was shown to improve yield and reproducibility, it was thereafter routinely used for all RNA isolation.

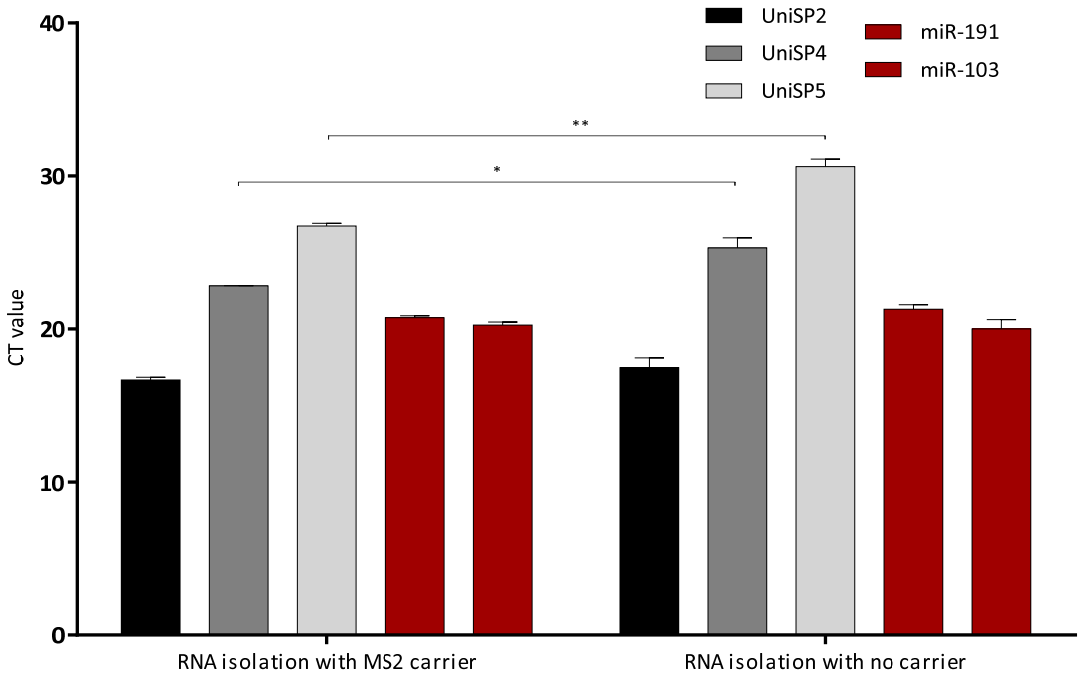

Figure 14: The effect of adding a carrier protein (Bacteriophage MS2, Roche) on RNA isolation. UniSP2/4/5 are synthetic spike-in RNAs, miR-191/103 are ubiquitous human miRs. Error bars show standard deviation. N=4 per group. Where unpaired t-testing revealed a statistically significant difference, this is shown (*=p≤0.05; **=p≤0.05).

Reverse transcription was carried out using miRCURY universal cDNA synthesis kit II (*Exiqon*) according to the manufacturer's protocol. *UniSP6* (a synthetic small RNA) and cel-miR-39-3p were spiked in to the master mix to allow assessment of the efficiency of this stage of the

process. The optimum cDNA concentration for PCR was unknown and therefore a dilution series was carried using a plasma venous sample from a patient at the time of acute myocardial infarction (Figure 15). For the spike in RNAs (UniSP2/4/5/6 and *cel-miR-39*) increasing cDNA concentration resulted in increased detection (lower CT value). For plasma microRNAs (*miR-103, -191, -1, -133a, -126*) this effect was not seen, with no significant difference in CT values between the different cDNA dilutions. A pragmatic decision was therefore made to use the 1:50 cDNA dilution from this point, as a reasonable compromise between miR detection sensitivity and economising use of RNA. Using the 1:50 concentration allowed the option of a second experiment if the first failed, which was not the case if 1:25 concentration.

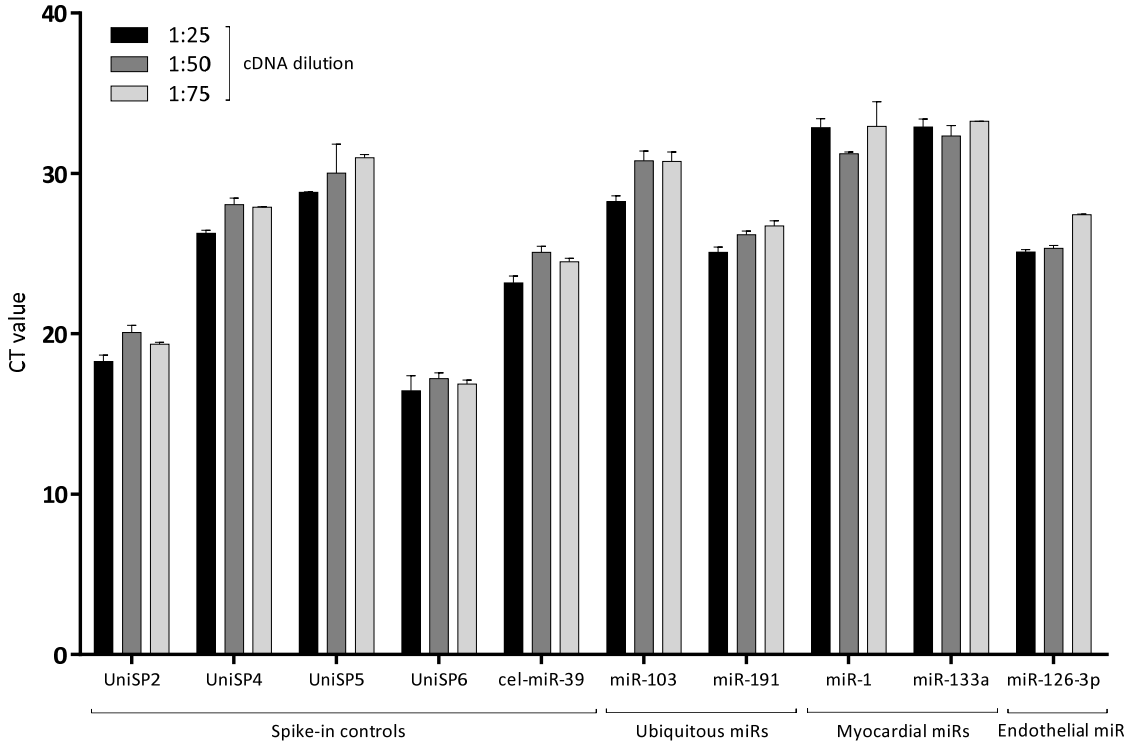

Figure 15: Dilution series to identify the optimum cDNA concentration for PCR.
RNA was isolated from a plasma venous sample from a patient at the time of acute myocardial infarction. Reverse transcription was carried out. Complementary DNA was diluted to three concentrations (1:25, 1:50 and 1:75, n=2 for each dilution). PCR was then carried out using these three cDNA dilutions to quantify multiple targets: RNA spike-in controls (UniSP2/4/5/6, cel-miR-39), ubiquitous biological positive controls (miR-103 and 191), myocardial miRs (miR-1 and -133a) and an endothelial miR (miR-126).

9.6 Quality Control

By this stage, a reliable and reproducible protocol for each of the stages of miR isolation and quantification had been developed. However, given the clinical challenges of collecting the samples, it was also important to be able to demonstrate experimental success or otherwise for each patient sample prior to analysis to reduce the risk of noise contaminating the results.

A thorough quality control process was therefore developed to assess each stage of the process using a dedicated 96-well plate which contained a well for each of the spike in controls, two positive controls and a red cell specific miR to identify haemolysed samples. The experimental algorithm is shown in Figure 16 and the quality control criteria are shown in Figure 17. If the QC criteria were achieved, the cDNA from that sample was then analysed using two 384-well plates containing 752 miRs (*Human Panels I + 2, version 3.M, Exiqon*). Statistical analysis was then used to determine changes in miR expression with clinical readouts (such as infarct size, troponin and microvascular function) and how these changes evolve over time.

The Quality Control parameters determining whether a sample 'passed' the quality control stage are shown in Figure 17. If a particular parameter was not achieved, then RT and PCR were repeated (RT is the most common source of quality control issues). If the sample still did not meet the pre-specified criteria, it was then excluded from analysis. If a sample was significantly haemolysed, either visually or by microRNA criteria then this was also excluded.

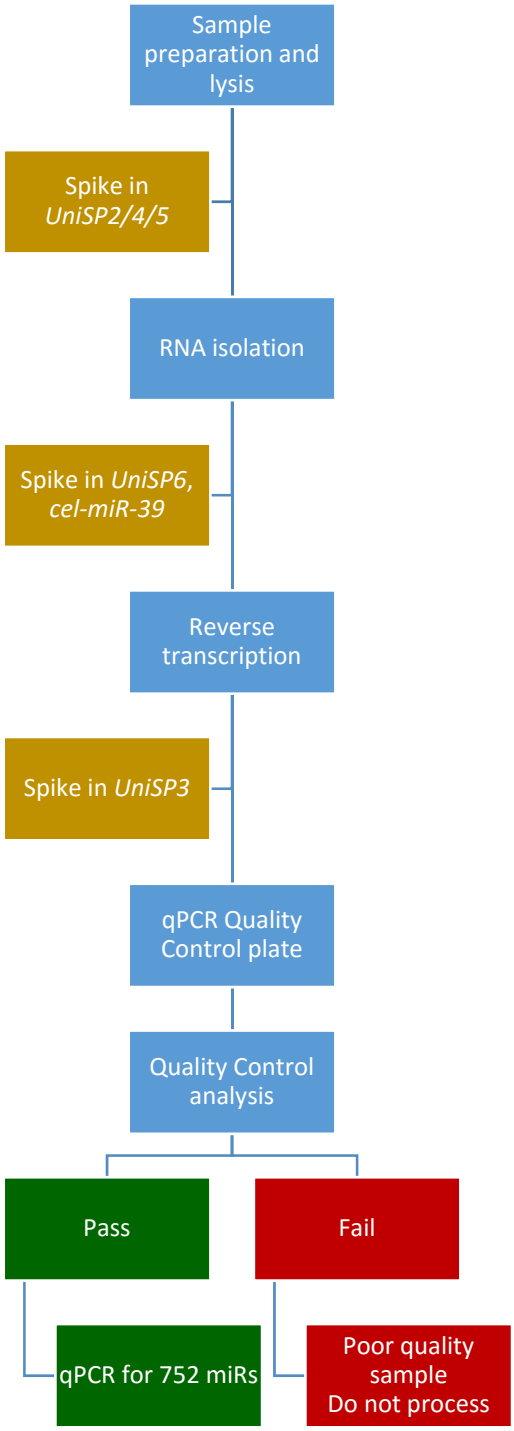

Figure 16: The Quality Control Process.
At each stage of the miR quantification process, control miRs are spiked in. These can then be analysed to measure the efficiency of each stage of the process. All plasma samples will undergo this analysis to determine sample quality and suitability for processing. Detailed miR analysis will then be carried out on samples that 'pass'. qPCR = quantitative real-time polymerase chain reaction; UniSPx = a synthetic miR; cel-miR-39 = C. Elegans miR 39.

	Parameter	Criteria	Action if not achieved
1	**RNA Isolation**	*UniSP2* and *UniSP4* should be detectible at CT values ≤37. CT values should be *SP2≤SP4*.	Exclude sample
2	**Reverse Transcription**	Both *UniSP6* and *cel-miR-39* should be detected at CT values ≤37.	Repeat RT and repeat PCR. If still not achieved, exclude sample
3	**PCR**	*UniSP3* CT value should be 18-22 across dataset	
5	**Positive controls**	Both positive controls (*miR-1*03 and *miR-191*) should be detected at CT values ≤37.	
4	**Haemolysis**	Significant haemolysis if ΔCT between *miR-23a* and *miR-451* ≥7	Exclude sample

Figure 17: Pre-specified quality control parameters.
At each stage of the miR analysis process, results were checked against these parameters. If a particular parameter was not achieved, then RT and PCR were repeated (RT is the most common source of quality control issues). If the sample still did not meet the pre-specified criteria, it was then excluded from analysis.

9.7 The microRNA Analysis Protocol

After these optimisation steps, the final microRNA analysis protocol was designed. The steps were as follows:

1. RNA isolation

   A dedicated RNAse free area was used. RNA was isolated using the column-based miRCURY RNA Isolation Kit for Biofluids (*Exiqon, Vedbaek, Denmark*) according to the manufacturer's protocol. Three synthetic miRs (*UniSP2*, *4* and *5*) at known concentrations (100, 10 and 1 fold respectively) were spiked in at the lysis step. *Bacteriophage MS2* (*Roche, Basel, Switzerland*) was added as a carrier RNA. For cell culture experiments, the miRCURY RNA Isolation Kit – Cell and Plant (*Exiqon, Vedbaek, Denmark*) was used. The spike-in controls were the same.

2. Reverse transcription

   A separate bench was used for all DNA work. Prior to reverse transcription, two spike-ins were introduced to assess the efficiency of this step. *UniSP6* (a synthetic small RNA) and

cel-miR-39-3p (a synthetic duplicate of a miR found in the *Caenorhabditis elegans* roundworm) were used for this purpose. Reverse transcription was carried out using the miRCURY universal cDNA synthesis kit II (*Exiqon*) according to the manufacturer's protocol.

3. Quantitative Real-Time PCR

Complementary DNA from the reverse transcription step was diluted to a 1:50 concentration. A PCR master mix was produced for each sample consisting of diluted cDNA, spike-in *UniSP3* (interplate calibrator/PCR control), ExiLENT SYBR Green (*Exiqon*) and ROX passive reference dye (*Life Technologies, Carlsbad, CA, USA*). 10µL was then pipetted into each well on the PCR plate.

9.8 Data Analysis

There is wide variation in the literature on the pre-processing steps taken on microRNA data before any statistical analysis is carried out, and these steps are frequently not reported in manuscripts. Additionally, the handling of missing data is highly variable, with some groups excluding entire samples or targets due to missing data and others imputing missing data using a variety of methods. These factors make it more challenging for other labs to scrutinise data and attempt to reproduce it. I have therefore developed the following process with the aim of excluding poor quality data based on pre-specified quality control parameters.

Before carrying out data analysis, the following pre-processing steps were carried out:

- Exclude CT values ≥38: Above this value, qPCR results are unreliable and inconsistent and reflect very low levels of detectable miR.
- Data normalisation is required to minimise the technical and experimental variation between samples. There are various methods commonly used to normalise miR data[93]. Initial analyses were carried out using reference genes identified using *Normfinder*[85] (*Moma Department of Molecular Medicine, Aarhus, Denmark*); the final analysis will be carried out using a global mean approach.

10 MicroRNA release in STEMI: Discovery

10.1 Introduction

The aim of this series of experiments was to describe patterns of microRNA release in patients with ST elevation myocardial infarction. While this field has been studied in the past, much of the existing research uses small groups of patients with focused, candidate based microRNA measurement rather than broad unbiased analysis[60,94,95].

Existing work has focused on microRNAs as biomarkers of myocardial injury with emphasis on identifying microRNAs that correlate with troponin and myocardial injury[94–100]. I aimed to validate this work, and to identify new relationships not only with myocardial injury but also with less well studied parameters, such as microvascular obstruction.

I carried out a detailed analysis of a cohort of patients presenting with STEMI, quantifying microRNA release in relation to multiple clinical parameters, such as ECG changes, biochemical markers, and cardiac MRI measurements. Plasma was isolated from samples of venous blood from patients during acute myocardial infarction and at multiple time points thereafter. I then analysed plasma microRNA using a quantitative real-time PCR array.

For the first six patients I analysed blood samples at all time points to identify which was likely to be the optimum time point to analyse with a larger cohort, based on technical and biological parameters. I then carried out a detailed microRNA analysis in the remainder of the patients at this single time point. These patients form the Discovery Experiment. A second larger cohort was

then recruited to validate these findings and this is discussed in the next chapter. The broad experimental plan is shown in Figure 18.

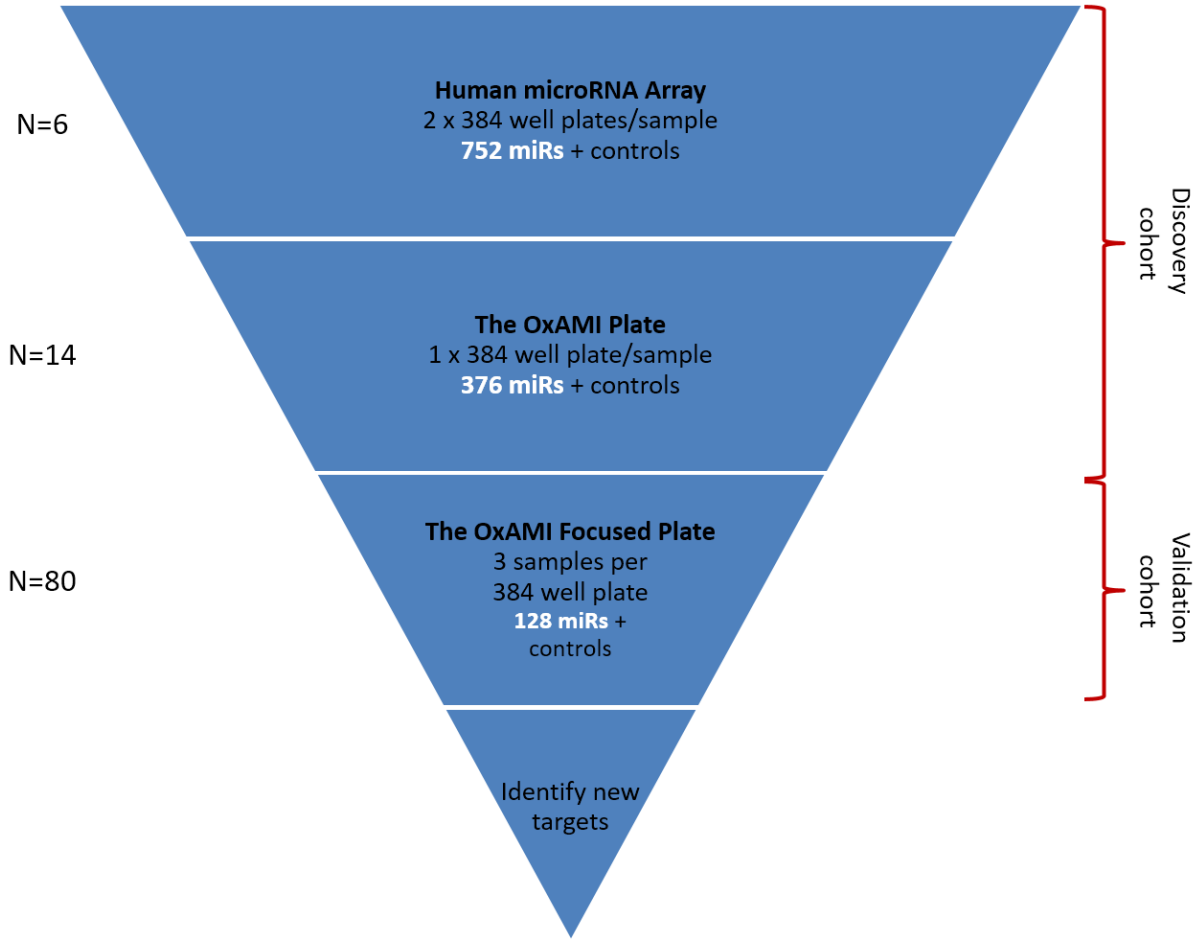

Figure 18: MicroRNA analysis in STEMI experimental design.
A pilot study of was carried out measuring 752 miRs and controls in six patients at four time-points to identify which time-point to use for the wider analysis, and to catalogue which miRs were detected in venous plasma samples in the STEMI population. The OxAMI plate was designed based on these findings, and the results of the endothelial cell culture experiment. Samples for a further 14 patients were analysed using the OxAMI plate and results (n=20) were combined to make the Discovery Experiment. To validate these findings, a further 80 patients were analysed using the OxAMI-focused plate, with a smaller number of targets (128 miRs and controls for each sample), allowing increased throughput.

10.2 Methods

Experimental Design

The experiment was carried out in two phases. Initially, microRNA analysis was carried out for six patients at four time-points (0, 6, 24 and 48 hours) using a comprehensive human microRNA array (Two 384-well plates - *Human Panels I + 2,* version 3.M, *Exiqon*). The aim was to identify which time-point should be used for the larger analysis, based on number of miRs detected, quality control measures and initial analysis of differential expression of microRNAs in relation to different clinical parameters.

It was anticipated that not all miRs on the panel would be detected in all samples, and therefore a secondary aim was to produce a list of miRs reliably detected in patients with STEMI to guide the design of a single 384-well plate, 'The OxAMI Plate', which could then be used for the analysis of further samples. A literature search and early results from the endothelial cell culture experiment (Chapter 11, page 121) were also used to identify miRs to be included on the OxAMI plate (Figure 19). This would allow one sample to be analysed per plate, doubling throughput compared with the two plate array.

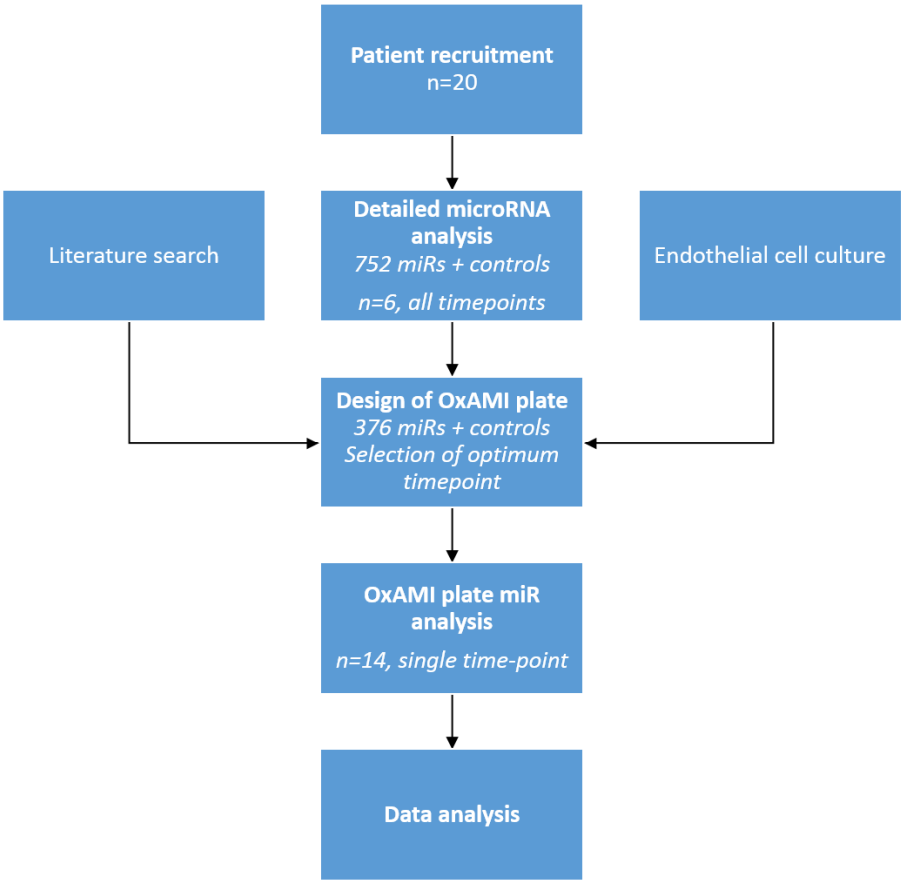

Figure 19: Experimental design for the Discovery Experiment.
20 patients were recruited to this cohort. Comprehensive microRNA analysis of plasma venous samples at four time-points was carried out on six patients which determined the optimum time point for further analysis. These initial results, combined with literature search and endothelial cell culture data determined the design of the OxAMI plate. MicroRNA analysis on samples from the next 16 patients was then carried out using the OxAMI plate.

Results from the Discovery Experiment were used to design of 'The OxAMI Focused Plate', which will have multiple samples per plate and this will be used to validate the findings from this experiment using a larger cohort of patients (Chapter 12, page 148).

Patient Recruitment

Patients were recruited to this part of the study using the criteria and protocols defined in the Patient Recruitment section (page 46). In order to be included, patients were required to have a

two MRI scans (at 48 hours and six months) and venous blood sample (serum and plasma) collection at 0, 6, 24 and 48 hours after hospital arrival.

MicroRNA Analysis and Quality Control

RNA isolation and reverse transcription were carried out according to the protocols in the MicroRNA analysis chapter (page 65). A 96-well plate was used to assess several quality control parameters in all samples prior to more detailed analysis. The plate design included wells for each spike-in, two miRs that are ubiquitous in human plasma and a red cell specific miR to identify haemolysed samples (Table 7).

Target	Description
miR-103 *miR-191*	Ubiquitous plasma miR (positive control)
miR-451 *miR-23a*	Haemolysis detection
UniSP2/4/5	RNA isolation spike-in
UniSP6 *Cel-miR-39*	Reverse transcription spike-in
UniSP3	PCR spike-in

Table 7: miRs used for quality control plate design.
miRs-103 and -191 are ubiquitous in human plasma samples and were used as a positive control. miR-451 is a red blood cell specific miR and signifies haemolysis if detected in plasma samples. miR-23a is detectable in plasma only and a miR-451:miR-23a ratio can be used to quantify haemolysis. UniSP2/4/5 are synthetic RNA spike-ins at differing concentrations (100/10/1 fold respectively) used to confirm efficient RNA isolation. UniSP6 and cel-miR-39 are reverse transcription spike-ins. UniSP3 is a spike-in added at the PCR stage.

The Quality Control plate was used to prospectively assess each sample before committing to carrying out a wider array analysis. Six patients with no quality control issues at any time point were then selected for analysis using the two-plate microRNA array.

Time-point Selection

The following parameters were used to select the optimum time point:

1. Sample quality

   The Quality Control plate results for all samples were analysed to identify whether a particular time point more commonly failed QC. For example, it might be anticipated that samples collected in the emergency setting of primary PCI may be more prone to technical deficiencies as opposed to samples collected in the more controlled ward environment at 6, 24 or 48 hours.

2. MicroRNA detection

   The absolute number of microRNAs detected at each time point in the six patients who underwent detailed microRNA analysis was compared to establish whether more miRs were detected at a particular time point. The mean CT value for all detected microRNAs in each sample was calculated to establish whether microRNAs were detected at higher levels at a particular time point. The acute inflammatory stimulus of myocardial infarction may increase both the number of detectible microRNAs and also the levels (CT values) of the microRNAs that are detected. This is important to establish both to identify the optimum time point and because it may have implications for normalisation.

3. Myocardial microRNA release

   MicroRNA release was measured at each time point to identify when the miR signal peaks. Levels of known myocardial miRs were plotted against troponin, the most commonly used clinical biomarker of myocardial necrosis.

The OxAMI Plate

The two-plate detailed microRNA analysis was both labour intensive and costly, and a large number of analysed miRs were not detected in any samples. It was therefore felt that reducing the analysis to one 384-well plate (the OxAMI-plate) would be reasonable. The method for selecting miRs for inclusion in the OxAMI plate was as follows:

1. Identifying miRs that are frequently detected

   If a microRNA was detected in >30% of samples analysed using the two plate process then it was included in the OxAMI plate design. If a miR was not detected in any sample, it was not included unless its importance in myocardial infarction had been previously published.

2. Literature search

   A literature search was carried out to identify microRNAs that have been reported in the myocardial infarction and ischaemia-reperfusion literature (Table 8). These were included in the OxAMI plate design, even if they were not detected in any sample as demonstrating their absence may be an important finding.

MiRs associated with myocardial infarction incorporated in OxAMI plate design
miR-1, miR-122, miR-133a, miR-133b, miR-145, miR-15, miR-155, miR-155, miR-195, miR-208b, miR-21, miR-24, miR-29, miR-30a, miR-30c, miR-320, miR-33, miR-494, miR-499

Table 8: MicroRNAs reported in the myocardial infarction and ischaemia-reperfusion literature[70–72,74,94,101–114].

3. Endothelial cell culture experiments

In parallel with this experiment, an in-vitro series of experiments was being carried out using endothelial cells in culture (see MicroRNA Release in Endothelial Cells, page 121). MiRs detected in the endothelial cell culture experiments were also included in the OxAMI plate design.

4. Controls

   Wells to detect the control spike-ins were included in the plate design. Additionally, two ubiquitous miRs were used as positive controls (*miR-103* and *-191*) and a non-template control well was included to detect sample contamination.

Once the OxAMI plate had been designed, this was used for microRNA analysis for the remainder of the samples (n=14) at the selected time point.

Data Pre-Processing

There is considerable variability in the way microRNA analysis data is processed in the literature. I adopted an approach designed to minimise manipulation of the data prior to analysis and to only use imputation of missing values where the chosen statistical test necessitates it. Where imputation was used, this was made clear in the text. The routine data pre-processing steps were as follows:

1. Data export

   Raw data were reviewed on the PCR Cycler (*QuantStudio™ 7 Flex Real-Time PCR System, ThermoFisher Scientific, Waltham, MA USA*) to ensure PCR had completed successfully, specifically that the controls and ubiquitous miRs were detected and that the melt curve morphology was as expected. The raw data were then exported as a comma delimited CSV file.

2. Quality control

Sample quality and experimental efficiency was assessed using the quality control algorithm (page 73). If the quality control parameters were not achieved, the results for that sample were excluded.

3. Data merge

   Raw data CSV files for each plate were merged into a single Excel (*Microsoft Corporation, Seattle, WA USA*) spreadsheet. The initial analysis of samples undergoing detailed miR analysis was straightforward as all samples were analysed on plates with the same layout. Raw data from all samples was merged into one worksheet with the CT values for one sample per column.

   The second phase of analysis (detailed microRNA analysis and OxAMI plate samples) was more complex due to the differing plate designs in the two groups. Briefly, all detailed miR analysis samples were merged into one worksheet and all OxAMI plate samples into another. A third worksheet was then used, in conjunction with the =VLOOKUP function to map data from all samples onto the OxAMI plate layout. The =EXACT function was used to check for errors in data transcription.

4. Normalisation

   At this stage the merged data that had passed the quality control step was imported into Genex (*MultiD, Göteborg, Sweden*) for further processing and normalisation.

Normalisation

Global mean normalisation was used for analysis of the Discovery Experiment. This was an appropriate normalisation method to use as there was a sufficiently large number of miRs in the

dataset and the OxAMI plate design only selected miRs on the basis of presence or absence rather than differential expression. In the Validation phase of the experiment in the next chapter, a more focused approach was used with a smaller number of miR targets. For this reason, global mean normalisation would not have been appropriate and therefore at this stage an alternative method for data normalisation needed to be found. The performance of global mean normalisation was compared with reference gene normalisation, using the *Normfinder* algorithm to identify potential reference genes, and spike-in normalisation which is commonly used in the microRNA literature.

The following analyses were carried out to compare the different normalisation strategies:

1. Global mean normalised CT values of known myomiRs were compared with the same miRs normalised using *Normfinder*-identified reference genes.
2. A similar analysis was carried out with miRs that were highly expressed and those at the limits of detection
3. Spike in normalisation with *cel-miR-39* and *UniSP2* was compared with global mean normalisation as shown in step 1 and 2 above.
4. For each normalisation method a Spearman correlation matrix was created to analyse the relationship between miRs and clinical parameters. Relationships identified between miRs and different clinical parameters were then compared using each normalisation method.

Data Analysis

The aims for data analysis of the Discovery Experiment were as follows:

1. Evaluate established miR relationships

Correlations between known myocardial miRs and existing biomarkers such as infarct size and troponin were assessed, and compared with the existing publications on the subject, as part of validation of the experimental protocol.

2. Examine correlation relationships with other clinical parameters

   A correlation matrix was generated to examine the relationship between microRNA release and the clinical parameters of each patient using SPSS version 23.0 (*IBM Corporation, Armonk, NY USA*). The relationship between miR release and the different clinical parameters was then assessed.

10.3 Results

Patient recruitment

Twenty patients were recruited between June 2012 and June 2013. Clinical parameters are shown in Table 9. As would be expected from a STEMI cohort, patients are predominantly male and in their seventh decade. Prevalence of smoking and renal impairment was similar to that seen in the hospital STEMI population, as was the length of hospital stay. The prevalence of diabetes was lower than would be expected in this group.

Time point selection

It would be impractical to carry out microRNA analysis at all time points in all patients with a patient group of this size, so the next phase of the experiment focused on identifying which time point to use. There were two factors to consider in this decision – which time point had the

highest quality samples, and which time point was likely to provide the most biological information.

Gender n (%)	
Male	15 (75.0)
Female	5 (25.0)
TOTAL	20

Age	
Median	65
Range	42-80

Diabetes n (%)	
Oral medication	0 (0)
Insulin	0 (0)
New diagnosis	0 (0)
TOTAL	0 (0)

Smoking n (%)	
Current	3 (15.0)
Ex	7 (35.0)
Never	10(50.0)

Creatinine (µmol/L)	
Median	82.0
Range	58.0-134.0

Culprit vessel n (%)	
LAD	10 (50.0)
Circumflex	1 (5.0)
RCA	9 (45.0)

Troponin-I (µg/L)	
Peak (median)	71.0
Peak (range)	7.6-847.2
AUC 0-48h (median)	1888.0
AUC 0-48h (range)	272.8-17201.0

Infarct size (g)	
Median	15.0
Range	2.3-43.7

LV ejection fraction at 6 months %	
Median	57.0
Range	35.1-69.6

Total hospital stay (days)	
Median	2.0
Range	1.2-6.4

Table 9: Discovery Experiment baseline patient characteristics for all patients recruited to the OxAMI microRNA substudy.
20 patients were recruited over 12 months. LAD=left anterior descending, RCA=Right coronary artery. Troponin-I AUC=area under the curve of four troponin-I measurements taken at 0/6/24/48 hours (µg/L) calculated using the trapezoid rule. Infarct size and ejection fraction are measured at the six month MRI scan. Infarct size is measured as late gadolinium enhancement.

Sample quality

To assess which time point had the highest quality samples, all 20 samples underwent RNA isolation and reverse transcription at all four time points. The samples were then analysed using the QC plate. Results for each QC parameter are shown in Table 10.

Six samples from each time point which had passed each stage of the QC assessment were then selected for comprehensive microRNA analysis (two 384-well plates – 752 microRNAs and controls).

	Parameter	Criteria	Time point (hours) 0	6	24	48
	Starting number of samples		20	20	20	20
1	RNA Isolation	*UniSP2/4/5 should be detectible at CT values ≤37 CT values should be SP2≤SP4≤SP5*	17	19	19	19
2	Reverse Transcription	*Both UniSP6 and cel-miR-39 should be detected*	18	20	20	19
3	PCR	*UniSP3 CT value should be 18-22 across dataset*	18	20	20	20
4	Positive controls	*Both positive controls (miR-103 and miR-191) should be detected*	18	20	20	20
5	Haemolysis	*Sample excluded if visibly haemolysed. Also excluded if ΔCT between miR-23a and miR-451 ≥7*	19	20	19	20
	TOTAL	*Number of samples passing all QC steps (%)*	16 (80)	19 (95)	18 (90)	18 (90)

Table 10: Quality control results for the first six patients analysed in the Discovery Experiment at four time-points (0, 4, 24 and 48 hours) after the start of the primary PCI procedure.
At each stage of the microRNA isolation and analysis process, the number of samples successfully reaching the pre-specified quality control criteria are shown. The Total row shows the number of samples successfully achieving all of the quality control criteria (percentages in brackets).

MicroRNA Detection

Once sample quality and microRNA isolation efficiency were confirmed, it was then important to assess the ability of a technique to detect microRNAs across the miRnome, and to determine whether the number of detected miRs was affected by the time point. While variations in detection between each time point may have had a biological rather than technical cause, it was important to ensure that no time point was associated with particularly low miR detection. Figure 20 illustrates the number of microRNAs detected at each time point using a cut-off of 37 cycles. A one-way repeated measures ANOVA was conducted to determine whether there was a statistically significant difference in the number of miRs detected at each time point. Although the number of miRs detected is lower when a cut-off is used, there is no statistically significant difference in the absolute number of miRs detected between each time point with or without a cut-off.

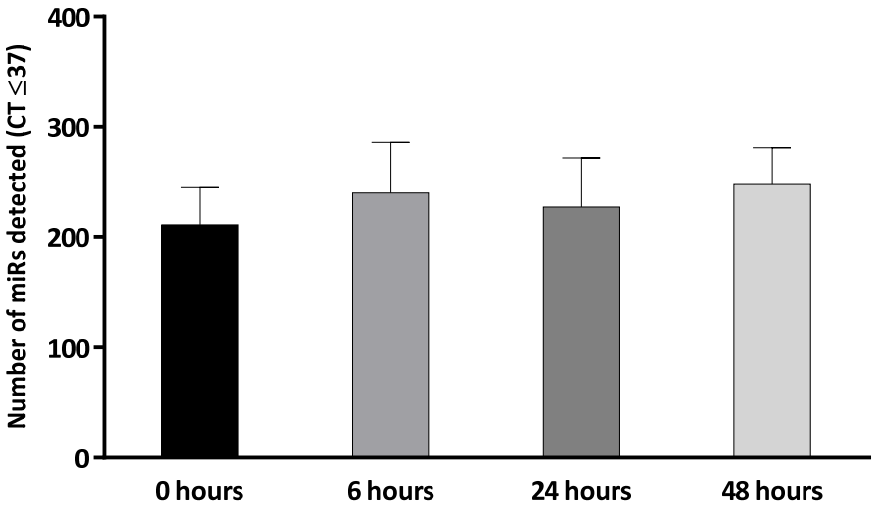

Figure 20: The absolute number of microRNAs detected at each time point with a CT value ≤37.
Each bar represents the mean of six samples (error bars show standard deviation). A one-way repeated measures ANOVA showed there was no statistically significant difference in the number of miRs detected between the four time-points. All miR analysis was carried out on two 384-well plates with wells for 752 unique miRs.

The mean CT value of all detected microRNAs in each sample was calculated and is shown in Figure 21. There was no significant difference in the mean CT value between the different time points using a one-way repeated measures ANOVA.

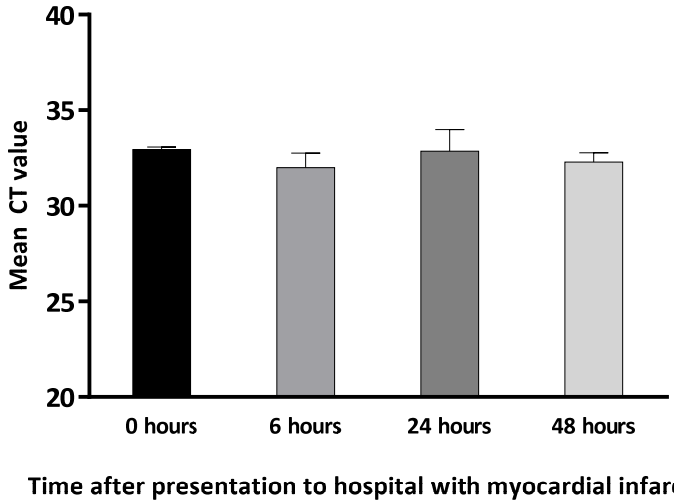

Figure 21: Mean microRNA detection with time after presentation with myocardial infarction (n=6 for each time point).
The geometric mean cycle threshold (CT) value was calculated for all miRs in all samples at each time-point. Raw (not normalised) CT values were used. Each bar shows the mean for six samples and the error bars show standard deviation. A one-way repeated measures ANOVA showed there was no statistically significant difference in miR expression between the four time-points.

Myocardial MicroRNA Release

Troponin is known to peak 6-12 hours after onset of chest pain. Less is known about the peak miR signal though existing publications suggest a similar pattern to troponin, albeit with an earlier peak (ref). Two patients, one with a small infarct and one with a large infarct, were selected to study the time course of miR release in comparison with troponin release (Figure 22).

The ΔΔCT method is a method for relative quantification in qPCR experiments, where relative expression of a miR is expressed as relative change to a control miR, which can be presented as fold change[115]. These results show that, like troponin, the magnitude of myocardial microRNA change relates to final infarct size, most dramatically shown with *miR-133a* which peaks with

approximately a 2000-fold increase in a large infarct compared with a 100-fold increase in the patient with a small infarct. In the small infarct, all miRs peak at six hours. In the large infarct all miRs peak at six hours except *miR-1* which peaks earlier at 0 hours.

Statistical Power

While it would seem an appealing prospect to analyse the entire miRnome for every sample, the statistical requirements of this approach would require sample numbers in the hundreds or even thousands to ensure adequate power. Initial screening to identify miRs of interest with subsequent analysis of a smaller subset of miRs in a larger number of samples is a reasonable compromise to ensure new miR signals can be identified and are statistically meaningful. A limitation in this work, and in the miR field in general, is that sample size and power calculations are difficult due to a lack of standardisation in experimental methods, normalisation or units of measurement. For the purposes of gaining an understanding of the number of samples required to detect a clinically important difference a power calculation was carried out using the Discovery Cohort data. It would seem reasonable to expect to detect a difference of 1 cycle threshold in a myocardial miR. The standard deviation for miR-1 in the Discovery Cohort was 1.91, with a normalised mean of 4.0. To detect a 1 cycle threshold difference with 80% power and a significance of 0.05, 16 samples would be required.

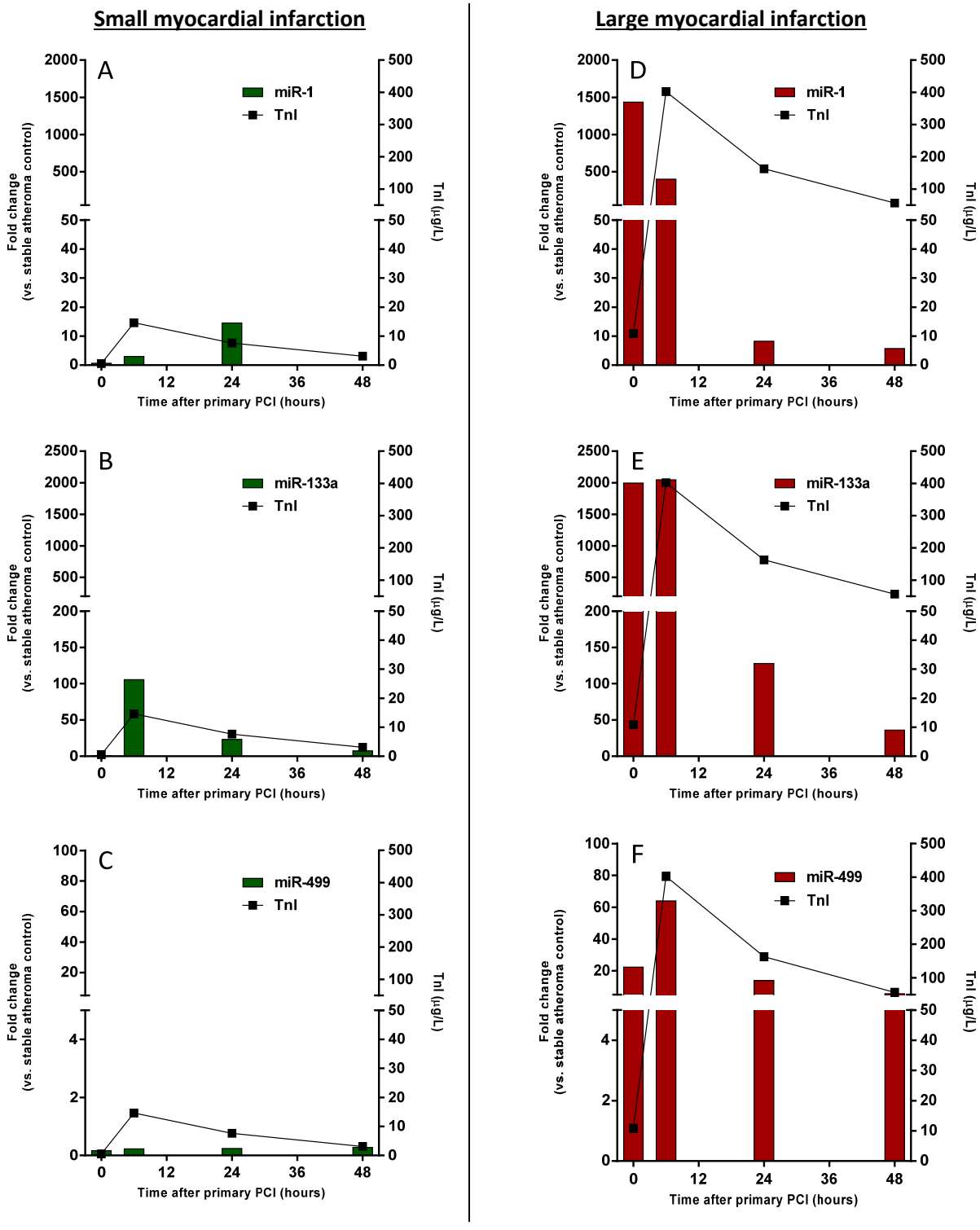

	Culprit vessel	Peak troponin	Troponin AUC (0-48 hours)	Infarct size (% LV)
Small infarct	LAD	14.6	45.7	4.4%
Large infarct	LAD	402.2	1239.0	38.7%

Figure 22: Expression of known myocardial miRs in two patients with ST elevation myocardial infarction.

Panels A/B/C show miR release in a patient with a small myocardial infarction, final infarct size 4.4% (coloured bar, left axis) and troponin-I release (black line, right axis). Panels D/E/F show the same

miRs and troponin-I release in a patient with a large myocardial infarction, final infarct size: 39.0%. TnI: troponin-I. Fold change values were calculated using the ΔΔCT method with a stable atheroma control (venous blood samples from a patient undergoing coronary angiography with visible atheroma but no flow-limiting coronary artery disease).

The OxAMI Plate

The above findings relating to sample quality, miR detection and likely peak miR release led to the six-hour time point being chosen as the optimum time point for further analysis. A further four patients underwent detailed miR analysis using two plates at the six-hour time point. The amalgamated results from these first ten patients were then used to aid design of the OxAMI plate. The intention was to reduce the number of miR analysed to less than 384 to allow a sample to be analysed on a single plate.

The combined miR results were analysed to identify the number of miRs detected in each sample. Figure 23 shows miR detection frequency. The majority of miRs were detected in fewer than half of all samples; 262 miRs are detected in at least 70% of samples.

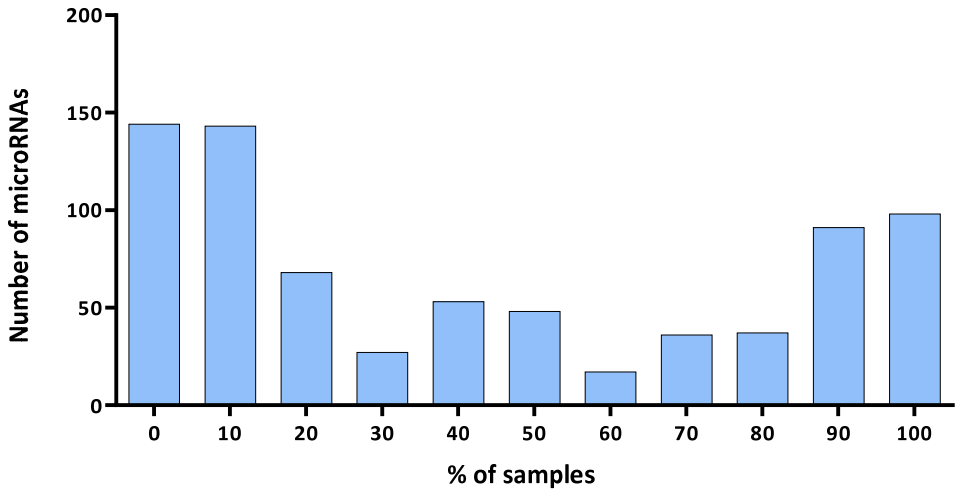

Figure 23: Frequency distribution histogram illustrating mIR detection in the detailed miR analysis of the first ten patients.

The percentage of samples that each miR was detected in was calculated. A frequency distribution was then created with this data with 10 equal sized bins spanning 100% of samples. Each bar represents the number of miRs detected in that bin i.e. 98 miRs are detected in all samples, 144 miRs are detected in no samples.

To identify important miRs to include in the OxAMI plate based on previously published studies, a PubMed search was carried out up to 28th February 2015. The word microRNA and any of the search terms myocardial infarction, myomiR, cardiac, vascular and endothelial were used to identify relevant studies, which were included if they were human studies with myocardial infarction or infarct size as an outcome. The miRs identified in this literature search were all detected in the early detailed miR analysis, so this strategy did not identify any extra miRs to include.

The endothelial cell culture experiment (page 121) identified miRs released into the supernatant when endothelial cells were exposed to hypoxia. MiRs detected in >30% of samples in this series of experiments were included in the OxAMI plate design.

Wells for the quality control parameters were also included: *UniSP2/4/5* for RNA isolation, *UniSP6* and *cel-miR-39* for reverse transcription and *UniSP3* for PCR. The ubiquitous *miR-103* and *-191* were included for use as positive controls. Erythrocyte specific *miR-451* and plasma specific *miR-23a* were included to allow a ratio to be calculated to exclude haemolysis. A non-template control well was included to monitor for contamination.

The 384-well OxAMI plate was therefore designed taking the above data into account. Any miRs detected in more than 30% of human samples, all miRs detected in the endothelial cell culture experiment and the controls were included in the final plate, allowing 373 miRs and 11 controls to be quantified on each plate. The final OxAMI plate design is shown in Appendix 1: The OxAMI Plate (page 198).

Normalisation

The analysis of the Discovery Experiment was carried out using global mean normalisation. While this method was appropriate for the broad non-selective qPCR arrays used for this cohort, in the next stage of the experiment a much more focused list of targets was analysed and therefore a different normalisation strategy was needed.

The *Normfinder* algorithm was used to identify potential stable reference genes. For selection, miRs had to have been detected in all samples at a CT value of less than 34. The reference genes selected for the Discovery Experiment are shown in Table 11. Six reference miRs were chosen for normalisation as there was minimal further reduction in the accumulated standard deviation with a larger number of miRs.

	MiRs ranked by standard deviation
Accumulated SD	0.22
Selected reference (miRs 1-6)	*hsa-miR-23a* *hsa-miR-92a* *hsa-miR-126* *hsa-miR-423* *hsa-miR-25* *hsa-miR-26b*
Other stable miRs (miRs 7-15)	*hsa-miR-223* *hsa-let-7a* *hsa-miR-215* *hsa-let-7g* *hsa-miR-23b* *hsa-miR-150* *hsa-miR-197* *hsa-miR-486* *hsa-miR-342*

Table 11: List of miRs identified by Normfinder ranked by standard deviation.
All PCR data from the Discovery Experiment 6-hour samples was imported into Genex for analysis. The Normfinder algorithm was used to identify the most stable miRs. Only miRs detected in all samples with a CT value <34 were included. This table shows the top 15 most stable miRs ranked by standard deviation. Acc SD is the accumulated standard deviation for the six most stable miRs.

Assessing Reference Gene Normalisation Performance

Making the assumption that global mean normalisation is the gold standard, this method was then used to test the performance of the various different normalisation strategies, including spike-in, single reference and multiple reference (*Normfinder*) normalisation (Figure 24-Figure 27). Spike-in normalisation performed poorly in comparison with single reference miR normalisation, with no significant correlation shown with two of the miRs tested, and a weaker correlation than other normalisation strategies for the other two miRs. *Normfinder* normalisation with the six most stable miRs showed a strong linear relationship with global mean normalisation with a correlation coefficient of ≥0.97 in all four miRs tested. Single reference miR normalisation using *miR-92a*, selected as a stable reference gene using the *Normfinder* algorithm, performed almost as well, with a correlation coefficient of ≥0.87.

A

miR-1
Global mean
versus
cel-miR-39 spike-in normalisation

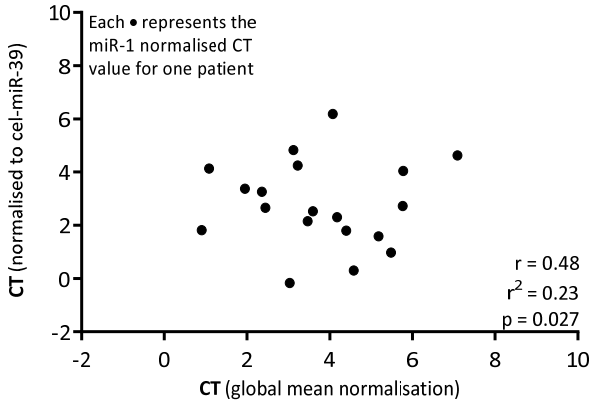

B

miR-1
Global mean
versus
UniSP2 spike-in normalisation

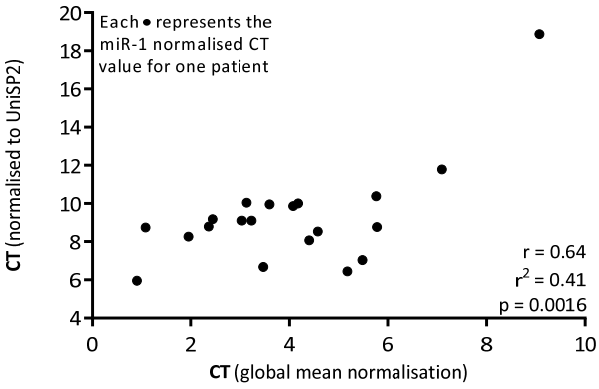

C

miR-1
Global mean
versus
single reference gene normalisation
(*miR-23a*)

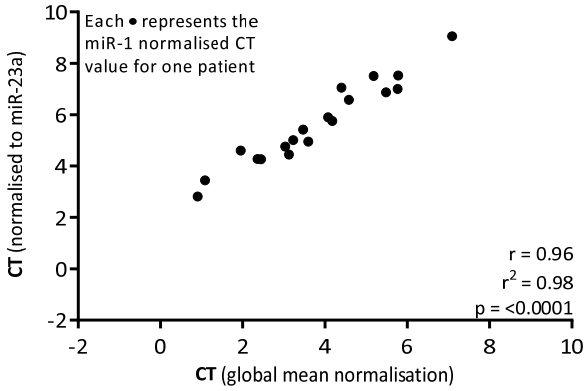

D

miR-1
Global mean
versus
Normfinder normalisation to six
reference miRs

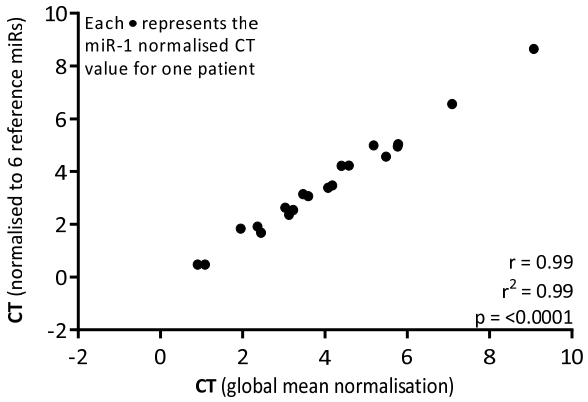

Figure 24: Discovery Experiment miR-1 (a known myocardial miR) normalised CT values using different normalisation strategies.
Each panel shows miR-1 (a known myomiR) global mean normalisation versus normalisation using **A:** spike in normalisation with cel-miR-39; **B:** spike in normalisation with UniSP2; **C:** single reference gene normalisation (most stable miR selected using the Normfinder algorithm, miR-23a); **D:** normalisation with the six most stable miRs identified using the Normfinder algorithm. A Pearson correlation was carried out for each pair of normalisation strategies. The strongest correlation with global mean normalisation was with Normfinder normalisation with the six most stable reference genes (r=0.99, p = <0.0001). CT=Cycle threshold. N=21.

A

miR-126
Global mean
versus
cel-miR-39 spike-in normalisation

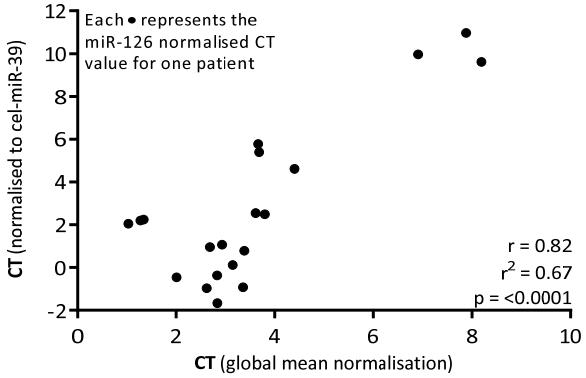

B

miR-126
Global mean
versus
UniSP2 spike-in normalisation

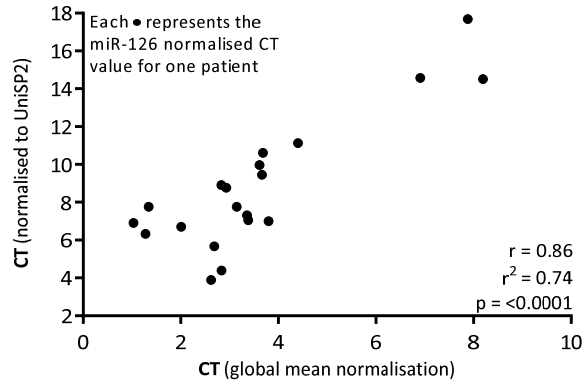

C

miR-126
Global mean
versus
single reference gene normalisation
(*miR-23a*)

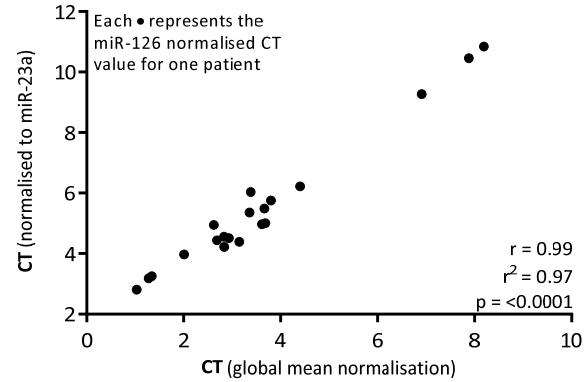

D

miR-126
Global mean
versus
Normfinder normalisation to six
reference miRs

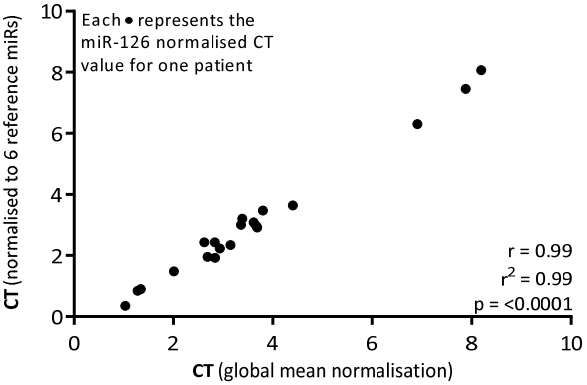

Figure 25: Discovery Experiment miR-126 (a known endothelial miR) normalised CT values using different normalisation strategies.

Each panel shows miR-1 (a known myomiR) global mean normalisation versus normalisation using **A:** spike in normalisation with cel-miR-39; **B:** spike in normalisation with UniSP2; **C:** single reference gene normalisation (most stable miR selected using the Normfinder algorithm); **D:** normalisation with the six most stable miRs identified using the Normfinder algorithm. A Pearson correlation was carried out for each pair of normalisation strategies. The strongest correlation with global mean normalisation was with Normfinder normalisation with the six most stable reference genes (r=0.99, p = <0.0001). N=21.

A

miR-877
Global mean
versus
cel-miR-39 spike-in normalisation

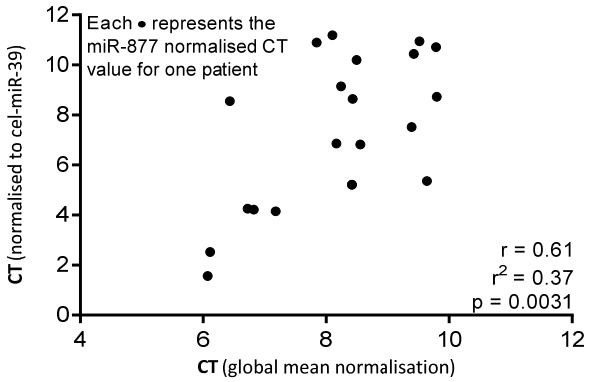

B

miR-877
Global mean
versus
UniSP2 spike-in normalisation

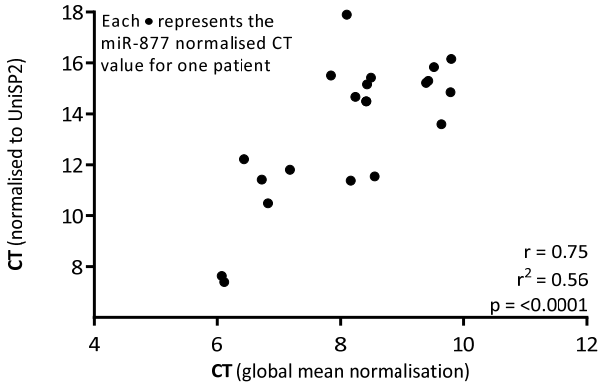

C

miR-877
Global mean
versus
single reference gene normalisation
(*miR-23a*)

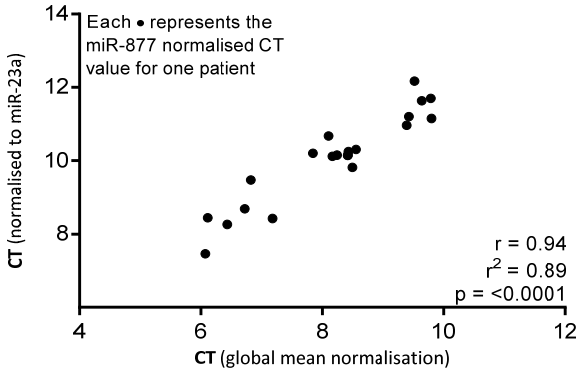

D

miR-877
Global mean
versus
Normfinder normalisation to six reference miRs

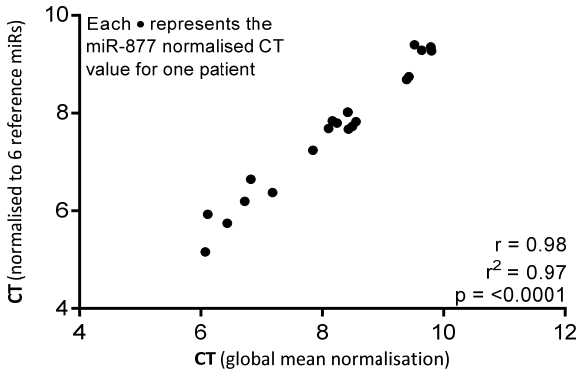

Figure 26: Discovery Experiment miR-877 (a miR with low expression in this cohort) normalised CT values using different normalisation strategies.
Each panel shows miR-1 (a known myomiR) global mean normalisation versus normalisation using A: spike in normalisation with cel-miR-39; B: spike in normalisation with UniSP2; C: single reference gene normalisation (most stable miR selected using the Normfinder algorithm); D: normalisation with the six most stable miRs identified using the Normfinder algorithm. A Pearson correlation was carried out for each pair of normalisation strategies. The strongest correlation with global mean normalisation was with Normfinder normalisation with the six most stable reference genes (r=0.99, p = <0.0001). N=21.

A

miR-16a
Global mean
versus
cel-miR-39 spike-in normalisation

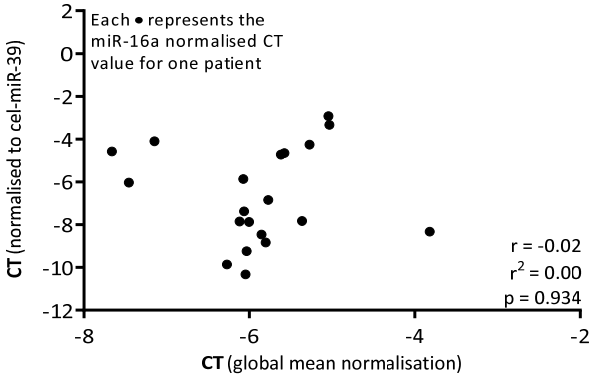

B

miR-16a
Global mean
versus
UniSP2 spike-in normalisation

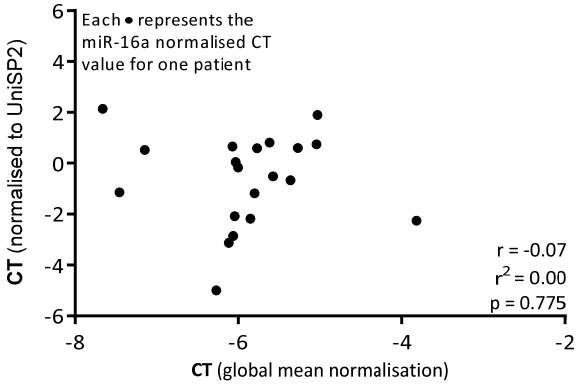

C

miR-16a
Global mean
versus
single reference gene normalisation
(*miR-23a*)

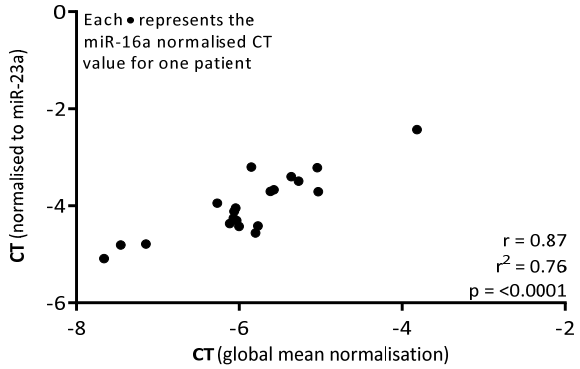

D

miR-16a
Global mean
versus
Normfinder normalisation to six
reference miRs

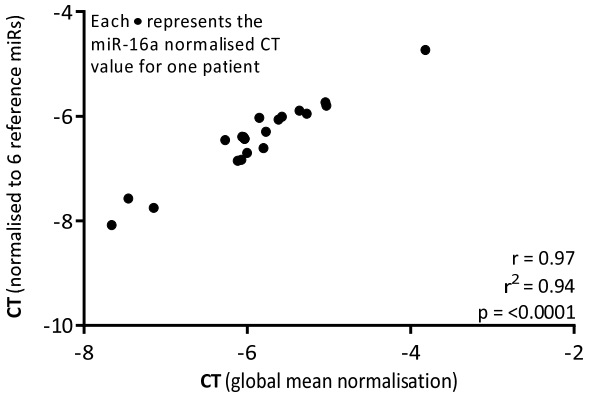

Figure 27: Discovery Experiment miR-16a (a miR with high expression in this cohort) normalised CT values using different normalisation strategies.
Each panel shows miR-1 (a known myomiR) global mean normalisation versus normalisation using **A:** spike in normalisation with cel-miR-39; **B:** spike in normalisation with UniSP2; **C:** single reference gene normalisation (most stable miR selected using the Normfinder algorithm); **D:** normalisation with the six most stable miRs identified using the Normfinder algorithm. A Pearson correlation was carried out for each pair of normalisation strategies. The strongest correlation with global mean normalisation was with Normfinder normalisation with the six most stable reference genes (r=0.99, p = <0.0001). Relationship between microRNA release and clinical parameters. CT=cycle threshold. N=21.

Infarct Size

The relationships between known myocardial miRs and infarct size measured by cardiac MRI six months after myocardial infarction were analysed (Figure 28). Normality was assessed visually using histograms and mathematically by calculating skewness and kurtosis and using the Shapiro-Wilk test. A variable was considered normally distributed if normality was demonstrated in two out of these three tests. Normalised CT values were normally distributed. Infarct size was positively skewed and was therefore $\log_{10}$ transformed prior to Pearson correlation analysis.

A

miR-1
vs
Log_{10} infarct size

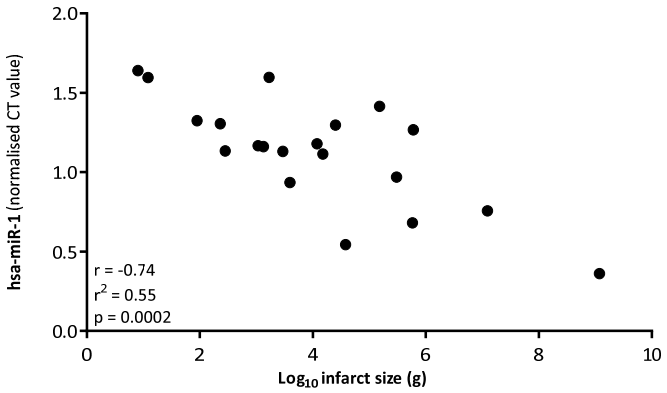

B

miR-133a
vs
Log_{10} infarct size

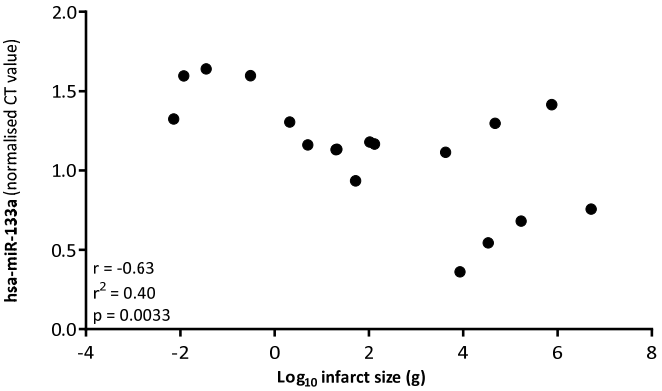

C

miR-499
vs
Log_{10} infarct size

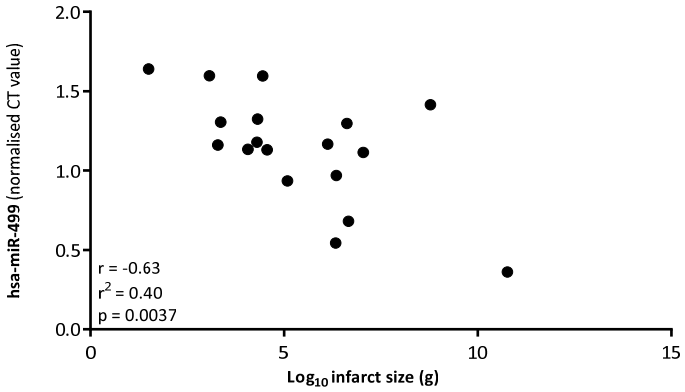

D

miR-208b
vs
Log_{10} infarct size

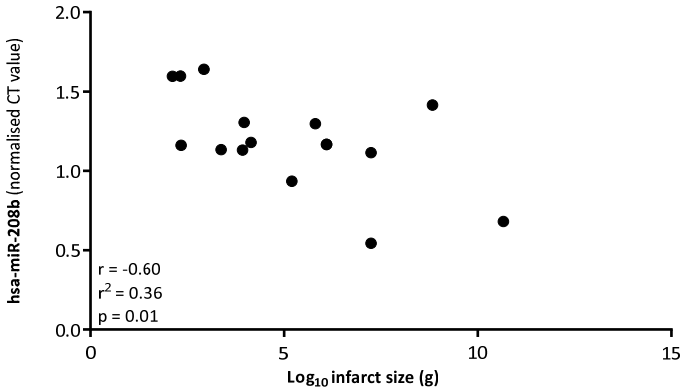

Figure 28: The relationships between known myocardial miRs and log_{10} infarct size measured by CMR at six months.
Each panel shows the relationship between a different miR and infarct size. Infarct size is not normally distributed and was therefore log_{10} transformed. After transformation, infarct size was normally distributed, assessed by analysing skewness and carrying out the Shapiro-Wilk test. All mIRs were normalised to the six most stable miRs (identified using the Normfinder algorithm). N=21.

Troponin

Troponin area under the curve was calculated using the trapezoid rule. The results were highly positively skewed both visually and mathematically (calculated skewness/kurtosis and Shapiro-Wilk) and were therefore log_{10} transformed. The normalised CT values analysed here were normally distributed. A Pearson correlation was carried out to assess the relationship between Log_{10} troponin AUC and previously described myocardial miRs. Strong correlations were found between the known myocardial miRs -1, -133b, 208b and -499 and troponin AUC (Figure 29).

A

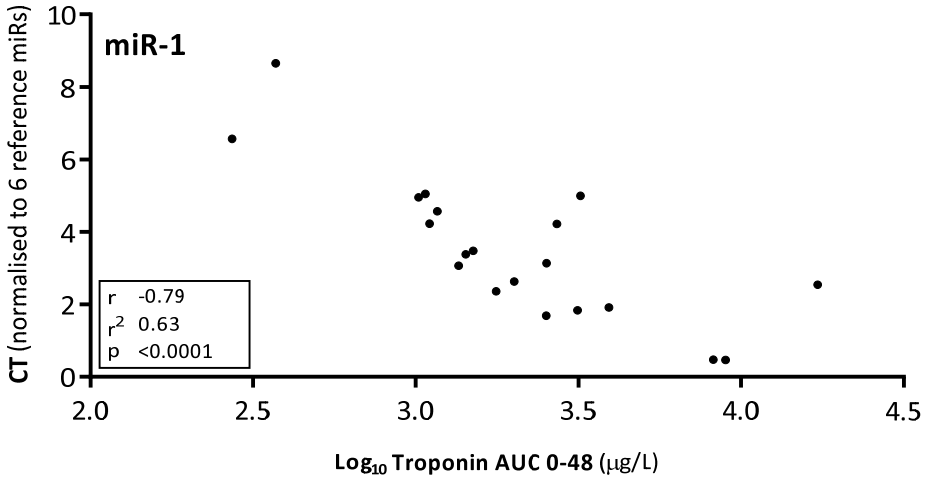
miR-1
CT (normalised to 6 reference miRs)
r -0.79
r2 0.63
p <0.0001
Log10 Troponin AUC 0-48 (μg/L)

B

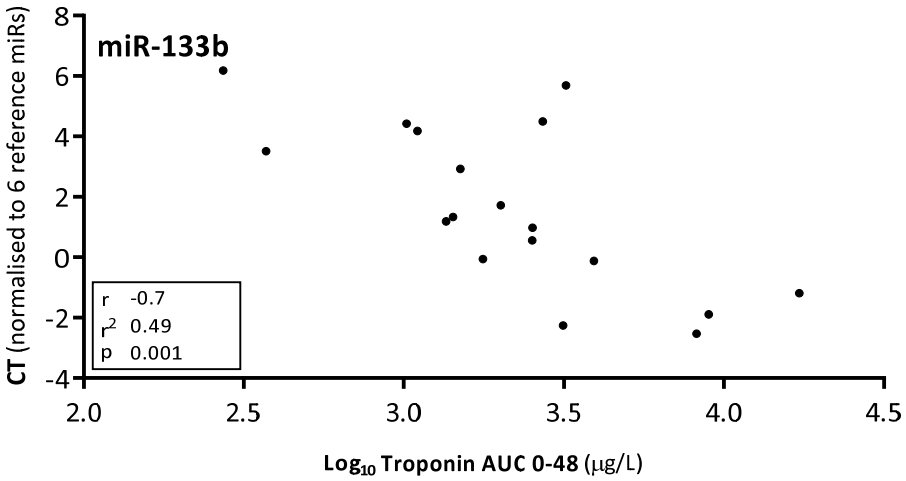
miR-133b
CT (normalised to 6 reference miRs)
r -0.7
r2 0.49
p 0.001
Log10 Troponin AUC 0-48 (μg/L)

C

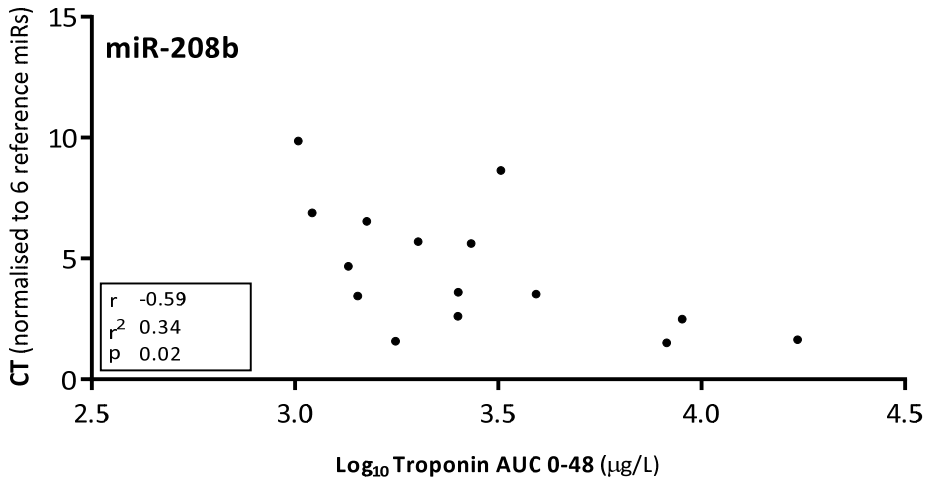
miR-208b
CT (normalised to 6 reference miRs)
r -0.59
r2 0.34
p 0.02
Log10 Troponin AUC 0-48 (μg/L)

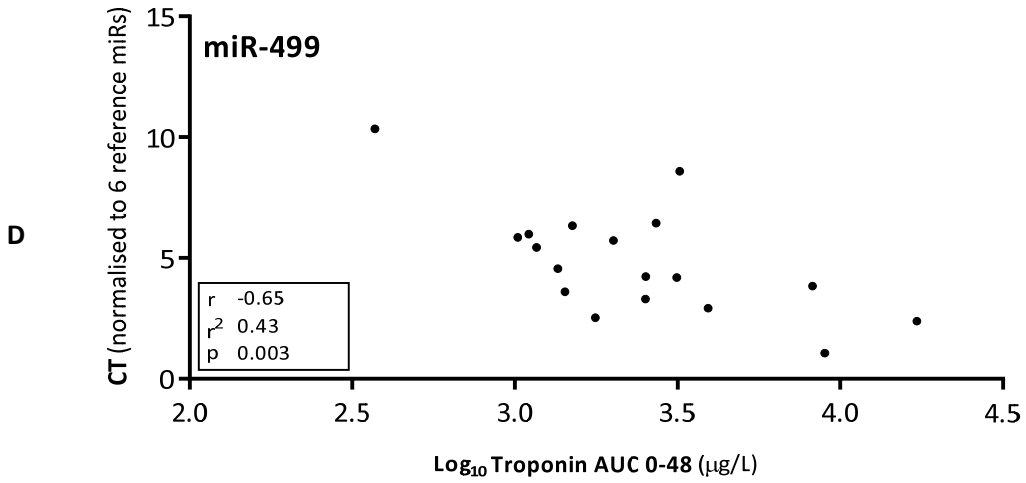

Figure 29: The relationships between known myocardial miRs and troponin AUC 0-48 hours for the Discovery Experiment.
Each panel shows the relationship between a different miR and troponin AUC 0-48 hours: A=miR-1, B=miR-133a, C=miR-208b, D=miR=499. Troponin AUC is not normally distributed and was therefore $\log_{10}$ transformed. All CT values were normalised to six reference miRs. A Spearman correlation was calculated between each miR and troponin AUC 0-48 hours for each cohort; correlation coefficient (r), coefficient of determination (r^2) and significance (p) are shown in the boxes. N=21.

A Pearson correlation matrix was constructed to show the relationship between $\log_{10}$ troponin area under the curve (0-48 hours) and each miR (Table 12). Known myocardial miRs are well represented in this list, in addition to multiple other miRs not previously reported to be associated with myocardial infarction. A smaller cohort of miRs have a negative concentration correlation with troponin AUC.

Log AUC 0-48 versus:	Correlation Coefficient (r)	Significance (p)	N
hsa-miR-1	-0.793	<0.0001	20
hsa-miR-378a-5p	-0.773	0.005	11
hsa-miR-302d-3p	-0.756	0.011	10
hsa-miR-144-5p	-0.727	0.001	17
hsa-miR-186-5p	-0.718	0.001	18
hsa-miR-133a-3p	-0.703	0.001	18
hsa-miR-27b-3p	-0.698	0.001	20
hsa-miR-152-3p	-0.697	0.001	20
hsa-miR-133b	-0.675	0.001	20
hsa-miR-30a-5p	-0.67	0.001	20
hsa-miR-452-5p	-0.66	0.004	17
hsa-miR-378a-3p	-0.656	0.002	20

hsa-miR-499a-5p	-0.654	0.003	18
hsa-miR-125b-5p	-0.65	0.002	20
hsa-miR-99a-5p	-0.64	0.002	20
hsa-let-7i-5p	-0.624	0.003	20
hsa-miR-148a-3p	-0.621	0.006	18
hsa-miR-30e-5p	-0.61	0.004	20
hsa-miR-193a-5p	-0.609	0.004	20
hsa-miR-362-3p	-0.603	0.023	14
hsa-miR-99b-5p	-0.596	0.007	19
hsa-miR-22-3p	-0.595	0.007	19
hsa-miR-423-3p	-0.592	0.01	18
hsa-miR-208b-3p	-0.587	0.022	15
hsa-miR-339-3p	-0.584	0.046	12
hsa-miR-22-5p	-0.568	0.011	19
hsa-miR-497-5p	-0.567	0.043	13
hsa-miR-29c-3p	-0.561	0.012	19
hsa-miR-193b-3p	-0.558	0.025	16
hsa-miR-221-3p	-0.557	0.016	18
hsa-miR-24-3p	-0.556	0.011	20
hsa-miR-320d	-0.547	0.015	19
hsa-miR-7-5p	-0.518	0.019	20
hsa-miR-23a-3p	-0.506	0.023	20
hsa-miR-181b-5p	0.513	0.025	19
hsa-miR-320c	0.531	0.023	18
hsa-miR-18a-3p	0.534	0.027	17
hsa-let-7e-5p	0.549	0.015	19
hsa-miR-10a-5p	0.567	0.043	13
hsa-miR-379-5p	0.603	0.038	12
hsa-miR-486-5p	0.609	0.004	20
hsa-miR-582-5p	0.612	0.035	12
hsa-miR-665	0.613	0.009	17
hsa-miR-218-5p	0.682	0.03	10
hsa-miR-636	0.74	0.004	13
hsa-miR-576-5p	0.838	0.001	12
hsa-miR-326	0.87	0.001	10

Table 12: Pearson correlation matrix for troponin area under the curve (0-48 hours) versus all detected microRNAs in the Discovery Experiment.

Troponin AUC (0-48 hours) values were not normally distributed and were therefore log transformed prior to analysis. Correlations are only shown where the correlation coefficient was ≥±0.5, the miR was detected in ≥50% of samples and p≤0.05. Correlations represent the relationship between troponin AUC and Normfinder normalised CT values, therefore a numerically negative correlation (shown in red) is in fact a positive correlation for miR concentration. Bold indicates previously reported myocardial miRs. N=21.

Microvascular Obstruction

Microvascular obstruction was measured by cardiac MRI within 48 hours of presentation. Although the MVO measurement is on a continuous scale (either mL, g or % LV), in the clinical context it is usually considered a binary variable. Therefore, for analysis, results were split into two groups: patients with >0g MVO were put into the 'MVO' group and patients with 0g MVO were put into the 'No MVO' group. Frequency distribution of MVO values is shown in Figure 30. 9 patients (45%) were in the 'No MVO' group and 11 patients (55%) were in the 'MVO' group. Spearman correlations were calculated for MVO versus miR detection and are shown in Table 13. Box plots of selected miRs which demonstrated a strong relationship with MVO are shown in Figure 31.

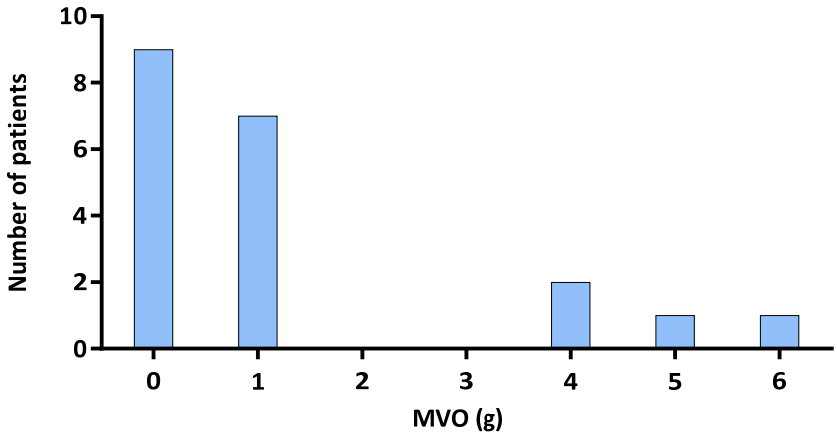

Figure 30: Frequency distribution histogram of microvascular obstruction (MVO) in the Discovery Experiment.
This was measured during the acute cardiac MRI scan which was carried out within 48 hours of presentation. MVO is measured in grams of affected myocardium. 9 patients (45%) had no microvascular obstruction detectible in the acute scan.

miR	Correlation coefficient (rho)	Significance (p)	N
hsa-miR-221-3p	-0.648	0.0036	18
hsa-miR-30a-5p	-0.6372	0.0025	20
hsa-miR-452-5p	-0.626	0.0054	18
hsa-miR-125b-5p	-0.5664	0.0092	20
hsa-miR-28-5p	-0.5611	0.025	17
hsa-miR-1	-0.5487	0.0122	20
hsa-miR-378a-3p	-0.5487	0.0122	20
hsa-miR-148a-3p	-0.5387	0.0211	18
hsa-miR-324-3p	-0.5382	0.0212	18
hsa-miR-335-5p	-0.5329	0.0418	16
hsa-miR-193b-3p	-0.5321	0.042	16
hsa-miR-29c-3p	-0.5255	0.0209	19
hsa-miR-99b-5p	-0.5255	0.0209	19
hsa-miR-133b	-0.5133	0.0206	20
hsa-miR-660-5p	-0.506	0.0271	19
hsa-miR-27b-3p	-0.4956	0.0263	20
hsa-miR-193a-5p	-0.4602	0.0412	20
hsa-miR-24-3p	-0.4602	0.0412	20
hsa-miR-30e-3p	-0.4602	0.0412	20
hsa-miR-532-3p	0.4942	0.0371	18
hsa-miR-342-5p	0.5354	0.0496	15
hsa-miR-320c	0.5601	0.0156	18

Table 13: The relationship between microvascular obstruction (MVO) and miR release.
Multiple Spearman correlations were carried out between individual miRs and MVO. Prior to analysis, MVO was transformed to a binary variable: no MVO or MVO present. As CT values are measured on an inverse scale, a negative correlation (shown in red) means that increased CV value is associated with increased MVO. Result only included if miR was detected in ≥50% of samples and p≤0.05. Bold indicates known myocardial miRs. N=21.

A

miR-221
vs
MVO

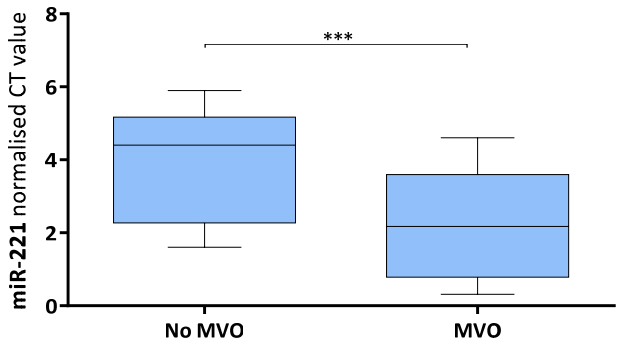

B

miR-30a
vs
MVO

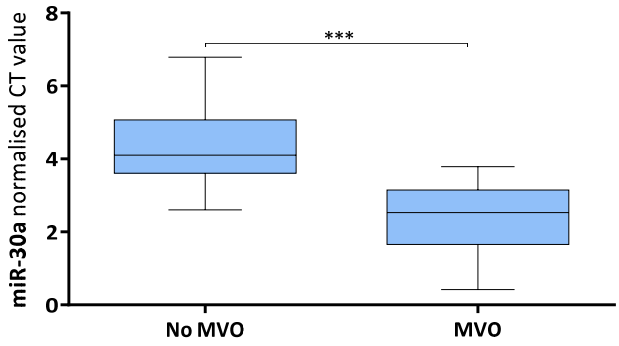

C

miR-320c
vs
MVO

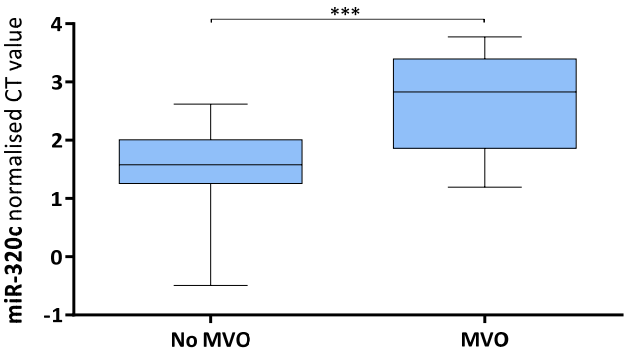

Figure 31: Box plots illustrating the relationship between MVO expressed as a binary variable and microRNA detection.

Two miRs with a strong positive correlation are shown in A and B (miR-221 and -30a respectively) and one with a strong negative correlation is shown in C (miR-320c). Box shows 25th-75th centiles, line represents median, whiskers represent range. An independent samples t-test showed that there was a statistically significant difference in detected CT values of the three miRs shown between the MVO and No MVO groups (p=<0.0001). N=21.

10.4 Discussion

Patients presenting with acute myocardial infarction are clinically unstable and they frequently have impaired consciousness. The clinical pathway is highly streamlined and designed to restore coronary artery patency as quickly as possible. Carrying out scientific research on these patients is challenging in many respects; identifying suitable patients, the ethics of consent and making measurements and collecting samples in the busy cardiac catheterisation laboratory where the clinical focus, quite rightly, is aimed towards rapid clinical care rather than detailed research. The results presented in this chapter showed that it is possible to consistently collect a complete, high quality dataset despite these complexities.

The twenty patients recruited into this Discovery Experiment were predominantly male and in their seventh decade. Other recent work looking at the STEMI population has shown similar patient demographics; for example, the TOTAL trial of primary PCI with or without manual thrombectomy and the CVLPRIT trial of complete versus target lesion revascularisation both had a similar male gender bias and they also recruited far fewer patients with a circumflex occlusion[116,117]. UK National PCI data records all PCI procedures, not just in STEMI patients, and this shows that the proportions of LAD/RCA/circumflex intervention are 42/31/21% respectively, with the remainder being left main stem and graft PCI, suggesting that although circumflex coronary artery disease is less commonly treated with PCI, this difference is far more pronounced in the STEMI population[118]. Diagnosing a lateral myocardial infarction (usually secondary to an occluded circumflex artery) can be more challenging than diagnosing anterior or inferior myocardial infarction (usually due to left anterior descending or right coronary artery occlusion respectively) which may explain why fewer of these patients receive primary PCI, or are recruited into clinical STEMI research.

The prevalence of diabetes mellitus in the primary PCI population in Oxford over the last three years was 12% (135 patients with diabetes mellitus, 1126 procedures between May 2012 and May 2015) so it is surprising that no patients in the Discovery Experiment had diabetes mellitus. However, of all patients recruited to OxAMI since 2012, the prevalence of diabetes mellitus was 12.7% so the absence of any patients with diabetes mellitus in the Discovery Experiment is likely to be related to random chance rather than any specific recruitment bias. Troponin-I measurements for the OxAMI cohort as a whole showed a median AUC 0-48 hours of 2,522μg/L (range 2,169-28,946) compared with a median of 1,888 (range 272.8-17,201) in the Discovery Experiment which suggests that the sample analysed included a range of infarct sizes.

It could be expected that blood samples collected while a patient is undergoing emergency PCI may be of inferior quality to those collected in the more controlled environment of the ward 6, 24 and 48 hours later. Table 10 (page 92) confirms this expectation with 83% of samples collected during the procedure passing all quality control steps, compared with 93-98% at the other time points. There were more failures of quality control at each step of the microRNA isolation and quantification process at the 0-hour time point than at any other. There are likely to be several explanations for this finding. At the first time point, samples needed to be collected rapidly so that the start of the procedure is not delayed. Drawing blood samples rapidly, particularly if strong negative pressure is generated with the syringe, increases the risk of haemolysis, though this issue was identified in the very early patients recruited to the OxAMI study so was avoided by the time this cohort was recruited.

Although laboratory space was acquired adjacent to the cath lab to allow rapid processing of blood samples, the challenge of trying to recruit the patient, collect blood samples, record clinical data, oversee the assent process and remind the operator to collect all the blood samples in a very short time sometimes did lead to delays in the centrifugation, aliquoting and snap freezing of blood

samples. This may explain why more samples at the 0-hour time point failed to meet the quality control criteria at the RNA isolation stage than the other time points. The quality control data for the 6, 24 and 48-hour time points was encouraging, with the majority of samples passing all QC steps.

Acute myocardial infarction is a large inflammatory insult and it may be expected that the absolute number of microRNAs detected, or their expression level, may be temporally related to vessel occlusion (or reperfusion). This would be an important finding as it may influence selection of one time point over another. In the Discovery Experiment, there was no significant difference in either the number of microRNAs detected (Figure 20, page 93), or the mean CT value of all microRNAs in all samples at each time point (Figure 21, page 94).

At this stage, taking into account quality issues at the 0-hour time point and the similar microRNA expression and detection at all time points it was felt that the six-hour time point would be the best option for more detailed microRNA analysis. The remainder of this experiment therefore used 6-hour venous samples, which were analysed together with the 6-hour samples analysed in the pilot experiment.

Previously published work has shown that release of some myocardial-specific miRs follows a similar (or slightly more rapid) timecourse as troponin-I. There are many different methods of isolating and processing plasma miR samples and an important part of the validation process was to confirm that in our patients, in our lab, with our own protocols, similar patterns were seen. Corsten et al. showed that the myocardial miRs are detectable at dramatically higher levels in MI patients versus controls[72]. Liebetrau et al. showed that myocardial miR release follows a timecourse with a peak detectable concentration between one and three hours[119]. Figure 22 showed that myocardial miRs followed a timecourse, peaking at the 6-hour timepoint. It also showed a relationship between miR fold change and infarct size.

MicroRNA isolation, reverse transcription and quantitative PCR takes approximately four hours for each 384-well plate. The highly detailed analysis carried out for the first six patients at time points required two 384-well plates each sample, and was therefore both time-consuming and expensive. Figure 20A illustrates that approximately 250 miRs were detected in each sample, though the detailed two plate analysis had target wells for 751 miRs; a substantial number of miRs were not detected in any samples. The decision was therefore made to design a single plate for the analysis of each sample, which would effectively double throughput. The identification of which microRNAs to include on the plate and perhaps more importantly which to exclude was carried out in several steps.

Figure 23 showed that the majority of miRs were detected in all (or almost all samples) or none at all. Few miRs were detected in between 30 and 60% of samples. There seemed no good reason to include microRNAs on the OxAMI plate which were not detected in any sample in the first six patients. It was also felt to be important to include miRs that have been shown to be released in human coronary microvascular endothelial cells in culture (Chapter 13, page 179), in an attempt to improve understanding of the biology of microvascular injury. The spike-in, biological and non-template controls provided useful information for assessing the processing effectiveness of samples from the first six patients and these wells were therefore also included in the OxAMI plate design (see *Appendix 1: The OxAMI Plate*).

There is considerable variation in the pre-processing steps used for microRNA data in the published literature, particularly in the exclusion of data, using CT value cut-offs and imputation of missing data. There is no consensus on the best approach, and frequently precise details on the steps taken are not reported. In this work I have consistently followed the same pre-processing steps (detailed on page 86) and there has been no imputation of missing data. The only point where a CT value cut-off was used was in carrying out global mean normalisation; only values <34 were used to calculate

the $CT_{AVERAGE}$ for a particular sample prior to normalisation. However, once normalisation was carried out, no data were excluded.

Global mean normalisation is the gold standard approach when carrying out a large (hundreds of targets) analysis on an unbiased selection of miRs. There is inconsistency in the literature about which normalisation strategy is used when global mean normalisation is not appropriate. In this chapter I tested the performance of the different normalisation methods currently in widespread use. The design of this phase of the experiment was challenging as there is no accepted method for doing this.

Figure 24-Figure 27 show the correlation between CT values for a single miR calculated using two different normalisation strategies. Each figure shows these findings for a different miR and each panel within the figure shows a comparison between global mean CT values and normalised CT values calculated using a different method. The most striking finding is that normalising to *cel-miR-39*, which is a widely used method in the literature, shows the weakest relationship with global mean normalisation. Using the *Normfinder* algorithm to select the six most stable reference miRs based on their variance correlates almost perfectly with global mean normalisation (correlation coefficient 0.97-0.99, p=<0.0001). Using a single reference miR, selected in the same way also offers very robust normalisation performance whether the method is used with a myocardial miR, and endothelial miR or a ubiquitous miR. These methods (single reference miR or six reference miR normalisation, selected using the *Normfinder* algorithm) can therefore reasonably be used in smaller miR analyses where global mean normalisation would be inappropriate due to a small number of miRs being analysed.

Once quality control steps had been completed and normalisation carried out, the final phase of the Discovery Experiment was to analyse the relationship between plasma miR release and the different

measured clinical parameters. Infarct size at six months is an important clinical endpoint used in many major scientific studies, though it has several disadvantages. Infarct size is usually measured by measuring late gadolinium enhancement at a cardiac MRI scan at six months; this introduces a delay in being able to analyse results, relies on the patient attending for follow-up and assumes the patient will be able to tolerate an MRI scan, which many find claustrophobic and unpleasant. Work in the previous chapter (Figure 8, page 61) has shown the strong correlation between infarct size measured at six months using cardiac MRI and troponin area under the curve using four measurements (0, 6, 24, 48-hours).

A strong correlation was shown between known myocardial miRs and infarct size at six months (Figure 28) with *miR-1, -133a, -499* and *-208b* showing a correlation coefficient ≥0.60. As would be expected, similar correlations were shown between these miRs and troponin AUC (0-48 hours) in Figure 29. A correlation matrix (Table 13) of all miRs versus troponin AUC (0-48 hours) showed multiple other miRs sharing this relationship, some of which not having been reported before. There were some miRs with a strong negative correlation which it could be speculated may reflect a protective process.

Microvascular obstruction (MVO) is less well studied in the field of microRNA research. The Discovery Experiment has, for the first time, shown the relationship between microvascular obstruction in STEMI patients and miR release. It is perhaps to be expected that some of the miRs showing a strong correlation with MVO showed a similar relationship with troponin release, for example *miR-1* and *-133b*. This is an interesting finding in itself, but further work in this thesis will aim to try and identify any miRs relating to MVO that do not relate to troponin release, which may offer insights into the underlying pathology of microvascular obstruction. Paired coronary sinus samples were collected from all of the Discovery Experiment patients and these will be analysed to confirm whether particular miRs are released from, or indeed consumed by, the myocardium.

In this chapter, a comprehensive miR analysis has been carried out on venous plasma samples from 20 patients who formed the Discovery Experiment. Careful analysis confirmed the sample quality and efficiency of each of the multiple steps required for miR isolation and quantification. Detection of myocardial miRs in these patients with ST elevation myocardial infarction is an important validation of the miR isolation protocol optimised in the previous chapter. The strong correlations shown between myocardial miR release and troponin AUC (0-48 hours) further confirms these findings and may suggest a future use for miRs in predicting infarct size in ST elevation MI patients.

11 MicroRNA Release in Endothelial Cells

11.1 Introduction

The Discovery Experiment has shown that ST elevation myocardial infarction results in a characteristic pattern of microRNA release and there are strong correlations between specific miRs and clinical parameters, such as infarct size. Previously published work has shown that there are different microRNA signatures across different cell types[120]. These studies analyse miRs expressed in tissues rather than the patterns of miR release into the plasma compartment.

It is likely that the detectable plasma miR signature reflects the miRs released from the different cell types impacted by myocardial infarction, both in the heart and potentially from other systemic sources.

The experiments in this chapter are designed to define the contribution of endothelial cells to the overall plasma miR signature, and to investigate how that signature changes in hypoxic conditions. To do this, endothelial cells were grown in cell culture and then exposed to hypoxic stress of different severity and duration.

11.2 Methods

Experimental Design

Human umbilical vascular endothelial cells (HUVECs) in cell culture medium were exposed to different hypoxic states (Figure 32). The purpose of these multiple experiments was to determine the effect of hypoxia, and determine whether there was a 'dose response' of increasing hypoxia.

- Control: HUVECs were cultured for 24 hours in a standard incubator at 37°C at 21% oxygen.
- 1% oxygen: HUVECs were exposed to hypoxia in a hypoxic chamber maintained at 37°C with 1% oxygen for 24 hours.
- 0.1% oxygen: HUVECs were exposed to hypoxia in a hypoxic chamber maintained at 37°C with 0.1% oxygen for 24 hours.
- 0.1% ischaemia reoxygenation: HUVECs were exposed to hypoxia in a hypoxic chamber maintained at 37°C with 0.1% oxygen for 12 hours and then transferred to a standard incubator (37°C, 21% oxygen) for 12 hours.

While HUVECs are a different cell subtype to human coronary microvascular endothelial cells, there is considerable commonality in the miR signature for different endothelial cell subtypes[73]. This factor, in addition to local expertise in working with HUVECs in hypoxic conditions drove the choice of HUVECs for this experiment.

At the end of the experiment the cell culture supernatant was removed, centrifuged, separated into aliquots and snap frozen. The cells were also removed, some wells were snap frozen for further analysis later and some were used for cell viability assessment.

Sample analysis was carried out in several phases. First, supernatant from the control samples was used to develop the microRNA isolation and analysis protocol. Once this had been achieved, microRNA from further control supernatant was isolated and analysed in order to determine which miRs where released from cultured endothelial cells. This information was used in the design of the OxAMI-focused plate, which is discussed in the next chapter.

The next phase was to identify the effect of hypoxia on the supernatant miR signature. Aliquots of supernatant from each hypoxic condition were analysed using quantitative real-time PCR. Numbers of miRs and their detected levels were measured in each hypoxic state.

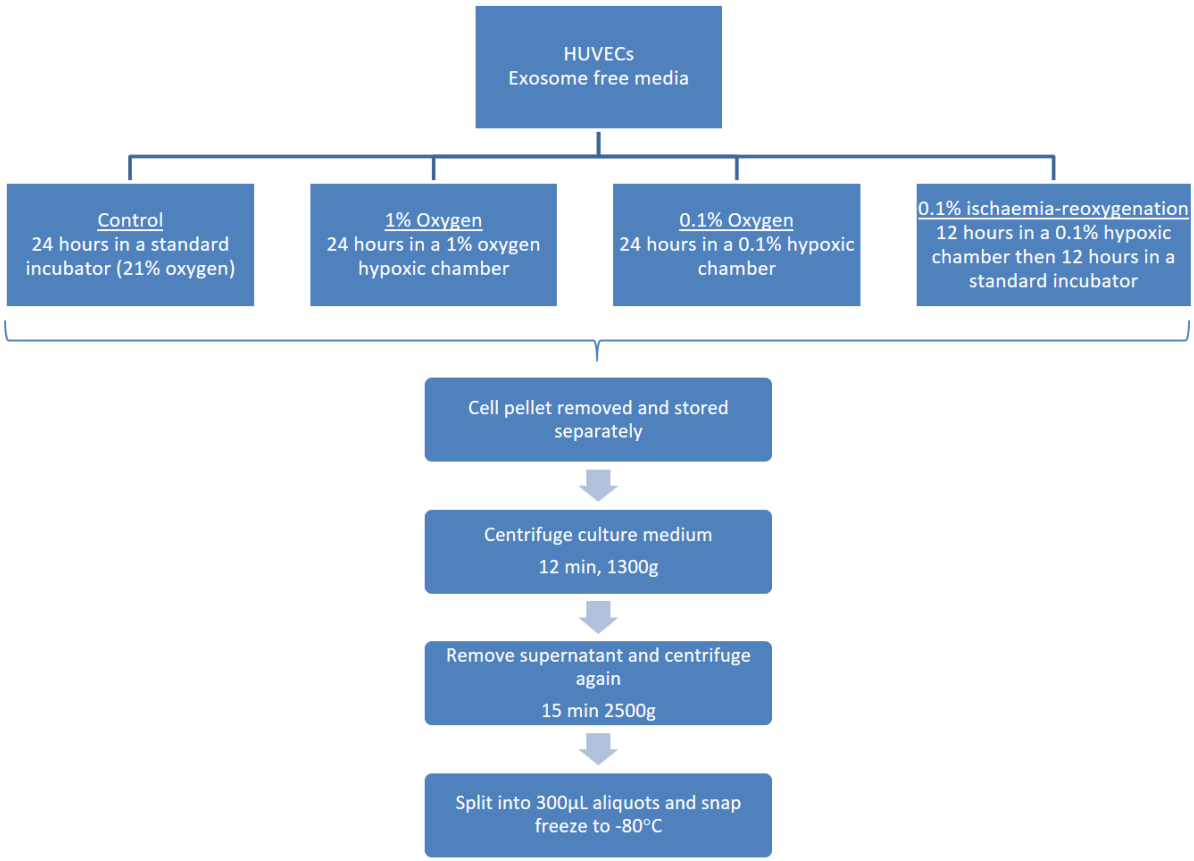

Figure 32: Experimental design for microRNA analysis of cultured endothelial cell supernatant microRNA signature under different hypoxia conditions.
HUVECs were cultured to passage 3 and transferred to four six-well plates and four 96-well plates. One of each plate type was then placed in each experimental condition (control, 1% oxygen, 0.1% oxygen or 0.1% ischaemia-reoxygenation(I-R)) for 24 hours, except in the 0.1% I-R condition where

the cells were exposed to 0.1% oxygen for 12 hours and a further 12 hours in a standard (21% oxygen) incubator.

Cell Culture

Cell Preparation

Cryopreserved pooled HUVECs (*PromoCell GmbH, Heidelberg, Germany*) were thawed according to the manufacturer's instructions and suspended in 7mL of endothelial cell growth medium MV2 (*Promocell*) containing foetal calf serum (0.05ml/ml), growth factors and hydrocortisone. They were then transferred to a T75 flask with a filter cap and placed in a standard incubator at 37°C, 21% oxygen and 5% carbon dioxide.

Every three days, culture medium was replaced; old culture medium was removed by pipetting and discarded and replaced with new culture medium (7mL) that had been warmed to 37°C in a water bath. When cells reached confluence, existing culture medium was removed and cells were washed with phosphate buffered saline. Accutase solution (*ThermoFIsher Scientific, Waltham, MA USA*) was then added to detach the cells. After 2-3 minutes, cells were examined under the microscope; if cells were still adherent, cells were bathed in Accutase solution for another 2-3 minutes. If cells had detached, 5mL culture medium was added to neutralise the Accutase. This cell suspension was then centrifuged for 5 minutes at 400g. Supernatant was discarded and cells were resuspended in warmed culture medium. This solution was then divided between two new T75 flasks and returned to the incubator.

Culture medium containing foetal calf serum is known to contain exosomes and signalling molecules within these may affect the behaviour of cultured cells[121]. Exosome-free medium was therefore used to minimise contamination from exosomes already present in the culture medium. This was prepared by taking endothelial cell growth medium and centrifuging at 120,000g for 18 hours[121]. The

supernatant was then separated and refrigerated ready for use. Three days before the start of the experiment, cells were detached, re-suspended in exosome free medium and transferred to the experimental plates: for each condition, two six-well plates and a single 96-well plate were prepared. Until the start of the experiment, all plates were stored in a standard incubator.

The Hypoxia Experiment

Two hypoxic chambers (*InvivO$_2$ 400 Hypoxia Workstation, Baker Ruskinn*) were used to create the hypoxic environment, and a standard incubator for the control environment. Oxygen was set to the required concentration (0.1% or 1% oxygen) 24 hours prior to starting the experiment to allow equilibration; carbon dioxide was set to 5%, temperature to 37°C and humidity 70%. The tanks (nitrogen, oxygen and carbon dioxide) were confirmed to have sufficient gas remaining for the experiment. The underwater seal was checked and replenished with sterile water if necessary. 12 hours and 1 hour before the start of the experiment, it was confirmed that the preset oxygen and carbon levels had been achieved and a separate oxygen gas analyser was used to confirm the correct oxygen level. A flask of exosome free medium was placed in each hypoxic chamber and the standard incubator 12 hours prior to the start of the experiment to equilibrate.

HUVECs were transferred to their allocated environment and the existing medium was removed and discarded. This was replaced with equilibrated exosome free medium. The experiment was deemed to have commenced as soon as the medium was changed. After 12 hours, the oxygen and carbon dioxide preset concentrations were re-checked, and the measured oxygen level was measured in duplicate with the built-in sensor in the chamber and the external oxygen analyser. The plates allocated to the ischaemia-reoxygenation experiment were removed and placed in a standard incubator (21% oxygen, 5% carbon dioxide, 37°C).

After 24 hours, the experiment was completed. Medium was removed from each well on the six-well plates into separate labelled microtubes. These were centrifuged at 1300g for five minutes to pellet the cell debris. The supernatant from each microtube was transferred to separate Eppendorf tubes and snap frozen on dry ice for later miR analysis.

The six-well plate was then prepared for RNA and protein analysis. Each well was first washed with phosphate buffered saline. RNA lysis solution (*miRCURY, Exiqon*) was added to the wells on one six-well plate and protein lysis solution (*CelLytic Mammalian Cell Lysis Reagent, Sigma*) was added to the wells on the other six-well plate. A cell scraper was used to dislodge the cells and the lysate was transferred to microtubes and snap frozen.

It was expected that the different hypoxic states would have an impact on cell viability, with more cell death in the 0.1% oxygen environment. Cell viability was assessed using an MTT (3-(4,5-dimethylthiazol-2-yl)-2,5-diphenyltetrazolium bromide) luminescent cell viability assay (*CellTiter Glo®, Promega, Madison, WI USA*) which quantifies cell viability by measuring the amount of ATP present and therefore the number of metabolically active cells. On incubation with metabolically active cells, MTT is converted to formazan which has a purple colour, which can then be quantified using a plate reading spectrophotometer[122]. For this analysis, a 96-well plate was prepared for each experimental hypoxia state with wells for endothelial cells and control wells (exosome-free medium only). At the end of the experiment, the *CellTiter Glo® buffer* and substrate were mixed and added to cultured cell and control wells according to the manufacturer's protocol. The cells were agitated using an orbital shaker for two minutes to induce cell lysis and then incubated for 10 minutes prior to measuring luminescence using a plate reader (*FLUOstar Omega microplate reader, BMG Labtech, Ortenberg, Germany*).

Although the oxygen levels in the hypoxic chambers had been checked and confirmed, it was important to confirm whether the hypoxic insult had any effect on the cultured cells. Light microscopy was helpful but qualitative. PCR for hypoxia inducible genes provided quantitative information on the cellular effect of hypoxia.

This analysis was carried out using the cells from the six-well plate that had been lysed and frozen. RNA isolation was carried out using the *miRCURY RNA isolation kit – Cell and Plant* (*Exiqon*). After defrosting, ethanol was added to the lysate and the solution was transferred to a silica gel column and centrifuged. The column was then washed and the isolated RNA was eluted into RNAse-free water. Reverse transcription was carried out and real-time PCR for the hypoxia inducible genes vascular endothelial growth factor (VEGF), vascular cell adhesion protein (VCAM) and transforming growth factor-β2 (TGF- β2) was carried out. Cyclophilin was used as a housekeeping gene and fold change expression (compared to control) was calculated using the delta-delta CT method[115].

MicroRNA Analysis

Although the protocols developed for the isolation and analysis of microRNA from human plasma were consistently reliable, it was important to confirm that these protocols were equally effective for cell culture samples and modify them as necessary.

A similar methods development process was carried out:

1. The same spike-in controls were used to allow quantification of the efficiency of each stage of microRNA processing.
2. MicroRNA analysis was carried out using different sample volumes (100, 200 and 400µL) with subsequent quantification of spike-in controls and ubiquitous miRs to determine the optimum sample volume.

3. The addition of *bacteriophage MS2* carrier protein improved RNA isolation efficiency in human samples; RNA isolation from cell culture supernatant was carried out with and without *MS2* to determine whether the same effect was seen.

MicroRNA isolation, reverse transcription and qPCR were carried out as previously described (page 75). The efficiency of RNA isolation and reverse transcription was assessed using a QC plate, and if the pre-defined QC parameters were achieved detailed microRNA analysis was carried out using the OxAMI qPCR plate (Figure 17, page 75). Normalisation was carried out using global mean normalisation.

The initial analysis focused on a description of miR release from cultured endothelial cells. The number of detectable miRs and their relative concentrations were measured and these values were compared with those from the human plasma samples. Another key question relates to which miRs are released into the cell supernatant. The miRs detected in the supernatant were compared with those released detected in human plasma.

This experiment allowed a detailed analysis of the effect of hypoxia on miR release from cultured endothelial cells. Analysis of the number of miRs detected in each hypoxic state was carried out and those miRs that were released in hypoxia but not normoxia (and vice versa) were reported. Finally, the effect of the severity of hypoxic insult was reported.

11.3 Results

Cell Preparation

Endothelial cell confluence was observed five days after thawing, and again three days after splitting. Doubling time was approximately 24 hours. At passage three, cells were transferred to the

final experimental plates. For each experimental condition, cells were added to two six-well plates ($1x10^6$ cells/well) and one 96-well plate ($2x10^4$ cells/well). After a further three days the cells were confluent and the supernatant was removed by pipetting and replaced with exosome-free medium. Cells were examined under light microscopy at this stage and confluence, adhesion and healthy morphology was confirmed (Figure 33). Cells were then transferred to their allocated experimental condition and medium was changed for exosome-free medium that had equilibrated to the experimental condition over the preceding 12 hours.

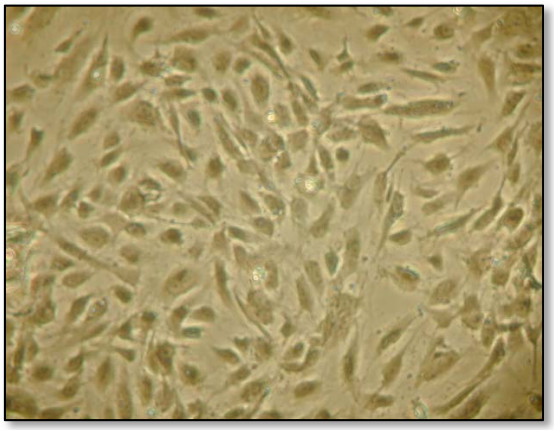

Figure 33: Light microscopy (10 x magnification) of cultured endothelial cells at passage 3 prior to the start of the hypoxia experiment.

A further microscopic examination was carried out at the end of the experiment which showed that in the control state the endothelial cells had continued to proliferate and were continuing to adhere to the flask (Figure 34). In the hypoxic states, endothelial cell proliferation was reduced and the amount of cell debris was increased. This was seen at 1% oxygen and was more pronounced in 0.1% oxygen. The visible features of cell damage were less severe in cells exposed to 0.1% ischaemia-reoxygenation.

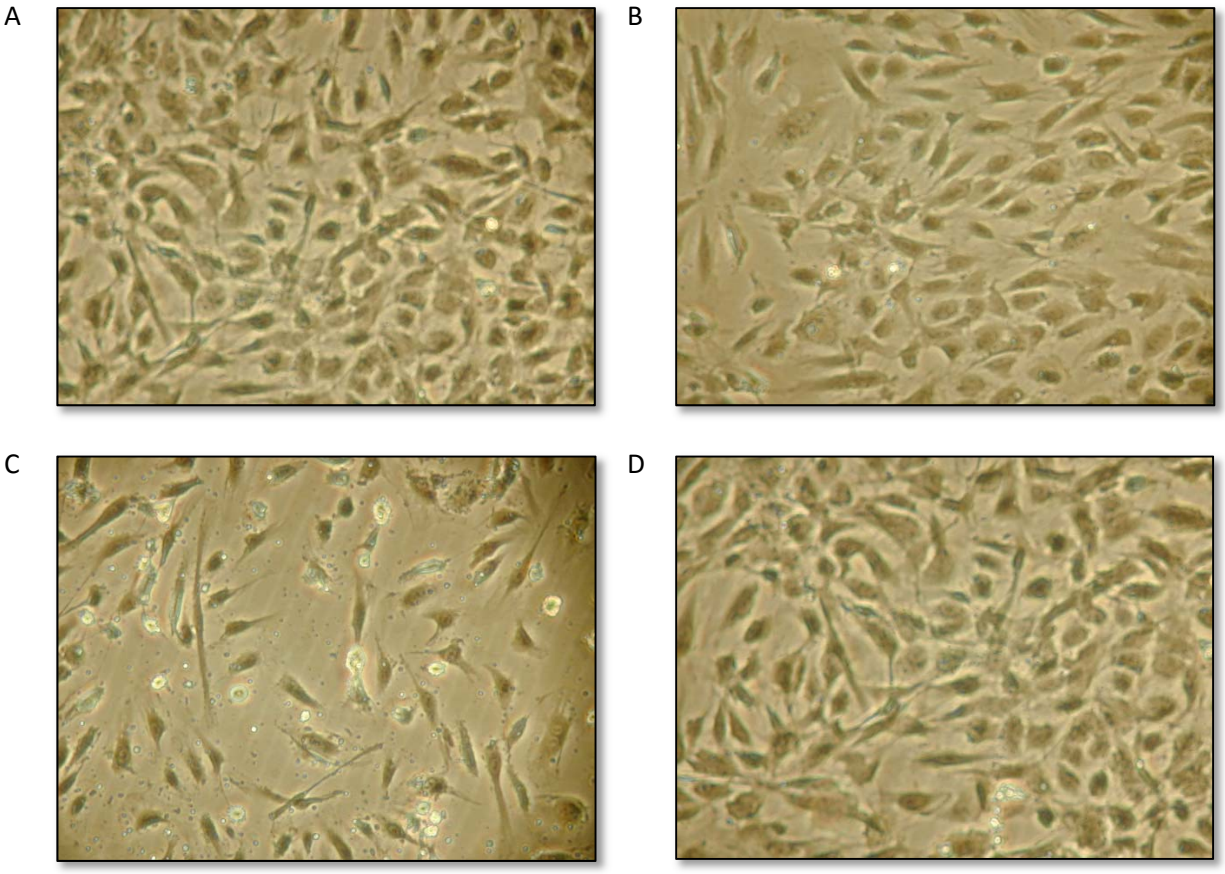

Figure 34: Light microscopy (10 x magnification) of cultured endothelial cells at the end of the experiment.
A: shows cells from the control (21% oxygen) group; **B:** the 1% oxygen group; **C:** the 0.1% oxygen group; **D:** the 0.1% ischaemia-reoxygenation group.

At the end of the experiment, endothelial cell viability was quantified using the *CellTiter Glo®* assay. HUVECs from the control sample showed the greatest luminescence, indicating the highest level of cell viability (Figure 35). Cells in the 1% O_2 and 0.1% O_2 environments showed reducing viability with the 0.1% sample showing the least viability. The 0.1% ischaemia-reoxygenation environment had increased viability compared with the 1% and 0.1% O_2 environments.

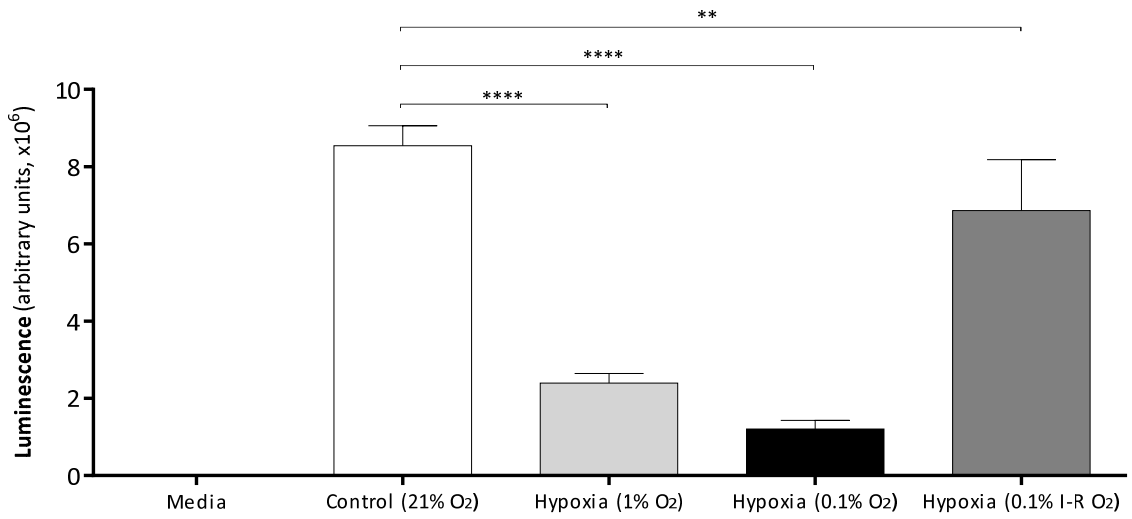

Figure 35: HUVEC cell viability in different hypoxic states measured using the CellTiter Glo® assay. Each bar represents an experimental condition. Exosome free medium was used as a control. Luminescence was measured using a plate reading spectrophotometer, with increased luminescence indicating increased viability. Control plates were placed in a standard incubator, hypoxia samples were placed in either a 1% or 0.1% oxygen hypoxic chamber for 24 hours. I-R=ischaemia-reoxygenation; plates in this group were placed in a hypoxic chamber for 12 hours and then a standard incubator for 12 hours. Multiple comparison ANOVA was carried out which showed a statistically significant difference between control and all other groups.

Confirming the Hypoxic Effect

The oxygen level was checked in each of the chambers prior to the start of the experiment. The internal sensor on each chamber confirmed that both chambers were had reached the preselected oxygen concentration (1% and 0.01%) and this was confirmed with an external oxygen detector.

The downstream effect of hypoxia was measured by carrying out RNA PCR for hypoxia inducible genes, with cyclophilin as a housekeeping gene used to calculate fold change using the delta-delta CT method (Figure 36). VEGF was upregulated in a stepwise fashion with increasing hypoxia, with maximal upregulation in the 0.1% group; it was downregulated in the 0.1% ischaemia-reoxygenation

group. VCAM was upregulated in all hypoxic states, maximally in 1% oxygen. TGF- β2 was upregulated in all hypoxic states, maximally in 0.1% oxygen.

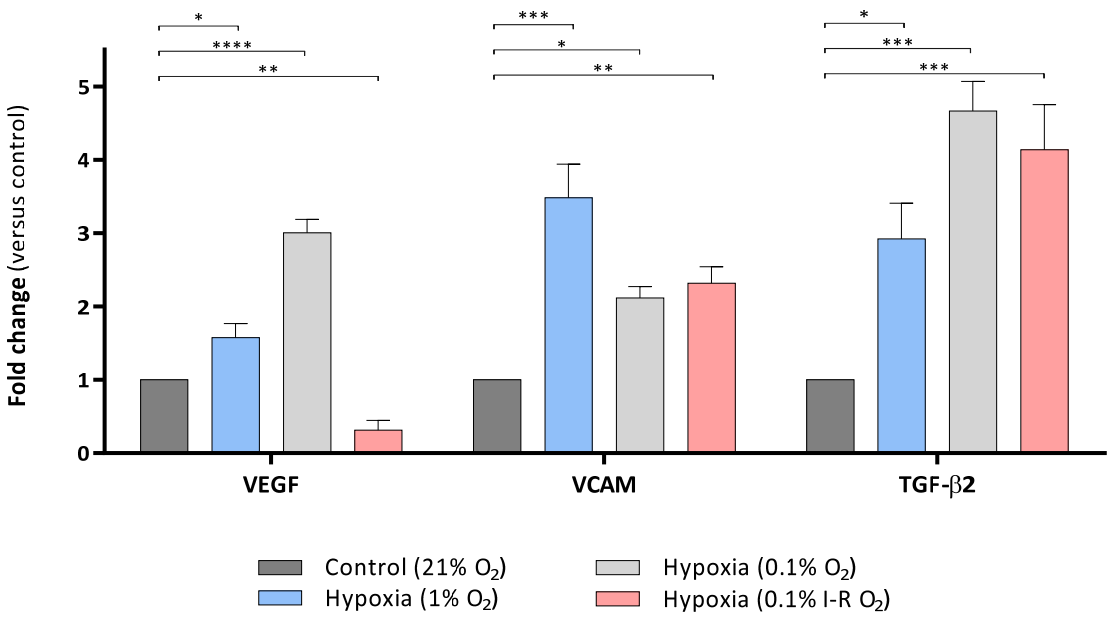

Figure 36: RNA PCR of cell pellets for hypoxia inducible genes after different hypoxic insults.
Fold change values were calculated using the delta-delta CT method with cyclophilin as a housekeeping gene. VEGF=vascular endothelial growth factor; VCAM=vascular cell adhesion protein; TGF-β2 transforming growth factor-β2. I-R=ischaemia-reoxygenation. N=6. A one-way ANOVA was conducted to determine whether there was a difference in fold change between control and different hypoxia states.

MicroRNA analysis

Figure 37 shows the effect of different cell culture medium sample volumes on RNA isolation efficiency. There was no significant difference in spike in control isolation efficiency between the different input sample volumes. For the ubiquitous human miRs -103 and -191, RNA isolation was

most efficient with a 200µL sample volume, and this volume was therefore selected for the remainder of the experiments.

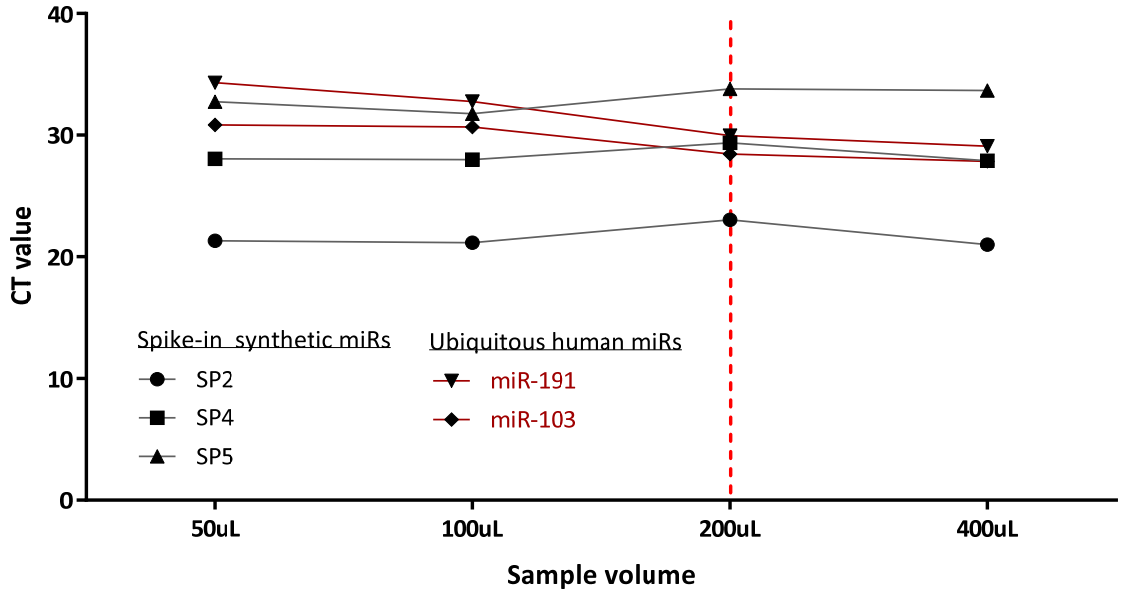

Figure 37: Determining the optimum sample volume in HUVEC culture medium supernatant. Different input volumes were used to determine the ideal sample volume (n=1 per sample volume tested). Levels of spike in miRs (grey) and ubiquitous miRs (red) were measured.

The RNA spike-in controls performed as shown previously in human plasma samples, with stepwise detection of synthetic RNAs *UniSP2*, 4 and 5 (Figure 38) and no difference of each spike in with hypoxia. The reverse transcription spike-in controls *UniSP6* and *cel-miR-39* and the PCR control *UniSP3* were stable across samples from the different hypoxic environments and each spike in was within 1 cycle in all samples, showing increased stability compared with the human plasma experiments (Figure 39).

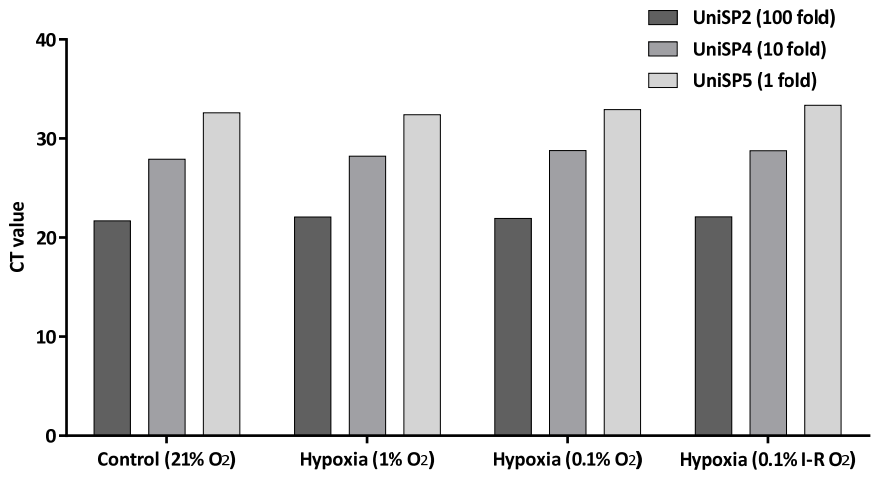

Figure 38: Detection of RNA spike-in controls in culture endothelial cells in each experimental state.
UniSP2, 4 and 5 (with relative concentrations of 100, 10 and 1 fold respectively) were spiked in prior to RNA isolation and provide information on the effectiveness of the RNA isolation process. A stepwise decreased concentration (increased CT value) was expected UniSP2>4>5. IR=ischaemia-reoxygenation.

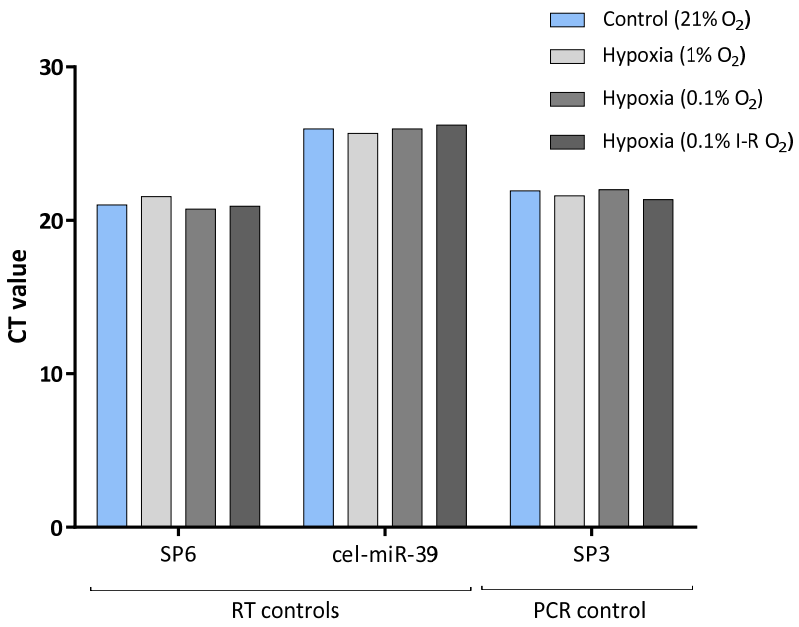

Figure 39: Detection of reverse-transcription and PCR spike-in controls in cultured endothelial cells in each experimental state.
UniSP6 and cel-miR-39 were spiked in prior to reverse transcription and UniSP3 was spiked in prior to PCR. IR=ischaemia-reoxygenation.

The Effect of Hypoxia on MicroRNA Release

RNA isolation and reverse transcription were carried out according to the protocols described previously. PCR analysis was carried out using the previously designed OxAMI plate (see Appendix 1: The OxAMI Plate, page 198) which had wells for all spike-in controls. Quality control results are shown in Table 14. The ubiquitous plasma miRs used previously (*miR-103* and -*191*) were not used as they had not been validated in endothelial cells, although they were detected. One control sample was excluded due to likely contamination; a signal was detected in the non-template control well and the reverse transcription spike-ins were detected at unusually high concentrations (CT value 10 vs. approximately 18 in all other samples). One sample from the 1% O2 group was excluded due to inefficient RNA isolation (*UniSP2* detected at low concentration (CT 31.9 vs. mean approximately 25 in the other samples) with no detection of *UniSP4* (detected in all other samples) or *UniSP5* (detected in 8/12 samples).

			Experiment group			
	Parameter	**Criteria**	Control	Hypoxia (1% O_2)	Hypoxia (0.1% O_2)	Hypoxia (0.1% O_2 I-R)
	Starting number of samples		4	4	4	4
1	RNA Isolation	*UniSP2/4/5 should be detectible at CT values ≤37 CT values should be SP2≤SP4≤SP5*	4	3	4	4
2	Reverse Transcription	*Both UniSP6 and cel-miR-39 should be detected*	3	4	4	4
3	PCR	*UniSP3 CT value should be 18-22 across dataset*	4	4	4	4
	TOTAL	*Number of samples passing all QC steps (%)*	3 (75)	3 (75)	4 (100)	4 (100)

Table 14: Quality control results for each stage of microRNA analysis of endothelial cell supernatant in the hypoxia experiment.
At each stage of the microRNA isolation and analysis process, the number of samples successfully reaching the pre-specified quality control criteria are shown. The Total row shows the number of samples successfully achieving all of the quality control criteria (percentages in brackets).

The number of miRs detected in cultured endothelial cell supernatant is shown in Figure 40. Although there is a trend towards fewer miRs being detected with increased hypoxia, this was not

statistically significant. The median number of miRs detected in all endothelial cell culture samples was 174 whereas in human plasma samples the median was 253, a difference that was statistically significant (one-way repeated measures ANOVA, p=<0.001). The mean raw CT value of all detected miRs was similar in cultured endothelial cell supernatant and plasma, with no statistical difference between the groups (Figure 41).

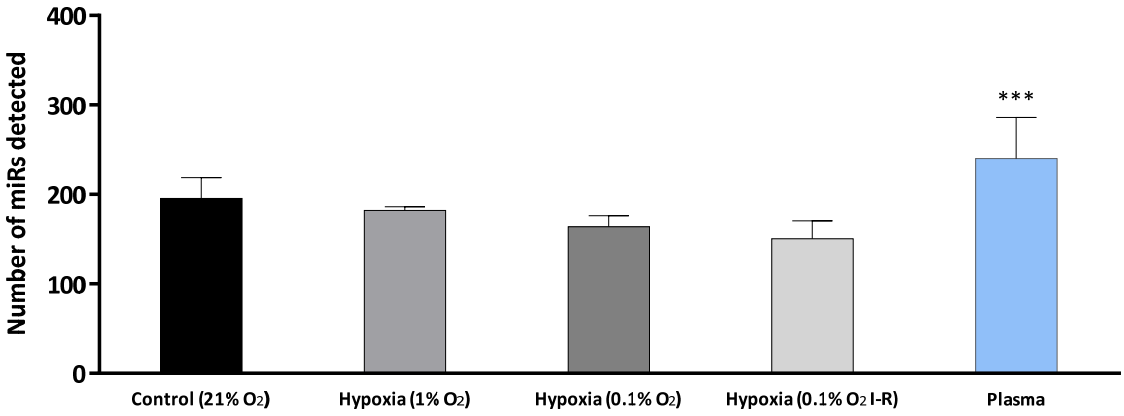

Figure 40: The number of microRNAs detected at each time point in cultured endothelial cells at the end of the experiment, compared with the number of miRs detected in human plasma.
miRs detected with CT≤37 in samples passing all quality control steps were included (error bars show standard deviation). Plasma refers to all human plasma samples at timepoint 1.2 analysed on the OxAMI plate in the Discovery Experiment (n=14). A one-way repeated measures ANOVA showed there was no difference in the number of miRs detected between the different endothelial cell groups, but there was a statistically significant difference between the number of miRs detected in human plasma and all four cultured endothelial cell groups (p=<0.001). The numbers shown in this graph are not directly comparable with figure 16 as this analysis was carried out on the OxAMI plate rather than plate I and II, therefore the maximum possible of miRs that could be detected was 383, rather than 752.

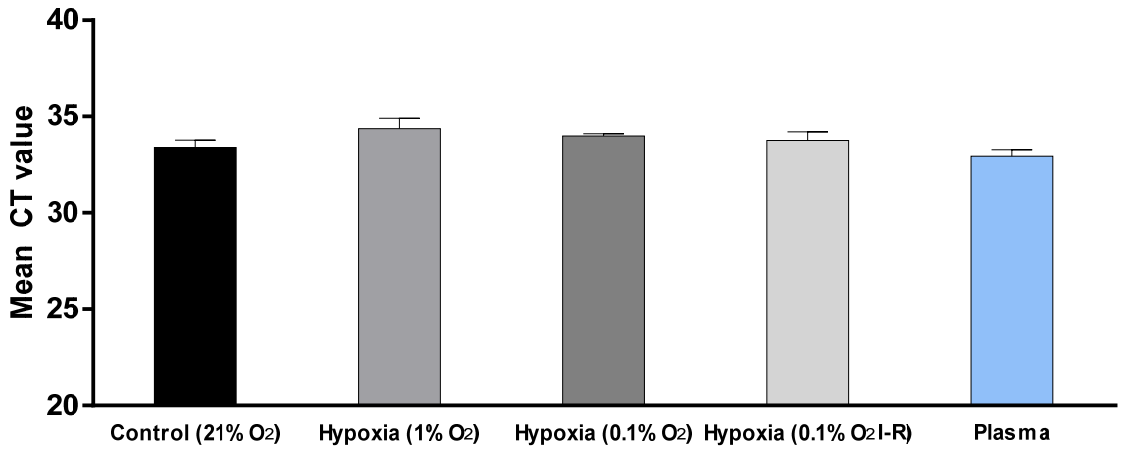

Figure 41: Mean microRNA detection at each time point.
The mean cycle threshold (CT) value was calculated for all miRs in all samples at each time-point. Raw (not normalised) CT values were used. Each bar represents the mean of all samples passing the quality control analysis (error bars show standard deviation). A one-way repeated measures ANOVA showed there was no statistically significant difference in miR expression between the four time-points, or with human plasma.

A Venn diagram was constructed to illustrate which miRs were detected in cultured endothelial cell supernatant, which were detected in human plasma, and which were detected in both (Figure 42). The only two miRs detected only in cultured endothelial cells were *miR-1*37 and *-433*. Although they were detected in a small number of human plasma samples, as the median CT value was 39 (above the upper level of reliable detection) they were therefore classified as 'not detected'.

A

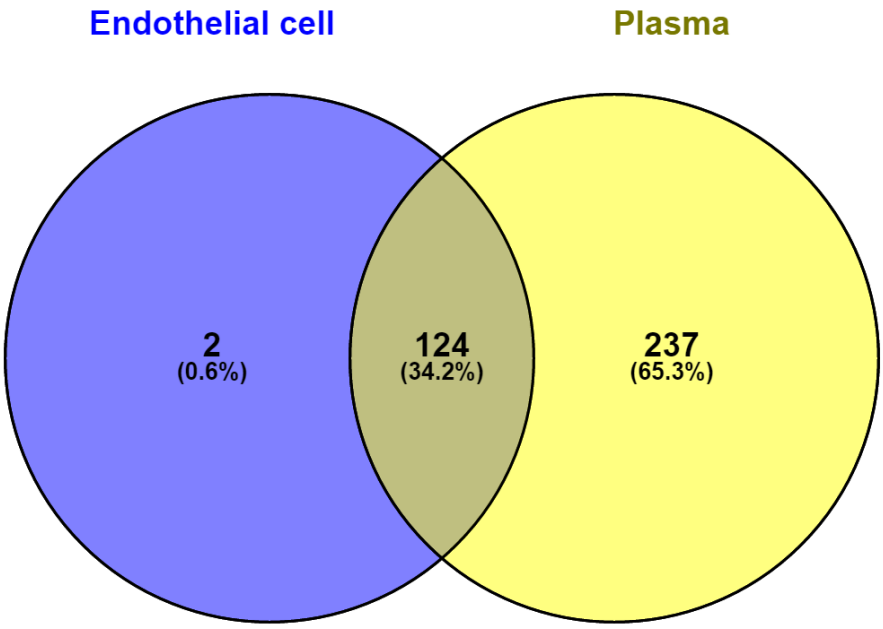

B

Endothelial only	Both		Plasma only		
hsa-miR-137	*hsa-let-7a-5p*	*hsa-miR-27a-3p*	*hsa-let-7a-3p*	*hsa-miR-20a-3p*	*hsa-miR-487b-3p*
hsa-miR-433-3p	*hsa-let-7b-5p*	*hsa-miR-27b-3p*	*hsa-let-7b-3p*	*hsa-miR-20b-5p*	*hsa-miR-490-3p*
	hsa-let-7d-3p	*hsa-miR-28-3p*	*hsa-let-7c-3p*	*hsa-miR-210-3p*	*hsa-miR-490-5p*
	hsa-let-7d-5p	*hsa-miR-29a-3p*	*hsa-let-7e-3p*	*hsa-miR-211-5p*	*hsa-miR-491-5p*
	hsa-let-7e-5p	*hsa-miR-29a-5p*	*hsa-let-7f-1-3p*	*hsa-miR-212-3p*	*hsa-miR-493-3p*
	hsa-let-7g-5p	*hsa-miR-30a-3p*	*hsa-let-7g-3p*	*hsa-miR-21-3p*	*hsa-miR-495-3p*
	hsa-let-7i-5p	*hsa-miR-30a-5p*	*hsa-let-7i-3p*	*hsa-miR-214-5p*	*hsa-miR-497-5p*
	hsa-miR-100-5p	*hsa-miR-30b-5p*	***hsa-miR-1***	*hsa-miR-216a-5p*	***hsa-miR-499a-3p***
	hsa-miR-103a-3p	*hsa-miR-30c-5p*	*hsa-miR-101-3p*	*hsa-miR-221-5p*	***hsa-miR-499a-5p***
	hsa-miR-106a-5p	*hsa-miR-30d-5p*	*hsa-miR-101-5p*	*hsa-miR-223-3p*	*hsa-miR-500a-5p*
	hsa-miR-107	*hsa-miR-30e-3p*	*hsa-miR-106b-3p*	*hsa-miR-223-5p*	*hsa-miR-501-5p*
	hsa-miR-10a-5p	*hsa-miR-31-5p*	*hsa-miR-106b-5p*	*hsa-miR-22-3p*	*hsa-miR-502-3p*
	hsa-miR-10b-5p	*hsa-miR-320a*	*hsa-miR-122-5p*	*hsa-miR-224-3p*	*hsa-miR-502-5p*
	hsa-miR-125a-3p	*hsa-miR-320b*	*hsa-miR-124-3p*	*hsa-miR-224-5p*	*hsa-miR-503-5p*
	hsa-miR-125a-5p	*hsa-miR-320c*	*hsa-miR-1245a*	*hsa-miR-22-5p*	*hsa-miR-505-5p*
	hsa-miR-125b-5p	*hsa-miR-320d*	*hsa-miR-1249*	*hsa-miR-23b-5p*	*hsa-miR-509-3p*
	hsa-miR-1260a	*hsa-miR-324-5p*	*hsa-miR-125b-1-3p*	*hsa-miR-24-1-5p*	*hsa-miR-511-5p*
	hsa-miR-126-3p	*hsa-miR-328-3p*	*hsa-miR-125b-2-3p*	*hsa-miR-24-2-5p*	*hsa-miR-517c-3p*
	hsa-miR-126-5p	*hsa-miR-337-3p*	*hsa-miR-1271-5p*	*hsa-miR-26b-3p*	*hsa-miR-518e-3p*
	hsa-miR-130a-3p	*hsa-miR-342-3p*	*hsa-miR-127-3p*	*hsa-miR-26b-5p*	*hsa-miR-518f-3p*
	hsa-miR-130b-5p	*hsa-miR-342-5p*	*hsa-miR-127-5p*	*hsa-miR-27a-5p*	*hsa-miR-520h*
	hsa-miR-132-3p	*hsa-miR-34a-5p*	*hsa-miR-128-3p*	*hsa-miR-28-5p*	*hsa-miR-524-5p*
	hsa-miR-134-5p	*hsa-miR-361-5p*	*hsa-miR-130b-3p*	*hsa-miR-296-5p*	*hsa-miR-525-5p*
	hsa-miR-139-3p	*hsa-miR-365a-3p*	***hsa-miR-133a-3p***	*hsa-miR-299-5p*	*hsa-miR-539-5p*
	hsa-miR-139-5p	*hsa-miR-365b-5p*	***hsa-miR-133b***	*hsa-miR-29b-2-5p*	*hsa-miR-542-5p*
	hsa-miR-140-3p	*hsa-miR-374b-5p*	*hsa-miR-135a-5p*	*hsa-miR-29b-3p*	*hsa-miR-545-3p*
	hsa-miR-146a-5p	*hsa-miR-376c-3p*	*hsa-miR-136-5p*	*hsa-miR-29c-3p*	*hsa-miR-548a-3p*
	hsa-miR-150-5p	*hsa-miR-379-5p*	*hsa-miR-140-5p*	*hsa-miR-29c-5p*	*hsa-miR-548c-5p*
	hsa-miR-151a-3p	*hsa-miR-382-5p*	*hsa-miR-141-3p*	*hsa-miR-301a-3p*	*hsa-miR-550a-3p*
	hsa-miR-151a-5p	*hsa-miR-409-3p*	*hsa-miR-141-5p*	*hsa-miR-302a-3p*	*hsa-miR-551a*
	hsa-miR-152-3p	*hsa-miR-411-5p*	*hsa-miR-142-3p*	*hsa-miR-302d-3p*	*hsa-miR-551b-3p*
	hsa-miR-155-5p	*hsa-miR-421*	*hsa-miR-142-5p*	*hsa-miR-30d-3p*	*hsa-miR-556-3p*
	hsa-miR-15a-5p	*hsa-miR-423-3p*	*hsa-miR-143-3p*	*hsa-miR-30e-5p*	*hsa-miR-570-3p*
	hsa-miR-15b-5p	*hsa-miR-423-5p*	*hsa-miR-143-5p*	*hsa-miR-323a-3p*	*hsa-miR-576-3p*
	hsa-miR-16-5p	*hsa-miR-425-5p*	*hsa-miR-144-3p*	*hsa-miR-324-3p*	*hsa-miR-576-5p*
	hsa-miR-181a-5p	*hsa-miR-432-5p*	*hsa-miR-144-5p*	*hsa-miR-32-5p*	*hsa-miR-582-5p*
	hsa-miR-181b-5p	*hsa-miR-455-3p*	*hsa-miR-145-3p*	*hsa-miR-326*	*hsa-miR-589-5p*
	hsa-miR-185-5p	*hsa-miR-455-5p*	*hsa-miR-145-5p*	*hsa-miR-329-3p*	*hsa-miR-590-3p*
	hsa-miR-18a-5p	*hsa-miR-484*	*hsa-miR-1468-5p*	*hsa-miR-330-3p*	*hsa-miR-595*
	hsa-miR-18b-5p	*hsa-miR-485-3p*	*hsa-miR-146b-5p*	*hsa-miR-331-3p*	*hsa-miR-598-3p*
	hsa-miR-1908-5p	*hsa-miR-501-3p*	*hsa-miR-148a-3p*	*hsa-miR-331-5p*	*hsa-miR-602*
	hsa-miR-1913	*hsa-miR-505-3p*	*hsa-miR-148b-3p*	*hsa-miR-335-3p*	*hsa-miR-610*
	hsa-miR-192-5p	*hsa-miR-532-3p*	*hsa-miR-149-5p*	*hsa-miR-335-5p*	*hsa-miR-615-3p*
	hsa-miR-193a-5p	*hsa-miR-532-5p*	*hsa-miR-154-5p*	*hsa-miR-337-5p*	*hsa-miR-624-5p*
	hsa-miR-196b-5p	*hsa-miR-543*	*hsa-miR-15b-3p*	*hsa-miR-338-3p*	*hsa-miR-625-3p*

	hsa-miR-1972	*hsa-miR-574-3p*	*hsa-miR-16-1-3p*	*hsa-miR-338-5p*	*hsa-miR-628-3p*
	hsa-miR-197-3p	*hsa-miR-584-5p*	*hsa-miR-16-2-3p*	*hsa-miR-339-3p*	*hsa-miR-628-5p*
	hsa-miR-200c-3p	*hsa-miR-590-5p*	*hsa-miR-17-3p*	*hsa-miR-339-5p*	*hsa-miR-629-5p*
	hsa-miR-20a-5p	*hsa-miR-632*	*hsa-miR-17-5p*	*hsa-miR-33a-5p*	*hsa-miR-636*
	hsa-miR-2110	*hsa-miR-665*	*hsa-miR-181a-2-3p*	*hsa-miR-340-3p*	*hsa-miR-642a-5p*
	hsa-miR-214-3p	*hsa-miR-7-5p*	*hsa-miR-181a-3p*	*hsa-miR-346*	*hsa-miR-643*
	hsa-miR-215-5p	*hsa-miR-877-5p*	*hsa-miR-181c-3p*	*hsa-miR-361-3p*	*hsa-miR-651-5p*
	hsa-miR-21-5p	*hsa-miR-92a-3p*	*hsa-miR-181c-5p*	*hsa-miR-362-3p*	*hsa-miR-652-3p*
	hsa-miR-217	*hsa-miR-92b-3p*	*hsa-miR-181d-5p*	*hsa-miR-362-5p*	*hsa-miR-660-5p*
	hsa-miR-218-5p	*hsa-miR-93-3p*	*hsa-miR-183-5p*	*hsa-miR-363-3p*	*hsa-miR-662*
	hsa-miR-221-3p	*hsa-miR-93-5p*	*hsa-miR-186-5p*	*hsa-miR-369-5p*	*hsa-miR-663a*
	hsa-miR-222-3p	*hsa-miR-98-5p*	*hsa-miR-187-3p*	*hsa-miR-370-3p*	*hsa-miR-664a-3p*
	hsa-miR-23a-3p	*hsa-miR-99a-5p*	*hsa-miR-188-5p*	*hsa-miR-371a-5p*	*hsa-miR-671-5p*
	hsa-miR-23b-3p	*hsa-miR-99b-3p*	*hsa-miR-18a-3p*	*hsa-miR-373-3p*	*hsa-miR-675-3p*
	hsa-miR-24-3p	*hsa-miR-99b-5p*	*hsa-miR-190a-5p*	*hsa-miR-375*	*hsa-miR-708-3p*
	hsa-miR-25-3p	*SNORD38B*	*hsa-miR-191-5p*	*hsa-miR-376a-3p*	*hsa-miR-708-5p*
	hsa-miR-26a-5p	*U6 snRNA*	*hsa-miR-193b-3p*	*hsa-miR-376b-3p*	*hsa-miR-7-1-3p*
			hsa-miR-193b-5p	*hsa-miR-378a-3p*	*hsa-miR-744-3p*
			hsa-miR-194-5p	*hsa-miR-378a-5p*	*hsa-miR-744-5p*
			hsa-miR-195-5p	*hsa-miR-381-3p*	*hsa-miR-760*
			hsa-miR-196a-5p	*hsa-miR-410-3p*	*hsa-miR-765*
			hsa-miR-199a-3p	*hsa-miR-412-3p*	*hsa-miR-766-3p*
			hsa-miR-199a-5p	*hsa-miR-424-3p*	*hsa-miR-769-5p*
			hsa-miR-199b-5p	*hsa-miR-424-5p*	*hsa-miR-874-3p*
			hsa-miR-19a-3p	*hsa-miR-425-3p*	*hsa-miR-885-3p*
			hsa-miR-19b-3p	*hsa-miR-431-5p*	*hsa-miR-885-5p*
			hsa-miR-200a-3p	*hsa-miR-450b-5p*	*hsa-miR-887-3p*
			hsa-miR-202-5p	*hsa-miR-451a*	*hsa-miR-940*
			hsa-miR-203a	*hsa-miR-452-5p*	*hsa-miR-941*
			hsa-miR-204-5p	*hsa-miR-454-3p*	*hsa-miR-942-5p*
			hsa-miR-205-5p	*hsa-miR-483-3p*	*hsa-miR-95-3p*
			hsa-miR-206	*hsa-miR-483-5p*	*hsa-miR-96-5p*
			hsa-miR-208a-5p	*hsa-miR-486-3p*	*hsa-miR-99a-3p*
			hsa-miR-208b-3p	*hsa-miR-486-5p*	*SNORD49A*

Figure 42: miR release in human plasma versus cultured HUVECs

A: Venn diagram to illustrate miR release from cultured endothelial cells and human plasma. B: List of all miRs identified by the Venn diagram. List of endothelial cell miRs generated from the control samples in the hypoxic chamber experiment. List of human plasma miRs generated from all time point 2.1 samples in the Discovery Experiment. In order to be included in this diagram, a miR had to be detected in >25% of samples with a CT value ≤38. Bold indicates a known myocardial miR. Venn diagram generated using Venny 2.1[123].

The miR qPCR raw data from the endothelial cell culture experiment was then global mean normalised to allow further analysis. miRs showing a dose-response relationship with hypoxia are shown in Table 15. 29 miRs decreased in concentration with increasing hypoxia (i.e. CT value control>1% oxygen>0.1% oxygen) and 34 miRs increased.

A MiR concentration reduces with hypoxia

	Mean normalised CT value			ΔCT between groups	
miR	**Control (21%)**	**1% oxygen**	**0.1% oxygen**	**Delta 21%-1%**	**Delta 1%-0.1%**
hsa-let-7d-5p	4.23	4.44	4.61	0.21	0.17
hsa-miR-1245a	8.56	10.05	10.35	1.49	0.30
hsa-miR-125b-5p	0.76	1.12	1.36	0.37	0.24
hsa-miR-139-3p	7.11	8.40	8.59	1.29	0.19
hsa-miR-146a-5p	3.89	3.93	4.90	0.05	0.97
hsa-miR-15b-5p	4.76	5.14	6.02	0.38	0.88
hsa-miR-185-5p	5.82	5.94	6.40	0.12	0.47
hsa-miR-193a-5p	4.60	4.68	4.85	0.09	0.17
hsa-miR-20a-5p	2.78	2.90	3.13	0.13	0.23
hsa-miR-217	2.07	2.14	2.51	0.06	0.37
hsa-miR-23a-3p	-2.45	-2.18	-2.06	0.27	0.11
hsa-miR-23b-3p	-0.56	-0.36	-0.30	0.20	0.05
hsa-miR-24-3p	-1.36	-0.93	-0.87	0.43	0.06
hsa-miR-25-3p	1.82	1.89	2.07	0.07	0.18
hsa-miR-27b-3p	2.23	2.33	2.83	0.10	0.50
hsa-miR-28-5p	5.92	6.61	6.83	0.69	0.22
hsa-miR-30a-3p	4.19	4.40	4.87	0.21	0.47
hsa-miR-320b	1.82	1.96	2.02	0.14	0.06
hsa-miR-320c	3.03	3.18	4.03	0.15	0.86
hsa-miR-331-3p	7.26	7.63	8.39	0.36	0.77
hsa-miR-361-5p	2.55	2.67	2.90	0.12	0.23
hsa-miR-382-5p	2.17	2.60	2.82	0.44	0.21
hsa-miR-423-3p	4.52	5.09	5.93	0.57	0.84
hsa-miR-584-5p	6.27	6.39	7.44	0.13	1.05
hsa-miR-744-5p	8.84	9.28	9.79	0.44	0.52
hsa-miR-92a-3p	0.69	0.94	0.96	0.25	0.02
hsa-miR-99a-5p	2.85	2.98	3.40	0.13	0.42
hsa-miR-99b-3p	4.54	4.75	5.36	0.21	0.62
hsa-miR-99b-5p	-0.05	0.49	0.79	0.54	0.30

B MiR concentration increases with hypoxia

	Mean normalised CT value			ΔCT between groups	
Target	**Control (21%)**	**1% oxygen**	**0.1% oxygen**	**Delta 21%-1%**	**Delta 1%-0.1%**
hsa-let-7g-5p	2.97	2.81	2.71	-0.17	-0.09
hsa-miR-1271-5p	9.07	8.06	7.39	-1.01	-0.67
hsa-miR-130b-3p	8.87	8.64	8.45	-0.23	-0.19
hsa-miR-18b-5p	7.27	6.74	6.24	-0.54	-0.50
hsa-miR-1908-5p	7.61	7.16	6.28	-0.46	-0.87
hsa-miR-195-5p	7.41	6.97	5.22	-0.44	-1.75
hsa-miR-196b-5p	3.53	3.33	3.13	-0.19	-0.20
hsa-miR-1972	2.78	2.54	1.99	-0.24	-0.55
hsa-miR-2110	6.98	5.61	5.57	-1.38	-0.04
hsa-miR-214-3p	7.67	6.65	6.44	-1.02	-0.21
hsa-miR-30c-5p	4.74	4.54	3.60	-0.20	-0.94
hsa-miR-30e-5p	8.44	7.02	7.02	-1.42	0.00
hsa-miR-328-3p	7.69	7.30	5.75	-0.40	-1.55
hsa-miR-329-3p	7.99	7.39	6.26	-0.59	-1.13
hsa-miR-335-3p	6.95	6.85	5.71	-0.11	-1.13
hsa-miR-362-5p	9.35	8.87	7.71	-0.48	-1.16
hsa-miR-365a-3p	5.97	5.64	5.30	-0.32	-0.34
hsa-miR-376a-3p	11.01	8.42	6.14	-2.59	-2.28
hsa-miR-378a-3p	7.52	6.35	6.22	-1.17	-0.13
hsa-miR-423-5p	4.69	4.61	3.51	-0.08	-1.09
hsa-miR-455-3p	3.28	3.08	3.04	-0.20	-0.04
hsa-miR-455-5p	6.56	6.42	6.28	-0.14	-0.13
hsa-miR-483-5p	9.05	8.64	6.67	-0.41	-1.97
hsa-miR-491-5p	11.29	10.55	8.13	-0.74	-2.42
hsa-miR-501-3p	7.69	7.06	6.85	-0.63	-0.21
hsa-miR-502-5p	9.98	9.28	7.00	-0.70	-2.28
hsa-miR-543	6.05	4.50	4.48	-1.55	-0.02
hsa-miR-548c-5p	8.33	7.33	7.26	-1.00	-0.07
hsa-miR-590-3p	9.34	8.70	7.57	-0.64	-1.13
hsa-miR-632	7.99	7.75	6.45	-0.23	-1.31
hsa-miR-766-3p	8.50	6.67	5.53	-1.83	-1.14
hsa-miR-92b-3p	7.14	6.39	5.48	-0.75	-0.91
SNORD49A	5.11	4.91	4.90	-0.20	0.00
U6 snRNA	1.77	0.70	0.70	-1.06	0.00

Table 15: Patterns of microRNA release in the supernatant of cultured endothelial cells after different hypoxic insults.

Cultured endothelial cells were exposed to normoxia (control), 1% oxygen or 0.1% oxygen for 24 hours. qPCR analysis was carried out on the supernatant. Raw data was global mean normalised. All miRs showing a dose-response relationship with hypoxia are shown here. **A:** all miRs with reducing concentration with hypoxia (Control>1% oxygen>0.1% oxygen); **B:** all miRs with increasing concentration with hypoxia (Control<1% oxygen<0.1% oxygen). Heat mapping was used to illustrate

direction and magnitude of change; blue indicates that a miR decreases in concentration with hypoxia and red indicates that it increases with hypoxia. CT=cycle threshold.

The effect of hypoxia on miR release into cultured endothelial cell supernatant is shown in Figure 43. 41 miRs were only detected in hypoxic samples and 13 were only detected in control samples. Incorporating the data for the 0.1% ischaemia-reoxygenation group revealed a further 13 miRs that were only detectable in this group (Figure 44).

A

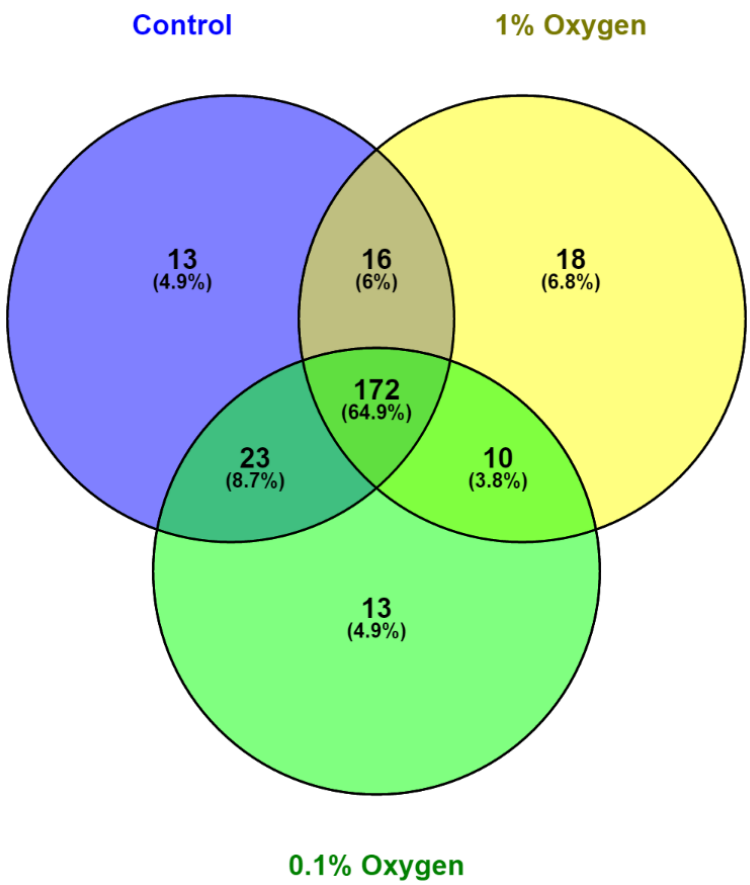

B

1. MiRs detected in control but not hypoxic samples	2. MiRs detected in hypoxic but not control samples
hsa-miR-101-3p	*hsa-let-7b-3p*
hsa-miR-122-5p	*hsa-let-7f-1-3p*
hsa-miR-125b-2-3p	*hsa-miR-106b-3p*
hsa-miR-140-5p	*hsa-miR-125b-1-3p*
hsa-miR-192-5p	*hsa-miR-148b-3p*
hsa-miR-203a	*hsa-miR-18a-3p*
hsa-miR-224-5p	*hsa-miR-190a-5p*
hsa-miR-330-3p	*hsa-miR-191-5p*
hsa-miR-335-5p	*hsa-miR-206*
hsa-miR-362-3p	*hsa-miR-210-3p*
hsa-miR-570-3p	*hsa-miR-216a-5p*
hsa-miR-662	*hsa-miR-219a-5p*
hsa-miR-885-3p	*hsa-miR-221-5p*
	hsa-miR-23b-5p

	hsa-miR-296-5p *hsa-miR-299-5p* *hsa-miR-29b-2-5p* *hsa-miR-337-5p* *hsa-miR-339-3p* *hsa-miR-361-3p* *hsa-miR-376b-3p* *hsa-miR-483-3p* *hsa-miR-486-3p* *hsa-miR-486-5p* *hsa-miR-509-3p* *hsa-miR-550a-3p* *hsa-miR-551b-3p* *hsa-miR-582-5p* *hsa-miR-589-5p* *hsa-miR-610* *hsa-miR-629-5p* *hsa-miR-660-5p* *hsa-miR-708-3p* *hsa-miR-708-5p* *hsa-miR-769-5p* *hsa-miR-874-3p* *hsa-miR-934* *hsa-miR-95-3p* *hsa-miR-99a-3p*

Figure 43: Patterns of microRNA release in the supernatant of cultured endothelial cells after different hypoxic insults.

A: Venn diagram illustrating the number of miRs detected in hypoxic samples but not control samples and vice versa; **B:** list of all miRs detected only in control samples (1) and list of miRs detected in hypoxic but not control samples. Venn diagram generated using Venny 2.1[123].

A

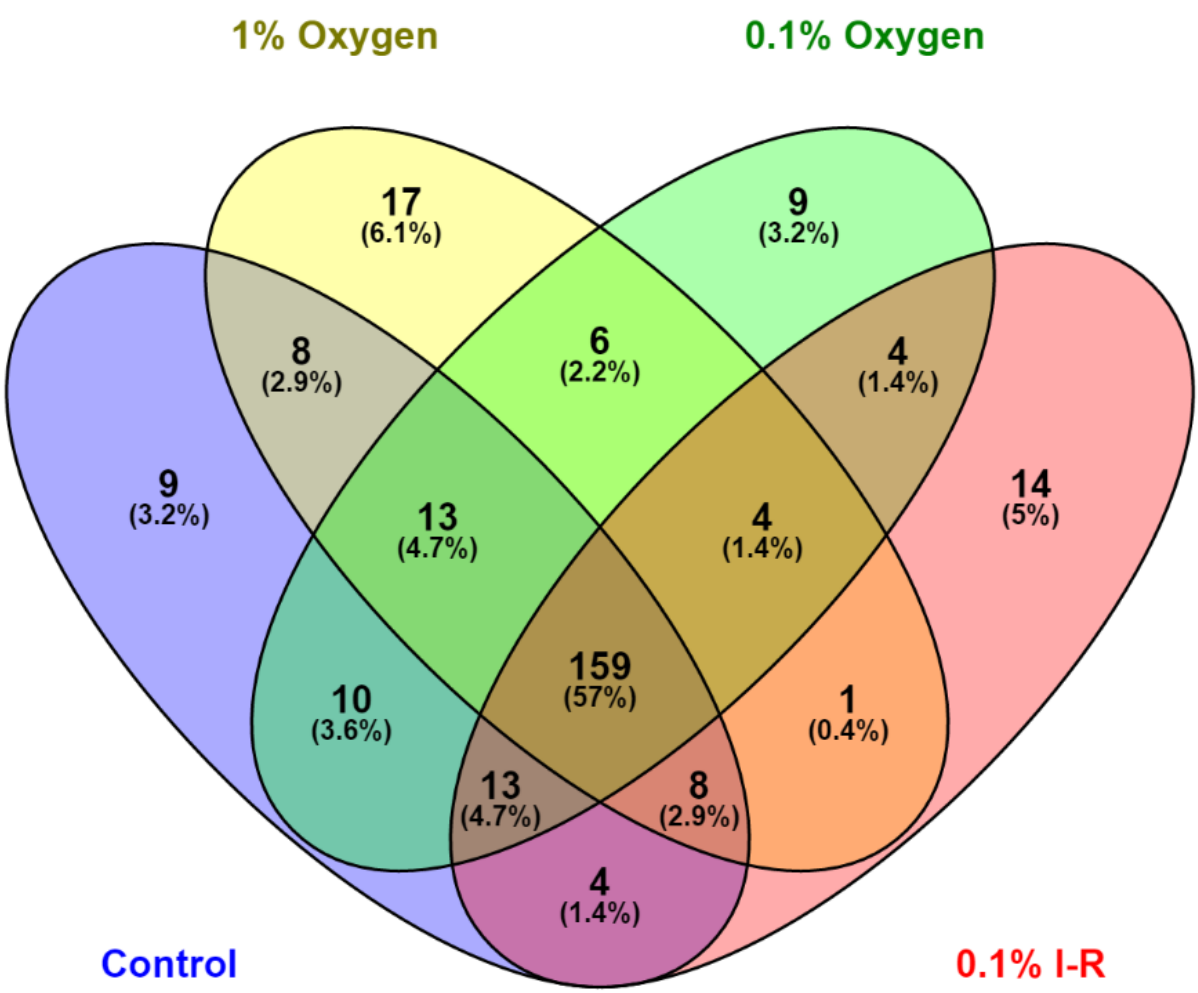

B

MiRs only detected in the 0.1% oxygen ischaemia-reoxygenation samples	
hsa-let-7c-3p	*hsa-miR-374a-3p*
hsa-miR-136-5p	*hsa-miR-410-3p*
hsa-miR-142-5p	*hsa-miR-450b-5p*
hsa-miR-186-5p	*hsa-miR-511-5p*
hsa-miR-199b-5p	*hsa-miR-517c-3p*
hsa-miR-20a-3p	*hsa-miR-576-3p*
hsa-miR-216b-5p	*hsa-miR-628-5p*

Figure 44: Patterns of microRNA release in the supernatant of cultured endothelial cells after different hypoxic insults, including 0.1% hypoxia-reoxygenation.
A: Venn diagram illustrating the number of miRs detected in each hypoxic condition, and overlap between the groups; **B:** list of all miRs detected only in the 0.1% ischaemia-reoxygenation group. Venn diagram generated using Venny 2.1[123].

11.4 Discussion

HUVECs were obtained, thawed and cultured in a standard fashion. Once they were confluent at passage 3 they were transferred to one of four different experimental conditions for 24 hours, a control experiment (21% oxygen in a standard incubator), 1% oxygen, 0.1% oxygen or 0.1% oxygen for 12 hours then 21% oxygen for 12 hours. At the end of the 24-hour period, the supernatant was collected, cell debris removed and samples from each experimental condition were snap frozen in aliquots. The cells from the plates were removed and either underwent viability assessment or were stored for RNA or protein analysis.

Light microscopy carried out at the start and end of the experiment showed that, in the control group, the endothelial cells continued to grow, becoming more confluent (Figure 33, Figure 34). In hypoxia, there was evidence of cell death; more debris was present and fewer cells were adherent to the plate. This was most evident in the most severe hypoxia (0.1% oxygen) and least evident in the ischaemia-reoxygenation group.

Viability assessment using the CellTiter Glo® assay showed greatest luminescence, which suggests the most viability, in the control cells (Figure 35). There was a stepwise decrease in luminescence (viability) in 1% and 0.1% hypoxia, confirming the findings from light microscopy – that the more hypoxic the environment, the fewer cells were viable. The ischaemia-reoxygenation sample showed more cell viability than either of the two other hypoxic conditions suggesting either that 12 hours of hypoxia caused less cell damage than 24 hours of hypoxia, or that there was a degree of recovery in the subsequent 12 hours, or both.

Measurement of hypoxia inducible genes using RNA PCR revealed upregulation of all three genes measured (VEGF, VCAM, TGF-B2) in conditions of hypoxia. The effect on VEGF was as might be

expected; detectable levels increased with severity of hypoxia. Ischaemia-reoxygenation led to a downregulation in VEGF, a phenomenon which has been demonstrated in renal ischaemia-reperfusion which may reflect reperfusion injury[124]. VCAM was upregulated in hypoxia and, unlike VEGF, this effect was greatest in 1% oxygen. TGF-β2 was upregulated in all hypoxia groups in a stepwise fashion, though upregulated less in the 0.1% ischaemia-reoxygenation group than the 0.1% oxygen group which may reflect a degree of recovery in this environment.

Confirmation of the effect of hypoxia using viability assessment, light microscopy and PCR of hypoxia-inducible proteins allowed the next phase of analysis to be carried out in the knowledge that the cells had received a measurable hypoxic insult. Previously optimised miR analysis protocols were validated for the analysis of cell culture supernatant and no changes were required with this new sample type. The same input volume (200µL) was appropriate and the multiple spike-in controls performed as expected. Pre-specified quality control criteria were met in the majority of samples.

The number of detectable miRs in cultured endothelial cell supernatant was significantly less than in plasma (Figure 40). Intuitively this would be expected, as the plasma miR signature is from multiple cell types whereas the endothelial cell supernatant is from only one cell type. It is possible, though perhaps less likely, that this phenomenon is related to technical rather than biological factors. The fact that there is no difference in CT value between cultured endothelial cell supernatant and plasma (Figure 41) would suggest that the difference in number of miRs detected is due to a true biological, rather than technical, difference between the two experiments.

Comparison of the miR signature in cultured endothelial call supernatant with human plasma revealed that very few miRs (two: *miR-137* and *-433*) were only detectable in cultured endothelial cell supernatant where they were detected at low concentration (median CT value 36.6) so it is conceivable that this weak signal was lost in the human plasma. All other miRs detected in cultured

endothelial cell supernatant were also detected in plasma, which was expected as the endothelial cell miR signature should be detectable in plasma. The known myocardial miRs (e.g. *miR-1*, *-133a/b*, *-208*, *-499*) are only detected in human plasma and not in endothelial cell supernatant and as these are known to be cardiomyocyte specific, this was also expected.

Figure 43 and Figure 44 illustrate the effect of hypoxia on miR release into endothelial cell supernatant. Some miRs are exclusively detectable in the supernatant of cells exposed to a hypoxic insult and these may relate to hypoxia inducible genes with a potential role in angiogenesis, whereas some are only detectable in control supernatant and these may be downregulated with hypoxia. Whether these relate to a protective mechanism that is inhibited by hypoxia would be an interesting question for future work. Finally, miRs released only into supernatant exposed to ischaemia-reoxygenation were identified.

This experiment has answered a number of important questions for the next phase of the project. By characterising which miRs are released from endothelial cells, these miRs can be included in the OxAMI focused plate design for the Validation Experiment. As a validation of previously published work, I have demonstrated that the myocardial miRs are not detectable in endothelial cell supernatant. Finally, I have identified the miRs which are increased and decreased with hypoxia, which may be important in understanding more about endothelial injury in myocardial infarction.

12 MicroRNA release in STEMI: Validation

12.1 Introduction

The work carried out in the Discovery Experiment demonstrated the feasibility of sample collection, microRNA isolation and quantification in patients undergoing primary PCI for ST elevation myocardial infarction. Detailed microRNA analysis confirmed previously published relationships, such as the association between troponin and myocardial microRNA release. In this chapter I validated these findings using a second cohort of patients, and analysed the relationship between miR release and other clinical parameters that have been less well studied in the microRNA field.

I used the microRNA analysis results from the Discovery Experiment, and further data from the endothelial cell analysis, to design a new plate, the 'OxAMI-focused plate' which allowed the analysis of three samples per plate, compared with one sample per plate using the OxAMI plate. This strategy increased throughput and allowed recruitment and analysis with a much larger cohort. The same methods for microRNA analysis, normalisation and data management were used.

Where relationships identified in the Discovery Experiment were replicated, I carried out more detailed statistical analysis. In the Discovery Experiment, univariate correlations were calculated; in this chapter, multivariate analysis was used to build a regression model to predict outcome.

12.2 Methods

Experimental Design

The first stage of this experiment was to design the OxAMI-focused plate. Whereas the OxAMI plate allowed the analysis of 384 targets per sample, the OxAMI-focused plate allowed three samples to be analysed per plate, with 128 targets measured for each sample (Figure 45). This tripled throughput allowing the analysis of a larger number of patients. Target selection for the OxAMI-focused plate was based on the results from the Discovery Experiment and the Endothelial Cell Culture Experiment. Six-hour venous plasma samples from 80 patients were then analysed using this plate with subsequent data processing and analysis as previously developed in the Discovery Experiment.

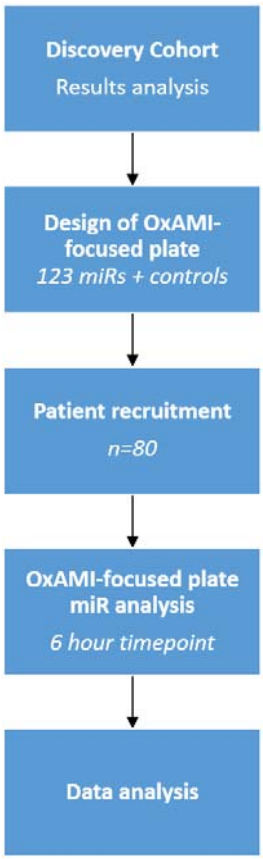

Figure 45: Experimental design for the Validation Experiment

Patient Recruitment

Patients were recruited according to the existing criteria and protocols defined in the patient recruitment section (page 46). In order to be included, patients were required to have venous blood samples collected at 0, 6, 24 and 48 hours. The six-hour venous plasma sample was used for miR analysis and serum samples at all four time points were used for troponin analysis. Patients were also required to have had an acute (within 48 hours of presentation) MRI scan; a six-month scan was considered desirable though not essential as troponin AUC (0-48 hours) was shown to be strongly predictive of infarct size in the Discovery Experiment.

MicroRNA Analysis and Quality Control

RNA isolation and reverse transcription were carried out according to the protocols in the MicroRNA analysis chapter (page 65). As the experimental protocol was reliable in the Discovery Experiment with few results excluded for quality control issues, a separate Quality Control plate was not used. Instead, all samples were analysed using the OxAMI focused plate which included wells for spike-in controls and quality control parameters were checked once PCR was complete using the pre-specified criteria set out in Table 10 (page 92).

Where samples did not meet these criteria, the RT step was repeated and PCR was carried out a second time on the OxAMI focused plate using this new cDNA. The rationale for this approach was that, in the Discovery Experiment, the RT step was the most common reason for failing QC and, with most samples, repeating RT resolved most QC problems.

Time-point Selection

As in the latter part of the Discovery Experiment, the six-hour time-point was used for microRNA analysis with venous plasma. Troponin-I measurements were made with the 0, 6, 24 and 48-hour serum samples.

The OxAMI-Focused Plate

Analysis of microRNA expression in the Discovery Experiment revealed differential expression of many microRNAs in STEMI; in addition, many other microRNAs were either rarely detected or not differentially expressed. These findings enabled the design of a new plate, the 'OxAMI focused plate'.

The following parameters were used to select microRNAs for inclusion:

1. Spike-in controls

   At this stage, the RNA isolation protocol was well defined and reliable so the multiple controls used in the early days of experimentation were not necessary. Instead, the RNA spike-ins *UniSP2*, 4 and 5 were used as the presence of these in the qPCR analysis at the expected detection levels confirmed efficiency of all stages of the process. A non-template control well was included for each sample to ensure samples contamination had not occurred.

2. Stable reference genes

   Global mean normalisation is the most robust method for normalisation a large unselected microRNA PCR array however for normalisation of a smaller subset of miRs on the OxAMI focused plate, selected for their differential expression in the Discovery Experiment, this method cannot be used as it could mask genuine differential expression. Instead, normalisation based on stable, statistically defined, reference miRs from the Discovery Experiment was used. These miRs were selected using the *Normfinder* algorithm (Table 11, page 99). The six most stable miRs were selected as reference miRs and included on the OxAMI-focused plate.

3. Clinical parameters

   Statistical analysis was used to test for a correlation between each microRNA and multiple clinical parameters. MicroRNAs were included where statistical significance was achieved ($p=\leq 0.05$) and they were ranked according to their correlation coefficient. MicroRNAs were

included in the OxAMI-focused plate where correlation coefficient ≥±0.4 and the miR was detected in ≥50% of samples; this figure was a reasonable compromise between not excluding miRs of interest, but also ensuring a manageable number of miRs were selected.

4. Literature search

   MicroRNAs reported to be differentially regulated in myocardial infarction, even if not detected in the Discovery Experiment, were also included (Table 8).

These selection methods culminated in a list of 128 microRNAs to be included in the OxAMI-focused plate. The final plate design is shown in Appendix 2: The OxAMI-Focused Plate (page 199).

Data Pre-Processing

Data pre-processing was carried out using the same protocol developed in the previous chapter (page 86).

Normalisation

Stable reference genes for normalisation were identified in the previous experiment (Table 11, page 99). Before carrying out normalisation on the Validation Experiment data, the stability of the reference genes was checked by ranking samples by standard deviation. Once their stability in this cohort was confirmed, normalisation was carried out using reference gene normalisation.

Data analysis

Validation of Discovery Experiment Findings

Analysis of the Discovery Experiment revealed relationships between microRNAs and the different clinical parameters, some of which had been previously reported in the literature and some which had not. Before proceeding with more detailed analysis of the Validation data, these relationships were checked individually. For example, *miR-1* had a strong correlation with troponin AUC in the Discovery Experiment; this correlation was therefore checked with the Validation Experiment for comparison.

Detailed Correlation Analysis

Once the Discovery Experiment findings had been validated with the new data, more detailed analysis was carried out and the larger number of patients offered more statistical power to identify relationships. Initially, simple correlation analysis was carried out between clinical parameters and each microRNA, using Pearson correlation for continuous variables and Spearman rank correlation for categorical variables, or variable that were not normally distributed.

Multiple Regression

The final aim of this experiment was to determine whether miR analysis from a six-hour blood sample could be used to predict outcome, such as infarct size at six months. Principal component analysis was used to identify miR networks and then identify a panel of miRs to build a multiple regression model. Principal component analysis and multiple regression were carried out using SPSS version 23.0.

12.3 Results

Patient Recruitment

Eighty-two patients with STEMI were recruited between June 2012 and March 2015. Clinical parameters are shown in Table 16. Patients were predominantly male and in their seventh decade. 12% of patients had diabetes mellitus. As in the Discovery Experiment, there was a wide range of infarct sizes and troponin AUC (0-48 hours) measurements (Table 16).

Gender n (%)	
Male	69 (84)
Female	13 (16)
TOTAL	82

Age	
Median	63.5
Range	31-90

Diabetes n (%)	
Oral medication	7 (9)
Insulin	2 (2)
New diagnosis	1 (1)
TOTAL	10 (12)

Smoking n (%)	
Current	32 (39)
Ex	26 (32)
Never	24 (29)

Creatinine (µmol/L)	
Median	73.0
Range	37.0-183.0

Culprit vessel n (%)	
LAD	40 (49)
Circumflex	10 (12)
RCA	32 (39)

Troponin-I (µg/L)	
Peak (median)	98.7
Peak (range)	0.6-1689
AUC (0-48h) (median)	2650
AUC (0-48h) (range)	21.7-28946

Infarct size (g)	
Median	16.4
Range	1.8-47.0

LV ejection fraction at 6 months %	
Median	53.4
Range	20.0-83.5

Total hospital stay (days)	
Median	2.3
Range	1.2-13.4

Table 16: Baseline patient characteristics for all patients recruited to the Validation Experiment.
82 patients were recruited over 33 months. LAD=left anterior descending, RCA=Right coronary artery. Troponin-I was measured at four time points and a troponin-I area under the curve (AUC) was calculated. Infarct size and ejection fraction were measured at the six-month MRI scan. Infarct size was measured as late gadolinium enhancement. Troponin AUC=area under the curve of four troponin measurements taken at 0/6/24/48 hours (μg/L) calculated using the trapezoid rule.

Quality Control

The quality control protocol, and the number of samples passing each stage is shown in Table 17. *UniSP2* and *UniSP4* were detected in the two samples that failed stage 1 but *UniSP5* was not. For these two samples, reverse transcription and qPCR was repeated and every QC step was then passed, so these samples (after the second RT and qPCR) were therefore included in the dataset.

	Parameter	Criteria	Number of samples (%)
	Starting number of samples		82
1	RNA Isolation	*UniSP2/4/5 should be detectible at CT values ≤37 CT values should be SP2≤SP4≤SP5*	80 (98)
2	PCR	*UniSP3 CT value should be 18-22 across dataset*	82 (100)
3	Positive controls	*Both positive controls (miR-103 and miR-191) should be detected*	82 (100)
4	Haemolysis	*Sample excluded if visibly haemolysed. Also excluded if ΔCT between miR-23a and miR-451 ≥7*	82 (100)
	TOTAL	*Number of samples passing all QC steps (%)*	80 (98)
	TOTAL (after repeat RT)	*Reverse transcription was repeated for the two samples failing QC*	82 (100)

Table 17: Quality control results for the 82 patients in the Validation Experiment.
Samples analysed were venous plasma samples six hours after presentation (time point 2.1). At each stage of the microRNA isolation and analysis process, the number of samples successfully reaching the pre-specified quality control criteria are shown. The Total row shows the number of samples that successfully achieved all of the quality control criteria (percentages in brackets).

To ensure similar miR analysis efficiency comparing the Discovery and the Validation Experiment, the median of the raw CT values (i.e. before normalisation) for each miR was calculated and is shown in Figure 46. To allow a direct comparison, only the miRs which were analysed in both cohorts were included in this analysis (i.e. only miRs on the OxAMI plate). There was no significant difference in the median raw CT values between the two groups.

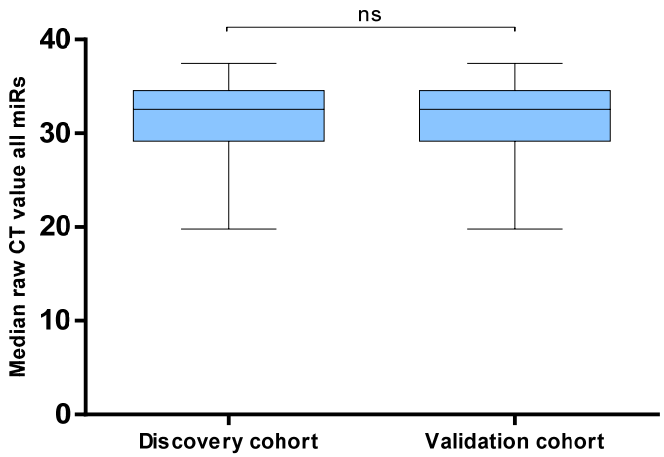

Figure 46: MiR detection in the Discovery and Validation Experiments.
Box shows median and interquartile range, whiskers show range. The median raw CT value of all miRs analysed in both the Discovery and Validation Experiments was calculated to determine whether there was a significant difference between groups, which might indicate a technical problem in the experiment. A Mann-Whitney test confirmed no significant difference between the two cohorts.

Normalisation

Provided the predefined quality control parameters had been met, the qPCR raw data were then processed and normalised using the reference genes identified in the Discovery Experiment using the *Normfinder* algorithm. Prior to normalisation, the accumulated standard deviation of the reference miRs identified in the Discovery Experiment was calculated as a final confirmatory check that normalisation with the same reference miRs was appropriate in the Validation Experiment (Table 18). The accumulated standard deviation for the six reference miRs was 0.22 in the Discovery Experiment and 0.25 in the Validation Experiment, and therefore reference gene normalisation was carried out on the Validation Experiment data using the same six reference miRs.

Experiment	Discovery	Validation
Accumulated SD	0.22	0.25
Selected reference miRs	*hsa-miR-23a* *hsa-miR-92a* *hsa-miR-126* *hsa-miR-423* *hsa-miR-25* *hsa-miR-26b*	

Table 18: List of miRs identified by Normfinder ranked by standard deviation.
Accumulated SD=accumulated standard deviation for the six most stable miRs. miRs in red are identified as potential reference genes in both cohorts.

Validating the Discovery Experiment Findings

Troponin

Troponin area under the curve was calculated using the trapezoid rule. As with the Discovery Experiment, the results were highly positively skewed both visually and mathematically (calculated skewness/kurtosis and Shapiro-Wilk) and were therefore log_{10} transformed. An unpaired t-test confirmed there was no statistically significant difference in infarct size measured by troponin AUC (0-48 hours) between the Discovery and Validation Experiments (Figure 47).

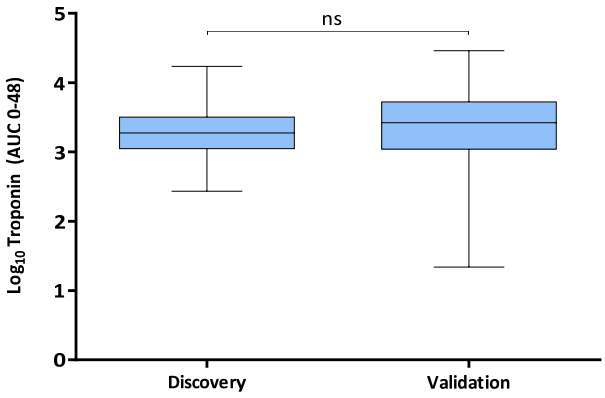

Figure 47: Serum plasma troponin-I detection in the Discovery and Validation Experiments.
Values shown are log10 troponin AUC (0-48 hours). Box shows median and interquartile range, whiskers show range. A Mann-Whitney test confirmed no significant difference between the two cohorts.

The normalised CT values were normally distributed. A Pearson correlation was carried out to assess the relationship between Log_{10} troponin AUC and previously described myocardial miRs. Strong correlations were found between miRs *-1, -133b* and *-499* and troponin AUC (0-48 hours) in both the Discovery and Validation Experiments, and the normalised CT values were in the same range in both cohorts (Figure 48). The two outliers in the Validation Experiment (patients with a troponin AUC (0-

48) of 1.3 and 1.5 were both patients with renal impairment (creatinine 183 and 141, eGFR 34 and 46 respectively).

A

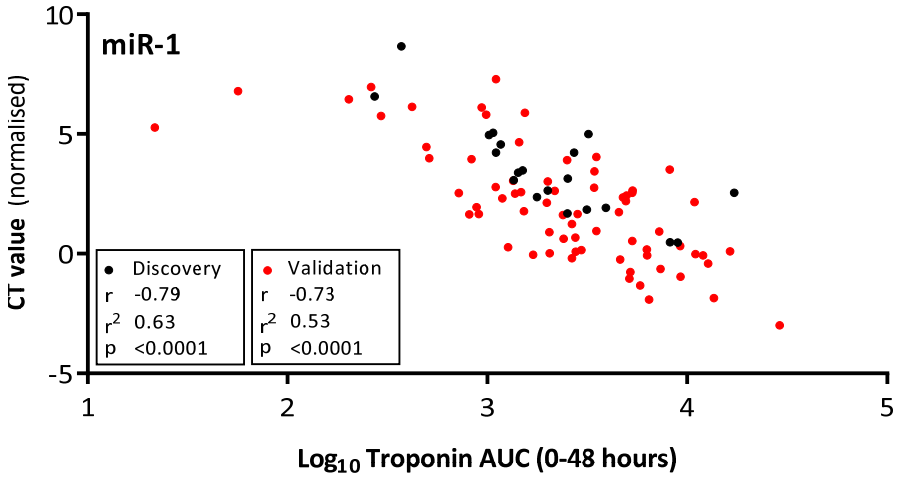

B

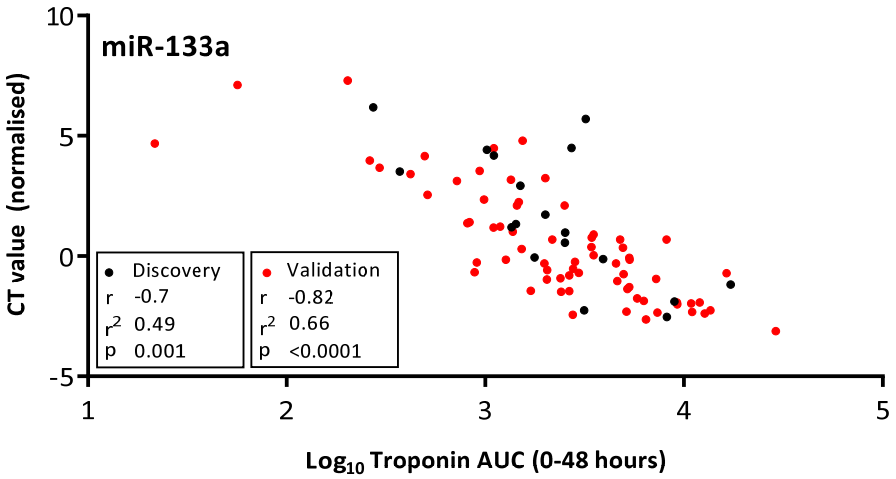

C

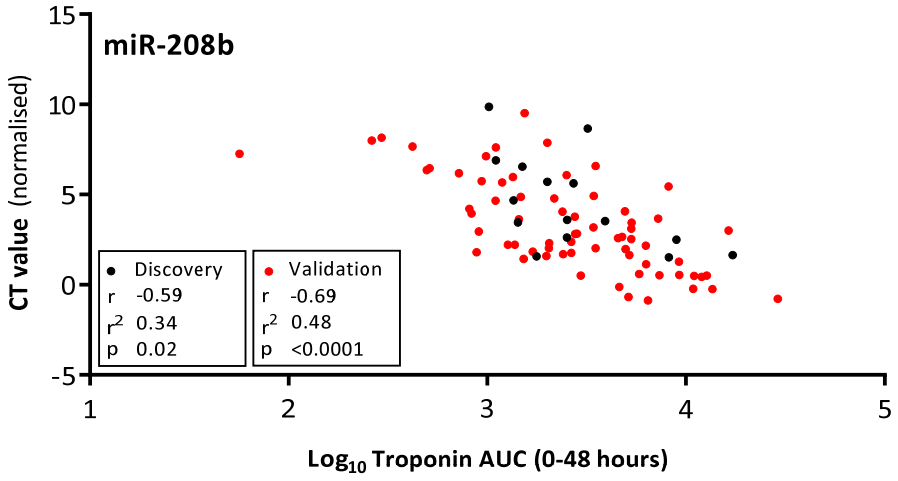

D

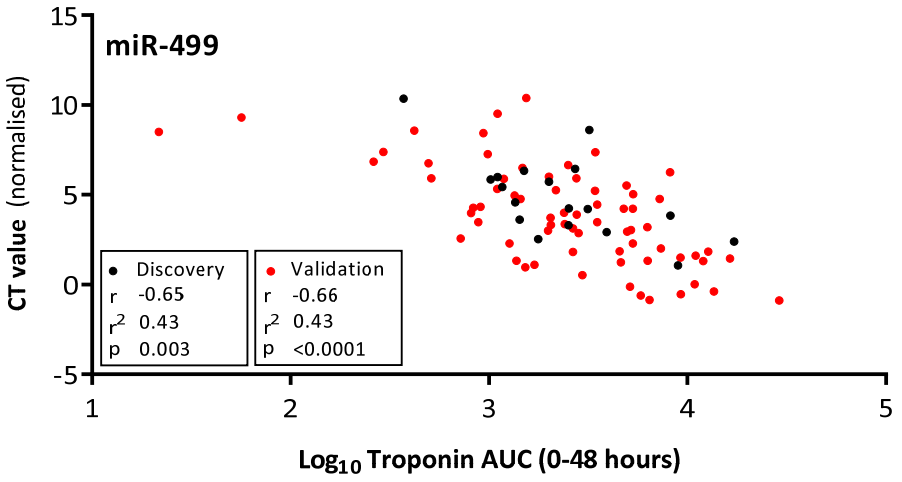

Figure 48: The relationships between known myocardial miRs and troponin AUC 0-48 hours for the Discovery (shown in black) and Validation (shown in red) cohorts.

Each panel shows the relationship between a different miR and troponin AUC 0-48 hours: A=miR-1, B=miR-133a, C=miR-208b, D=miR-499. Troponin AUC is not normally distributed and was therefore $\log_{10}$ transformed. All CT values were normalised to six reference miRs. A Spearman correlation was calculated between each miR and troponin AUC 0-48 hours for each cohort; correlation coefficient (r), coefficient of determination (r^2) and significance (p) are shown in the boxes. Troponin AUC=area under the curve of four troponin measurements taken at 0/6/24/48 hours (µg/L) calculated using the trapezoid rule. N=21 in Discovery Cohort; N=102 in Validation Cohort.

For the next stage of analysis, all miRs detected in both cohorts were included, not including controls. A correlation matrix was generated for each Experiment showing the Pearson correlation between troponin AUC (0-48 hours) and normalised CT values of detected miRs. A Venn diagram was used to illustrate the correlation concordance between the two groups. In order to be included in the diagram, a miR had to be detected in ≥50% samples with a correlation coefficient of ≥±0.4 and a significance (p) of ≤0.05.

119 miRs were detected in both Experiments. In the Discovery Experiment, 101 miRs were detected in ≥50% of samples. Of these, 81 had a correlation efficient ≥±0.4 and 77 had a significance (p) of ≤0.05. 76 had a positive correlation (i.e. miR detection increased (and CT values decreased) with increasing troponin AUC (0-48). In the Validation Experiment, 21 miRs showed a positive correlation with troponin AUC and all 21 had a significance (p) of ≤0.05. Of the 21 miRs increased with troponin AUC (0-48 hours) in the Validation Experiment there was strong concordance with the Discovery Experiment; all 21 showed a similar correlation (Figure 49). One miR in the Discovery Experiment (*miR-576*, r=0.67, p=0.02) and one in the Validation Experiment (*miR-181*, r=0.42, p=0.003) had a negative correlation with troponin AUC but neither of these relationships were validated in the other cohort.

A

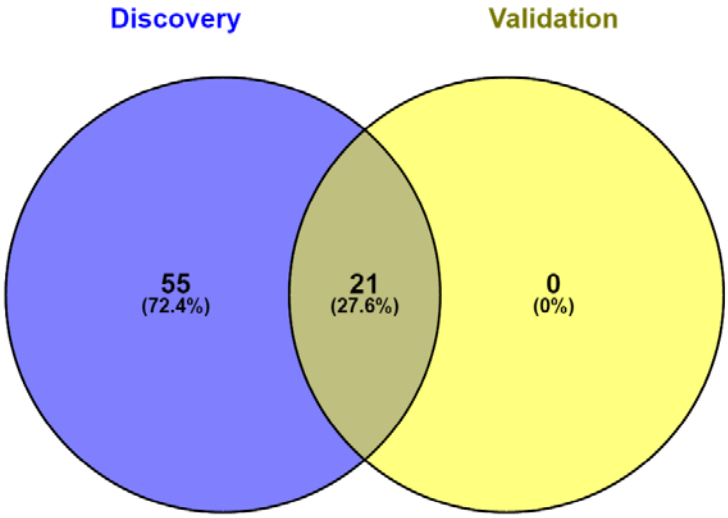

B

	Discovery Experiment			Validation Experiment		
	r	p	N	r	p	N
hsa-miR-197-3p	-0.603	0.005	20	-0.43	<0.0001	70
hsa-miR-193b-5p	-0.728	0.005	13	-0.44	<0.0001	55
hsa-miR-24-3p	-0.586	0.007	20	-0.453	<0.0001	71
hsa-miR-95-3p	-0.669	0.002	19	-0.457	<0.0001	67
hsa-miR-302d-3p	-0.833	0.003	10	-0.466	<0.0001	46
hsa-miR-30a-3p	-0.586	0.013	17	-0.481	<0.0001	66
hsa-miR-99a-5p	-0.584	0.007	20	-0.502	<0.0001	71
hsa-let-7d-3p	-0.685	0.001	20	-0.534	<0.0001	71
hsa-miR-145-5p	-0.665	0.002	19	-0.535	<0.0001	71
hsa-miR-452-5p	-0.73	0.001	17	-0.546	<0.0001	64
hsa-miR-152-3p	-0.678	0.001	20	-0.547	<0.0001	71
hsa-miR-193b-3p	-0.668	0.005	16	-0.552	<0.0001	68
hsa-miR-378a-5p	-0.777	0.005	11	-0.556	<0.0001	65
hsa-miR-125b-5p	-0.661	0.002	20	-0.646	<0.0001	71
hsa-miR-499a-5p	-0.583	0.011	18	-0.656	<0.0001	69
hsa-miR-208b-3p	-0.624	0.013	15	-0.69	<0.0001	68
hsa-miR-1	-0.555	0.011	20	-0.729	<0.0001	70
hsa-miR-378a-3p	-0.624	0.003	20	-0.739	<0.0001	71
hsa-miR-30a-5p	-0.648	0.002	20	-0.787	<0.0001	70
hsa-miR-133a-3p	-0.647	0.004	18	-0.815	<0.0001	70
hsa-miR-133b	-0.551	0.012	20	-0.818	<0.0001	69

Figure 49: miRs showing a positive correlation with troponin AUC (0-48 hours).

A: Venn diagram showing the number of miRs positively correlating with troponin AUC (0-48 hours) in each cohort. A positive correlation was defined as a correlation coefficient ≥0.4 and p≤0.05 where the miR was detected in ≥50% of samples. **B:** List of the 21 miRs showing a positive (Pearson) correlation with troponin AUC (0-48 hours) with correlation data for each miR with a positive correlation in both cohorts. miRs are sorted according to correlation coefficient in the Validation Experiment. NB. Correlations are between miR detection as a CT value (which is an inverse scale – i.e. higher CT value = lower concentration) and troponin AUC (0-48) so a negative correlation coefficient in fact reflects a positive correlation. r=correlation coefficient; p=significance; n=number of patients this miR was detected in within the cohort.

Microvascular obstruction

A similar analysis to that carried out with troponin AUC (0-48 hours) was also carried out with microvascular obstruction. A correlation matrix was generated for each Experiment showing the Pearson correlation between troponin AUC (0-48 hours) and normalised CT values of detected miRs. 120 miRs in the Discovery Experiment had a strong correlation with MVO (r=≥±0.4, p=<0.05, n≥50%). As with troponin, the majority (119) of these correlations were positive (i.e. miR detected concentration increases with MVO) and one was negative. Unlike troponin, concordance between the Experiments was much weaker with only two miRs meeting the criteria for a strong correlation in both Experiments (Table 19).

	Discovery Experiment			Validation Experiment		
	r	p	N	r	p	N
hsa-miR-378a-3p	-0.701	0.001	19	-0.425	<0.001	81
hsa-miR-30a-5p	-0.674	0.002	19	-0.417	<0.001	80

Table 19: All miRs showing a positive correlation between miR detection and MVO in the Discovery and Validation Experiments.
A Pearson correlation was carried out between MVO (in grams) and all miRs (normalised CT value). r=correlation coefficient; p=significance; n=number of patients this miR was detected in within the cohort.

Microvascular obstruction was then considered as a categorical variable. Patients were divided into 'MVO present' (n=40, 49%) and 'MVO absent' (n=42, 51%) groups. Spearman correlation was carried out between these groups and normalised miR CT values. In the Discovery Experiment, 33 miRs had a statistically significant strong correlation with MVO (r=≥±0.4, p=<0.05, n≥50%). All of these correlations were positive; no miRs were shown to decrease with microvascular obstruction. In the Validation Experiment, 40 miRs had a statistically significant correlation with MVO though the strength of correlation was weaker with 12 of these having a correlation coefficient ≥±0.4. Table 20 shows all miRs with a statistically significant correlation with grouped MVO. The direction of correlation was concordant in nine miRs and not concordant in two. *MiR-30a-5p* was shown to

correlate with MVO in Table 19 but although there was a correlation with grouped MVO, this did not reach statistical significance and is therefore not shown in Table 20.

	Discovery Experiment			Validation Experiment		
	r	p	N	r	p	N
hsa-miR-200a-3p	-0.683	0.021	11	0.411	0.002	52
hsa-miR-99b-5p	-0.626	0.005	18	0.355	0.001	79
hsa-miR-302d-3p	-0.704	0.023	10	-0.283	0.04	53
hsa-miR-378a-5p	-0.689	0.028	10	-0.329	0.004	74
hsa-miR-95-3p	-0.673	0.002	18	-0.332	0.003	77
hsa-miR-193b-3p	-0.618	0.014	15	-0.391	<0.0001	78
hsa-miR-452-5p	-0.52	0.032	17	-0.467	<0.0001	74
hsa-miR-1	-0.503	0.028	19	-0.475	<0.0001	80
hsa-miR-133b	-0.509	0.026	19	-0.508	<0.0001	79
hsa-miR-133a-3p	-0.635	0.006	17	-0.519	<0.0001	80
hsa-miR-378a-3p	-0.49	0.033	19	-0.546	<0.0001	81

Table 20: miRs showing a statistically significant correlation (p=<0.05) with MVO in both the Discovery and Validation Experiments.
Patients were divided into 'No MVO' and 'MVO' groups and a matrix was generated to compare Spearman correlation between MVO group and microRNA reference gene normalised CT value. r=correlation coefficient; p=significance; n=number of patients this miR was detected in within the cohort. Heat mapping was used to illustrate direction and magnitude of change; blue indicates that a miR decreases in concentration with MVO and red indicates that it increases with MVO.

The results from the troponin and MVO analysis were then compared. All miRs showing a correlation between troponin release and miR concentration were listed with the corresponding results for grouped MVO (Table 21). Although not all of the MVO results were statistically significant (and therefore not shown in Table 20) the direction of the grouped MVO correlation was the same for all miRs increased with troponin release.

	Troponin-I						Microvascular Obstruction					
	Discovery			Validation			Discovery			Validation		
	r	p	N	r	P	N	r	p	N	r	p	N
hsa-miR-197-3p	-0.603	0.005	20	-0.43	<0.0001	70	-0.371	0.118	19	-0.122	0.279	80
hsa-miR-193b-5p	-0.728	0.005	13	-0.44	0.001	55	-0.393	0.206	12	-0.246	0.05	64
hsa-miR-24-3p	-0.586	0.007	20	-0.453	<0.0001	71	-0.304	0.205	19	-0.402	<0.0001	81
hsa-miR-95-3p	-0.669	0.002	19	-0.457	<0.0001	67	-0.673	0.002	18	-0.332	0.003	77
hsa-miR-302d-3p	-0.833	0.003	10	-0.466	0.001	46	-0.704	0.023	10	-0.283	0.04	53
hsa-miR-30a-3p	-0.586	0.013	17	-0.481	<0.0001	66	-0.249	0.352	16	-0.416	<0.0001	76
hsa-miR-99a-5p	-0.584	0.007	20	-0.502	<0.0001	71	-0.372	0.117	19	-0.296	0.007	81
hsa-miR-145-5p	-0.665	0.002	19	-0.535	<0.0001	71	-0.455	0.058	18	-0.315	0.004	81
hsa-miR-452-5p	-0.73	0.001	17	-0.546	<0.0001	64	-0.52	0.032	17	-0.467	<0.0001	74
hsa-miR-152-3p	-0.678	0.001	20	-0.547	<0.0001	71	-0.348	0.145	19	-0.342	0.002	81
hsa-miR-193b-3p	-0.668	0.005	16	-0.552	<0.0001	68	-0.618	0.014	15	-0.391	<0.0001	78
hsa-miR-378a-5p	-0.777	0.005	11	-0.556	<0.0001	65	-0.689	0.028	10	-0.329	0.004	74
hsa-miR-125b-5p	-0.661	0.002	20	-0.646	<0.0001	71	-0.407	0.083	19	-0.46	<0.0001	81
hsa-miR-499a-5p	-0.583	0.011	18	-0.656	<0.0001	69	-0.384	0.128	17	-0.425	<0.0001	78
hsa-miR-208b-3p	-0.624	0.013	15	-0.69	<0.0001	68	-0.462	0.097	14	-0.43	<0.0001	78
hsa-miR-1	-0.555	0.011	20	-0.729	<0.0001	70	-0.503	0.028	19	-0.475	<0.0001	80
hsa-miR-378a-3p	-0.624	0.003	20	-0.739	<0.0001	71	-0.49	0.033	19	-0.546	<0.0001	81
hsa-miR-30a-5p	-0.648	0.002	20	-0.787	<0.0001	70	-0.365	0.124	19	-0.567	<0.0001	80
hsa-miR-133a-3p	-0.647	0.004	18	-0.815	<0.0001	70	-0.635	0.006	17	-0.519	<0.0001	80
hsa-miR-133b	-0.551	0.012	20	-0.818	<0.0001	69	-0.509	0.026	19	-0.508	<0.0001	79

Table 21: Comparing the identified relationships between miR release, troponin-I and MVO.
All miRs showing a positive correlation with troponin-I release were listed with the corresponding results for grouped MVO. r=correlation coefficient; p=significance; N=number of patients.

The next analysis carried out was to determine which miRs were detected in patients with MVO and which were not, and to understand whether some miRs were more likely to be released in patients (and therefore detected) with MVO. MiRs were listed with the percentage of samples in which they were detected for patients with and without MVO. The same analysis was carried out for both the Discovery and Validation Experiments and then displayed by difference in percentage detection between the two MVO groups (Table 22). Ten miRs were more likely to be detected in patients with MVO in both the Discovery and Validation Experiments.

	% of samples in which miR detected				Difference in detection between No MVO and MVO	
	Discovery Experiment		Validation Experiment			
	No MVO	MVO	No MVO	MVO	Discovery	Validation
hsa-miR-224-3p	0%	64%	43%	76%	64%	33%
hsa-miR-302a-3p	25%	55%	25%	56%	30%	31%
hsa-let-7c-3p	13%	73%	30%	61%	60%	31%
hsa-miR-181c-3p	0%	27%	40%	68%	27%	28%
hsa-miR-346	25%	55%	30%	56%	30%	26%
hsa-miR-125a-3p	0%	55%	35%	54%	55%	19%
hsa-miR-214-5p	0%	55%	35%	54%	55%	19%
hsa-miR-193b-5p	50%	73%	70%	88%	23%	18%
hsa-miR-30d-3p	50%	73%	78%	93%	23%	15%
hsa-miR-378a-5p	38%	64%	85%	98%	26%	13%

Table 22: The number of samples in which each miR was detected.
miRs are shown where the difference between No MVO and MVO was >10% in each group. Sorted by delta in the Validation group.

Principal Component Analysis

Factor reduction was carried out using Principal Component Analysis in the Validation Experiment dataset. The purpose of this was to identify signals within the microRNA signature and to aid variable selection for the design of a regression model to predict outcome following STEMI.

Principal component analysis cannot be carried out with missing data. A conservative approach was used to impute missing data. Prior to analysis, miRs that were detected in fewer than 70% of samples were excluded (26/128). In the remainder, missing data were imputed with the maximum recorded CT value +1 for that microRNA. Normalisation was then carried out using reference gene normalisation as previously described. Eigenvalues for the top 20 principal components are shown in Table 23 and the scree plot is shown in Figure 50.

There are various accepted methods for selecting the optimal number of components to extract: visual inspection of the scree plot to identify the inflection point and selecting all components before this; selecting all components with an Eigenvalue greater than 1; or selecting enough components to explain 70% of the variance. A combination of these approaches was used. Visual inspection demonstrated seven components before the inflection point, 20 components had an Eigenvalue greater than 1 and 10 components would be needed to explain 70% of the variance. Based on this information 10 components were retained.

	Total Variance Explained		
	Eigenvalue	**% of Variance**	**Cumulative %**
1	22.54	22.32	22.32
2	13.23	13.09	35.41
3	8.25	8.17	43.58
4	7.38	7.30	50.88
5	6.13	6.07	56.95
6	5.13	5.08	62.03
7	2.55	2.52	64.55
8	2.27	2.25	66.80
9	2.11	2.09	68.88
10	2.04	2.02	70.91
11	1.83	1.81	72.72
12	1.78	1.76	74.48
13	1.64	1.63	76.11
14	1.47	1.45	77.56
15	1.36	1.34	78.90
16	1.34	1.33	80.23
17	1.27	1.26	81.49
18	1.23	1.22	82.70
19	1.20	1.19	83.89
20	1.02	1.01	84.90

Table 23: Total variance explained for the first 20 principal components.
Within the dataset, the total variance explained by each component is shown, as is the cumulative variance. The most variance is explained by the first component.

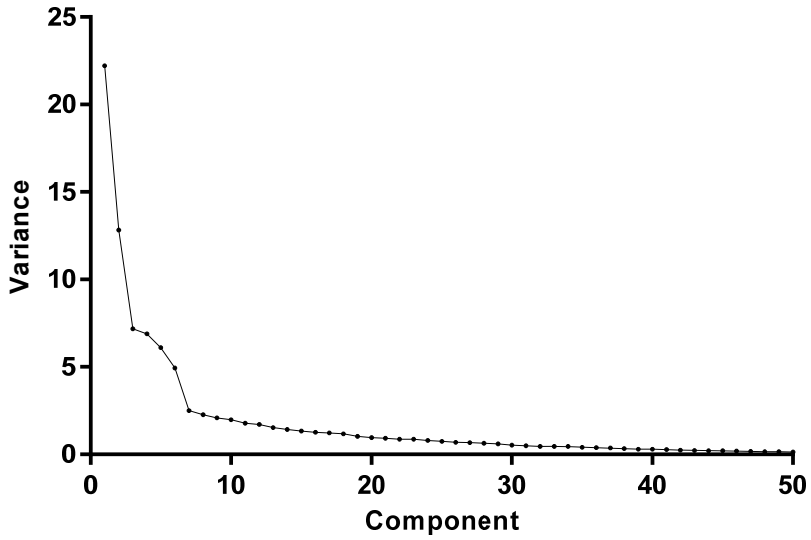

Figure 50: Scree plot of total variance explained by each component against its respective component.
The inflection point is at the seventh component. Each data point reflects the variance explained by one component.

Component scores for each principal component were generate and analysed with the miR data from the Validation Experiment. A Pearson correlation analysis was carried out between the component scores and the individual miRs. Correlation coefficients are shown in Table 24.

Component									
1		2		3		4		5	
miR-22-3p	-0.873	*miR-30a-5p*	0.852	*miR-27a-3p*	0.603	*miR-193a-5p*	0.742	*miR-28-5p*	0.581
miR-208b-3p	-0.836	*miR-378a-3p*	0.803	*miR-215-5p*	0.587	*miR-665*	0.639	*miR-335-3p*	0.572
miR-22-5p	-0.822	*miR-95-3p*	0.664	*miR-885-5p*	0.565	*miR-27a-5p*	0.529	*let-7e-5p*	0.506
miR-378a-5p	-0.819	*miR-24-3p*	0.618	*miR-362-5p*	0.561	*miR-548c-5p*	0.511	*miR-376c-3p*	0.474
miR-499a-5p	-0.803	*miR-125b-5p*	0.616	*miR-30e-5p*	0.554	*miR-145-3p*	0.487	*miR-664a-3p*	0.473
miR-133a-3p	-0.789	*miR-30a-3p*	0.598	*miR-186-5p*	0.522	*miR-663a*	0.486	*miR-221-3p*	0.441
miR-133b	-0.753	*miR-452-5p*	0.58	*miR-576-5p*	0.513	*miR-128-3p*	0.43	*miR-199a-3p*	0.433
miR-1	-0.739	*miR-361-5p*	0.579	*miR-532-5p*	0.463	*miR-197-3p*	0.371	*miR-26a-5p*	0.432
miR-210-3p	-0.696	*miR-23b-3p*	0.576	*miR-222-3p*	0.457	*miR-22-5p*	0.362	*miR-27a-3p*	0.392
miR-193b-3p	-0.66	*miR-152-3p*	0.575	*miR-195-5p*	0.435	*miR-362-5p*	0.335	*miR-154-5p*	0.378
miR-148a-3p	-0.614	*miR-197-3p*	0.567	*miR-7-1-3p*	0.413	*miR-1*	0.328	*let-7a-5p*	0.371
miR-99a-5p	-0.591	*miR-145-5p*	0.543	*miR-664a-3p*	0.407	*miR-23b-3p*	0.326	*miR-190a-5p*	0.362
miR-221-3p	-0.579	*miR-421*	0.521	*miR-204-5p*	0.399	*miR-30a-3p*	0.303	*miR-103a-3p*	0.361
miR-125b-5p	-0.564	*let-7d-3p*	0.521	*miR-324-3p*	0.392	*miR-30e-5p*	-0.31	*miR-146b-5p*	0.361
miR-145-3p	-0.538	*miR-214-3p*	0.512	*miR-376c-3p*	0.391	*miR-652-3p*	-0.315	*miR-152-3p*	0.333
miR-30e-5p	-0.507	*miR-193b-5p*	0.474	*miR-335-3p*	0.39	*miR-7-1-3p*	-0.344	*let-7d-5p*	0.316
miR-30d-3p	-0.427	*miR-133b*	0.44	*miR-424-3p*	0.36	*miR-222-3p*	-0.357	*miR-126-3p*	0.309
miR-34a-5p	-0.41	*miR-133a-3p*	0.407	*miR-335-5p*	0.351	*miR-103a-3p*	-0.364	*miR-320a*	-0.315
miR-874-3p	-0.389	*miR-195-5p*	0.387	*miR-452-5p*	0.349	*miR-376c-3p*	-0.371	*miR-320b*	-0.321
miR-128-3p	-0.373	*miR-1*	0.365	*miR-30d-3p*	0.349	*miR-107*	-0.39	*miR-532-5p*	-0.423
miR-378a-3p	-0.353	*miR-155-5p*	0.344	*miR-190a-5p*	0.334	*miR-28-5p*	-0.39	*miR-324-3p*	-0.427
miR-107	-0.337	*miR-193b-3p*	0.334	*miR-431-5p*	0.316	*miR-423-3p*	-0.496	*miR-92a-3p*	-0.456
miR-652-3p	-0.328	*miR-151a-3p*	0.32	*miR-328-3p*	0.312	*miR-744-5p*	-0.693	*miR-25-3p*	-0.486
miR-27a-3p	-0.325	*miR-30d-3p*	0.309	*miR-221-3p*	-0.345				
miR-452-5p	-0.32	*miR-210-3p*	-0.329	*let-7a-5p*	-0.374				
miR-215-5p	0.308	*miR-424-3p*	-0.329	*let-7d-3p*	-0.432				
miR-532-5p	0.309	*miR-576-5p*	-0.336	*let-7d-5p*	-0.476				
miR-663a	0.312	*miR-431-5p*	-0.339						
miR-181b-5p	0.329	*miR-193a-5p*	-0.357						
miR-671-5p	0.346	*miR-27a-5p*	-0.384						
miR-335-3p	0.351	*miR-324-3p*	-0.464						
miR-197-3p	0.354	*miR-148a-3p*	-0.562						
miR-7-1-3p	0.357	*miR-199a-3p*	-0.575						
miR-548c-5p	0.362	*miR-128-3p*	-0.578						
miR-361-5p	0.407	*miR-140-5p*	-0.612						
miR-18a-3p	0.411	*miR-107*	-0.616						
miR-130b-3p	0.423	*miR-652-3p*	-0.616						
miR-665	0.427	*let-7g-5p*	-0.631						
let-7d-5p	0.432	*miR-103a-3p*	-0.649						
miR-664a-3p	0.434								
miR-146b-5p	0.461								
miR-421	0.496								
miR-155-5p	0.526								
let-7e-5p	0.537								
miR-23b-3p	0.552								
miR-1972	0.602								
miR-342-5p	0.615								
miR-150-5p	0.633								
miR-132-3p	0.654								
miR-92a-3p	0.662								
miR-99b-5p	0.663								
let-7a-5p	0.678								
miR-320d	0.718								
miR-25-3p	0.752								
miR-26a-5p	0.764								
miR-151a-3p	0.787								
miR-342-3p	0.797								
miR-126-5p	0.802								
miR-126-3p	0.804								
miR-320b	0.825								
miR-320a	0.844								

Component									
6		7		8		9		10	
miR-423-3p	0.56	*miR-130b-3p*	0.453	*miR-122-5p*	0.429	*miR-154-5p*	0.557	*miR-190a-5p*	0.389
miR-671-5p	0.486	*miR-122-5p*	0.353	*miR-190a-5p*	-0.31	*miR-663a*	0.366	*miR-193b-3p*	0.327
miR-652-3p	0.446	*miR-193b-5p*	0.344	*miR-214-3p*	-0.324	*miR-885-5p*	-0.373	*let-7g-5p*	0.304
miR-431-5p	0.384	*miR-34a-5p*	0.341	*miR-1972*	-0.325	*miR-34a-5p*	-0.405		
miR-1972	0.35	*miR-155-5p*	0.324	*miR-186-5p*	-0.343				
miR-320d	0.346	*miR-885-5p*	0.305	*miR-941*	-0.395				
miR-421	0.336	*miR-664a-3p*	-0.343						
miR-548c-5p	0.33								
miR-221-3p	0.321								
miR-665	0.318								
miR-18a-3p	-0.301								
miR-122-5p	-0.304								
miR-125b-5p	-0.324								
miR-126-5p	-0.325								
miR-126-3p	-0.336								
miR-150-5p	-0.345								
miR-146b-5p	-0.349								
miR-140-5p	-0.365								
miR-215-5p	-0.382								
miR-130b-3p	-0.384								
let-7g-5p	-0.422								

Table 24: Component loading matrix showing the relationship between principal component scores and individual miRs.
The table was calculated by carrying out Pearson correlation analysis between component scores and normalised CT values. Values shown are correlation coefficients.

To link these findings to the clinical attributes of the cohort, a further correlation analysis was carried out between the component scores and the clinical parameters. Positive and negative correlations between clinical parameters and each principal component are shown in Table 25.

Component	Positive correlation	Negative correlation
1	Troponin-I Infarct size Grouped MVO Myocardial oedema	6-month ejection fraction Acute salvage index 6-month salvage index
2	% ST segment resolution after PCI 6-month ejection fraction Peripheral venous pCO_2 during PCI	Troponin-I Length of hospital stay Max ST segment deviation on presenting ECG
3	Haemoglobin (6 hours) Total cholesterol (6 hours) LDL cholesterol (6 hours)	Peripheral venous pO_2 during PCI
4	Troponin-I Peripheral venous pCO_2 during PCI Haemoglobin (during PCI) Neutrophil count (during PCI)	No strong correlations with clinical parameters
5	Creatinine (during PCI) Creatinine (6 hours) Creatinine (24 hours) Urea (6 hours)	Salvage area Oedema (%) TP2 Trop eGFR Max dev
6	No strong correlations with clinical parameters	No strong correlations
7	Peripheral venous pCO_2 during PCI	Venous pH Coronary sinus pH
8	No strong correlations with clinical parameters	No strong correlations with clinical parameters
9	No strong correlations with clinical parameters	No strong correlations with clinical parameters
10	No strong correlations with clinical parameters	No strong correlations with clinical parameters

Table 25: Correlation between the first ten principal components and clinical parameters.
To be included, correlation coefficient had to be ≥±0.3 and statistically significant (p=<0.05).

Regression Model to Predict Infarct Size

The final aim was to design a multiple regression model to predict outcome in patients after ST elevation myocardial infarction. The outcome measure used was infarct size, measured by cardiac MRI at six months. The results from this experiment – miR correlation with troponin, miR correlation with MVO and principal component analysis – have identified the microRNA signal for myocardial necrosis, which determines infarct size. These findings were therefore used for variable selection for the model. MiRs associated with troponin release, MVO and miRs from each component shown to have a correlation with clinical markers of myocardial injury were tested in multiple combinations to identify variables to build the most robust multiple regression model.

Of all clinical parameters available during the index hospital admission, troponin AUC (0-48) has the strongest correlation with infarct size measured at six months. A linear regression established that troponin AUC (0-48) could statistically significantly predict infarct size (r^2=0.41, p=<0.0001). The purpose of this model was to be able to predict infarct size at the six-hour time point to allow optimisation of treatment and therefore all the measurements to calculate troponin AUC would not be available. A linear regression established that the six-hour troponin-I measurement could also statistically significantly predict infarct size, albeit less effectively than troponin AUC (0-48) (r^2=0.29, p=<0.0001).

A multiple regression model was run to predict infarct size at six months using seven miRs, which were selected using the principal component analysis results. This model was able to predict final infarct size with a correlation coefficient of 0.68 (r^2=0.47, p=0.001), compared with 0.54 with six-hour troponin. The miRs used for this model, the rationale for their selection and potential roles is shown in Table 26. The miRs selected for the regression model represent the major myocardial cell types and adding two miRs known to originate from platelets increased the statistical power of the mode.

	Reason for inclusion	Origin	Roles
hsa-miR-378a-3p	PC 1,2 Increased in MVO, correlates with troponin	Cardiomyocytes[125]	Regulator of cardiac hypertrophy and neovascularisation under hypoxic conditions[126,127]
hsa-miR-30a-5p	PC 2 Correlates with troponin	Myocardial[128]	Tumour suppressor[129]
hsa-miR-1	PC 1,2 Strong relationship troponin and MVO	Cardiomyocytes Smooth muscle	Known myocardial miR[94,99,101,119,130,131] Regulates cardiomyocyte proliferation suppresses smooth muscle gene expression[130]
hsa-miR-320a	PC 1,5	Platelets[132,133]	Downregulated in patients without coronary disease[134]
hsa-miR-208b-3p	PC 1 Increased in MVO, correlates with troponin	Myocardial[72]	Known myocardial miR[94,99,101,119,130,131]
hsa-miR-320b	PC 1	Platelets[132,133]	Downregulated in patients without coronary disease[134]
hsa-miR-22-5p	PC 1 Released from endothelial cells	Myocardial[135]	Regulates stress-induced cardiac hypertrophy[136]

Table 26: Rationale for miR inclusion in regression model.
These miRs were selected for the linear regression model to predict outcome (infarct size at six months). They were selected on the basis of relationships between miRs and clinical parameters

identified during the Validation Experiment and in Principal Component Analysis. PC=Principle Component.

12.4 Discussion

In the Discovery Experiment (Chapter 10, page 78), a reliable and reproducible microRNA analysis protocol was developed and the miRs detected in human plasma samples in patients with ST elevation myocardial infarction were identified. Subsequent work in cultured endothelial cells (Chapter 11, page 121) showed which miRs were detectable in endothelial cell supernatant, and how this miR signature changed with hypoxia. Cross-referencing these results showed that myocardial miRs were detected in plasma but not endothelial cell supernatant, which would suggest they are cardiomyocyte associated.

The OxAMI focused plate was designed based on the results from these two experiments and this allowed throughput to be increased to three samples per plate. Where in the pilot experiment, the analysis of a single sample, which involved two 384 well plates, took approximately seven hours, with the OxAMI plate, three samples could be analysed in less than five hours; a time scale and economy that could be clinically useful.

The 82 patients recruited into the Validation Experiment shared similar baseline characteristics to those recruited into the Discovery Experiment. They were predominantly male and in their seventh decade. Unlike the earlier Experiment, 12% of these patients had diabetes mellitus which is more reflective of the Oxford STEMI population as a whole. As before, the left anterior descending and right coronary artery were the most common culprit vessels (49% and 39% respectively), with fewer patients being recruited with an occluded circumflex (12%), likely reflecting the challenges of diagnosing posterior myocardial infarction.

As with the clinical population, there was a wide range of infarct size and final left ventricular function, which is important for an experiment where one aim is to define whether the relationship between infarct size and miR release is linear across the range of infarct size. Hospital stay was a median of 2.3 days, reflecting contemporary management of ST elevation myocardial infarction, and also illustrating that being recruited to the OxAMI research programme did not extend hospital stay.

The range of renal function shown in the Validation Experiment again reflected real-world experience. Interestingly the two patients who were outliers in Figure 48 were those with significant renal impairment (creatinine 141 and 183) and detectable levels of the myocardial miRs were lower than expected, if the myocardial miR-troponin relationship is linear. This may demonstrate features of troponin or miRs in chronic kidney disease. Troponin is known to be renally excreted and in patients with chronic kidney disease the troponin 'lag' – the time it takes for troponin to become undetectable after an acute myocardial infarction – is increased and these patients may actually have presented long after their myocardial infarction. Both patients had chest pain with a stuttering course, waxing and waning over more than 24 hours so their MI may have occurred longer before presentation than appreciated at the time. Levels of circulating miRs have been shown to be lower in patients with chronic kidney disease, which may also be a factor[137].

Quality control results improved in the Validation Experiment (Table 17) compared with the Discovery Experiment with 98% of samples reaching the pre-specified quality control criteria. The improvement was likely partly related to greater experience at microRNA analysis and also running samples in large batches, which had been found previously to produce the most consistent results.

There was no significant difference between mean raw CT value between the two cohorts (Figure 46) which was expected, but reassuring. The miRs selected for reference gene normalisation in the Discovery Experiment were also stable in the Validation Experiment and were therefore used for

normalisation. Normalising with the same identified reference miRs allowed the Discovery and Validation results to be directly comparable.

The strong correlations shown in the Discovery Experiment between the myocardial miRs and troponin AUC (0-48) were confirmed in the Validation Experiment, with similar strength and direction of correlation seen in all myocardial miRs (Figure 48). In the Discovery Experiment, multiple miRs were shown to have a correlation with troponin, not just the previously reported myocardial miRs. In 21 of these, a similar relationship was shown in the Validation Experiment (Figure 49).

Microvascular obstruction was present in 51% of patients in the Validation Experiment. Of all the miRs with a concordant correlation relationship in both cohorts (9 miRs, Table 20), all also had a positive correlation with troponin-In both cohorts (Figure 49). Only one of these miRs was detected in cultured endothelial cells – *miR-278a* – and this miR also increased with hypoxia (Table 15). These findings provide some insight into the biology of microvascular obstruction. Previously published work has suggested that microvascular obstruction is caused by endothelial dysfunction, but my findings show that the miRs related to MVO are, apart from *miR-278a*, not endothelial in origin, rather they are released from the other myocardial cell types, such as cardiomyocytes.

Of the miRs more likely to be detected in patients with MVO (Table 22), two of these showed a strong relationship with troponin release (*miR-193b* and *-378a*, Figure 49). Two other miRs were released from cultured endothelial cells (*miR-125a* and *-30d*). The remainder of miRs did not show strong relationships with the analysed clinical parameters.

The final stage of this experiment was to construct a regression model to predict outcome. While every miR analysed on the OxAMI-focused plate could potentially be used in such a model, it was likely that many miRs increased or decreased as part of wider networks of other miRs moving in a similar way. The number of components generated in a principal component analysis is the same as

the number of variables (miRs). To include all principal components in an analysis would defeat the main purpose of PCA which is factor reduction - to explain as much variance as possible using as few variables as possible.

The Total Variance Explained showed that the first ten components explained 70% of the variance within the dataset (Table 23). The correlation between each miR and the principal components is shown in Table 24 and it shows that a large amount of variance in the dataset is explained by the myocardial miRs which are strongly represented in component 1 (which accounts for 22% of the variance in the dataset).

The rich clinical phenotyping carried out in the OxAMI programme allowed the principal component analysis to be of clinical, as well as statistical, relevance. The principal component scores were extracted and a correlation matrix was generated with the clinical parameters. Given the finding that the myocardial miRs relate to component 1, it is perhaps unsurprising that this component also correlates with troponin and infarct size (Table 25). The fact that it also correlates with grouped MVO may support the finding earlier in this experiment that MVO is strongly linked with troponin release. Other components demonstrate the importance of other clinical parameters in the miR signature in myocardial infarction, such as renal function, haemoglobin and acid-base status.

Being able to predict infarct size early in a patient's hospital admission would be clinically important because it would allow earlier risk stratification, targeting of treatment, identification of patients for clinical trials and could be used to identify patients who could safely be discharged earlier and those who may benefit from a longer stay. Although troponin is helpful, it is not strongly predictive of infarct size until at least 24 hours after admission, and is most predictive when using four readings over 48 hours to calculate area under the curve.

The seven miRs used to build the regression model were selected for both statistical and biological reasons. Principal component analysis allowed the identification of miRs specifically related to myocardial injury which is a predictor of final infarct size. As MVO is known to predict outcome, and patients with MVO are likely to have worse outcome (Figure 10), three of the miRs were selected because of their strong relationship with MVO. Finally, platelet activation is important in acute myocardial infarction, both in the pathogenesis of plaque rupture and coronary thrombosis. Two miRs were selected for their roles in platelet activation (*miR-320a* and *-b*). All miRs contributed to the statistical power of the model which model statistically significantly predicted final infarct size and was more predictive of final infarct size than either a single measurement of troponin at six hours or troponin AUC (0-48).

13 Transcoronary MicroRNA Analysis

13.1 Introduction

MicroRNAs are known to be tissue and organ specific. For example, *miR-1* and *-133a* are expressed in both skeletal and cardiac muscle whereas *miR-499* is cardiomyocyte specific[74]. These miRs can also be detected in the circulating plasma but less is known about the biology or kinetics of miR release.

In this chapter, paired blood samples which were collected at the time of primary PCI were analysed. These samples were taken from the proximal coronary artery and the coronary sinus, which is part of the venous drainage of the heart (Figure 51). Around 85% of coronary venous blood drains via the coronary sinus system[138–140]. The remainder drains into the Thebesian venous system, thin walled veins that drain directly into all chambers of the heart. The coronary sinus is the terminal vein of the heart and it follows the atrioventricular groove to drain into the right atrium around the junction of the septal and posterior tricuspid valve leaflets.

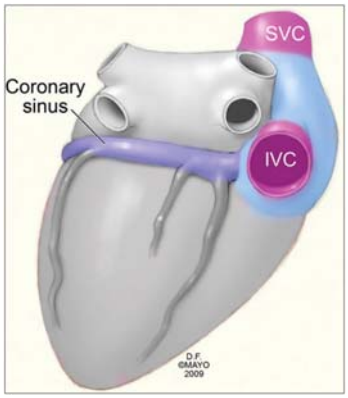

Figure 51: Coronary sinus anatomy. From Habib A, et al. Europace 2009; 11 Suppl 5: v15-21.

Collecting both samples allowed the calculation of a miR gradient from coronary artery to coronary sinus which could then be used to identify which components of the miR signature already identified in the previous chapters originated from the myocardial tissue and which originated elsewhere.

13.2 Methods

Patient Recruitment

Patients were recruited using the criteria and protocols as previously described (Chapter 8). In order to be included in this part of the study, patients were required to have had coronary artery and coronary sinus blood samples collected during primary PCI.

Experimental Design

Paired coronary artery and coronary sinus samples were collected at the time of primary PCI from a subset of patients recruited to the OxAMI programme. The sample collection methods are shown in the Patient Recruitment section on page 47. Briefly, two EDTA and one SST test tubes were collected from each sample site and processed to isolate serum and plasma.

Collecting blood from the coronary sinus can be technically challenging due to the difficulty of obtaining a stable catheter position and in the early patients the position was sometimes lost during sample collection. It became common practice to place a coronary guide wire into the coronary sinus to provide some catheter stability which resolved this issue.

This problem identified, it was important to confirm that any sample analysed was actually taken from the coronary sinus, rather than from the right atrium. An extra 2ml blood sample was collected from a peripheral vein and the coronary sinus for blood gas analysis. If the pO_2 in a presumed

coronary sinus sample was less than the pO_2 in the venous sample, then this sample was confirmed as a true coronary sinus sample. If this criterion was not met, then the sample was excluded from this part of the study.

MicroRNA Analysis and Quality Control

RNA isolation and reverse transcription were carried out according to the protocols in the MicroRNA Processing section (page 65, MicroRNA analysis). Samples were analysed using the OxAMI-focused plate which included wells for quality control assessment (Appendix 2: The OxAMI-Focused Plate, page 199).

Normalisation

Data pre-processing was carried out as described previously (page 86). As the OxAMI focused plate was used, global mean normalisation was not a suitable normalisation method. Therefore, once qPCR of all samples was complete, an initial analysis was carried out to determine whether previously identified reference miRs were stable in this particular sample type. Once confirmed reference gene normalisation could be carried out.

Data Analysis

Paired analyses were carried out to identify which miRs were detected in samples from each site. Median CT values were calculated for each miR from each site and these values were subtracted to calculate the change in miR across the myocardial gradient, and miRs increasing or decreasing were listed and cross-referenced with the findings from the Validation Experiment.

13.3 Results

Patient Selection and Quality Control

92 patients underwent coronary sinus blood sampling between September 2012 and May 2014. All patients had coronary artery, peripheral venous and coronary sinus blood samples taken during primary PCI at time point 1.3 (immediately after coronary stent deployment). Blood gas analysis was carried out on all samples. Patients were included in this part of the study if the following criteria were met:

- Paired coronary artery, peripheral venous and coronary sinus samples were collected during primary PCI
- The patient had undergone an acute (48 hour) cardiac MRI scan
- Blood gas analysis confirmed a true coronary sinus sample ($pO_{2\ (CS)} < PO_{2\ (venous)}$)

Patient selection and quality control results are shown in Figure 52 and Table 27. As this experiment was designed as a paired analysis, only paired samples underwent further analysis; if one sample was excluded for a quality control issue, the other sample was also excluded. On this basis, a further six samples were excluded thus 23 patients (46 paired samples) underwent statistical analysis.

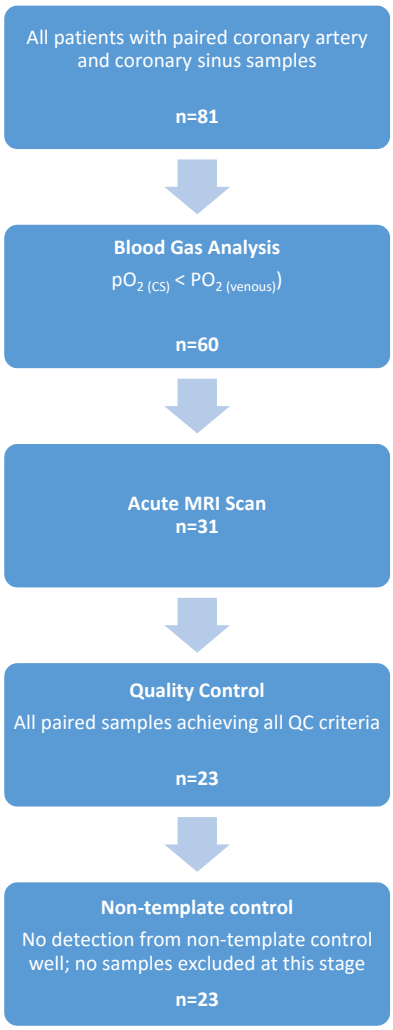

Figure 52: Sample selection process for the paired coronary artery-coronary coronary sinus analysis.

	Parameter	Criteria	Number of samples (%) Coronary artery	Number of samples (%) Coronary sinus
	Starting number of samples		29	29
1	RNA Isolation	*UniSP2/4/5 should be detectible at CT values ≤37. CT values should be SP2≤SP4≤SP5*	27 (93)	24 (83)
2	PCR	*UniSP3 CT value should be 18-22 across dataset*	29 (100)	29 (100)
3	Positive controls	*Both positive controls (miR-103 and miR-191) should be detected*	29 (100)	29 (100)
4	Haemolysis	*Sample excluded if visibly haemolysed. Also excluded if ΔCT between miR-23a and miR-451 ≥7*	29 (100)	28 (97)
	TOTAL	*Number of samples passing all QC steps (%)*	27 (93)	23 (79)
		Number of paired samples undergoing detailed analysis	23	

Table 27: Quality control results for the 23 paired coronary artery and coronary sinus samples collected at the time of primary PCI.

At each stage of the microRNA isolation and analysis process, the number of samples successfully reaching the pre-specified quality control criteria are shown. The Total row shows the number of samples that successfully achieved all of the quality control criteria (percentages in brackets).

Twenty-three patients were selected for inclusion and were recruited between September 2012 and May 2014; their clinical parameters are shown in Table 28.

Gender n (%)	
Male	16 (69.6)
Female	7 (30.4)
TOTAL	23

Age	
Median	66
Range	42-87

Diabetes n (%)	
Oral medication	4 (17.4)
Insulin	0 (0)
New diagnosis	0 (0)
TOTAL	4 (17.4)

Smoking n (%)	
Current	8 (34.8)
Ex	8 (34.8)
Never	7 (30.4)

Creatinine (µmol/L)	
Median	73.0
Range	37.0-141.0

Culprit vessel n (%)	
LAD	10 (43.5)
Circumflex	4 (17.4)
RCA	9 (39.1)

Troponin (µg/L)	
Peak (median)	54.7
Peak (range)	1.1-929.5
AUC 0-48h (median)	1440.0
AUC 0-48h (range)	34.0-12697.0

Infarct size (g)	
Median	15.1
Range	2.0-40.0

LV ejection fraction at 6 months %	
Median	59.5
Range	37.1-83.5

Total hospital stay (days)	
Median	1.8
Range	1.2-10.8

Table 28: Baseline patient characteristics for all patients recruited to the coronary sinus cohort.
23 patients were recruited over 20 months. LAD=left anterior descending, RCA=Right coronary artery. Troponin-I was measured at four time points and a troponin area under the curve (AUC) was calculated. Infarct size and ejection fraction are measured at the six month MRI scan. Infarct size is measured as late gadolinium enhancement.

MiR detection parameters are shown in Figure 53. A greater number of miRs were detected in the coronary sinus samples (median=9 additional miRs) compared with the coronary artery samples. A Wilcoxon signed-rank test determined that this was a statistically significant increase ($p=0.01$). There was no statistically significant difference in the median raw CT values between the different sample sites.

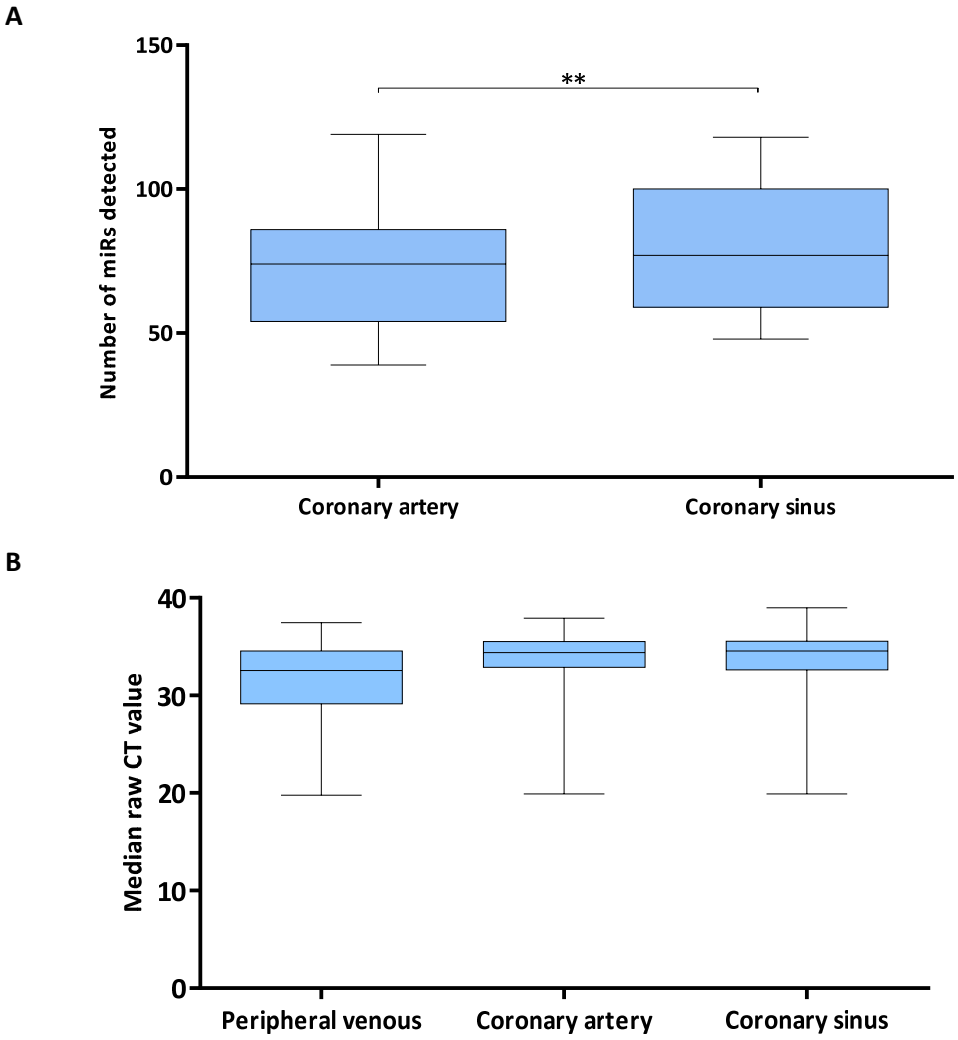

Figure 53: MiR detection in the paired coronary artery-coronary sinus experiment.
A: the number of miRs detected with a raw CT value ≤38 in each group. There was a significantly larger number of miRs detected in the coronary sinus group (p=0.01). **B:** Median raw CT value (all detected miRs with a raw CT value ≤38) in the three different sample types – peripheral venous, coronary artery and coronary sinus. There was no significant difference between any of the three groups. Box shows median and interquartile range, whiskers show range.

Normalisation

Reference genes were once again selected using the *Normfinder* algorithm. Table 29 shows the most stable miRs in each cohort and sample site. As before, the six most stable miRs were used for normalisation.

Experiment	Discovery	Validation	Transcoronary	
Sample site	Peripheral venous		Coronary artery	Coronary sinus
Accumulated SD	0.22	0.25	0.40	0.40
Selected reference miRs	*hsa-miR-23a* *hsa-miR-92a* *hsa-miR-126* *hsa-miR-423* *hsa-miR-25* *hsa-miR-26b*			

Table 29: Accumulated standard deviation (SD) of the Normfinder selected reference genes across all cohorts and sample sites.

Myocardial MicroRNAs

Initially the known myocardial miRs were analysed. CT values for each sample at each site were plotted, also with grouped results (Figure 54). *MiR-1*, *-499* and *-133b* all increased down the myocardial gradient. A paired samples t-test confirmed that this increase was statistically significant in all myocardial miRs.

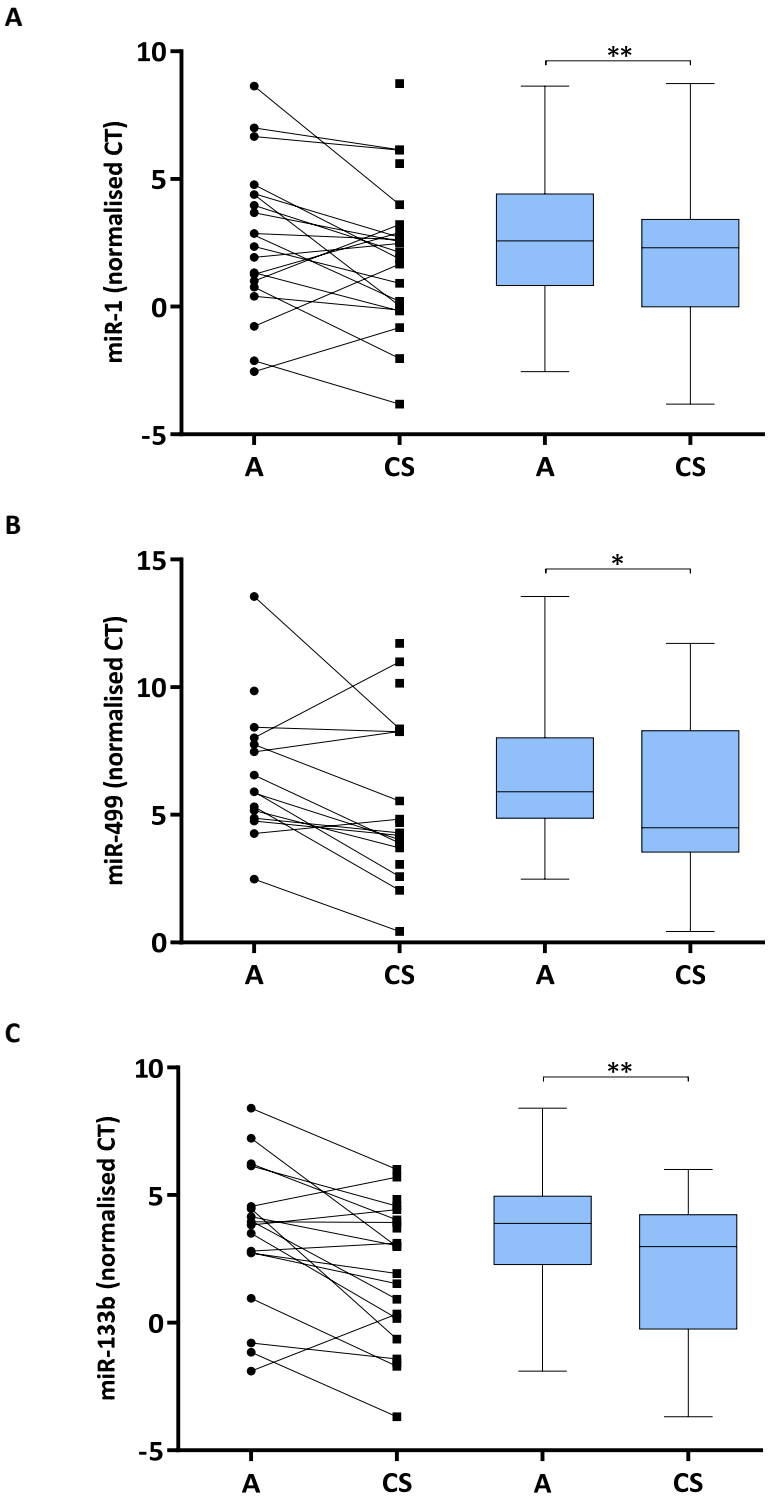

Figure 54: Detection of myocardial microRNAs across the myocardial gradient.
MiR-1 (panel A), miR-499 (panel B) and miR-133b (panel C) levels increase (CT decreases) from coronary artery to coronary sinus. A=coronary artery; CS=coronary sinus; CT=cycle threshold. N=22.

Paired samples t-test was used to test for a significant difference between miR detection in coronary artery versus coronary sinus samples.

In addition to the myocardial miRs, some others were shown to increase down the myocardial gradient (Figure 54, panel A) and some decreased (panel B).

A

miR	Δ median CT
hsa-miR-193b-3p	-2.49
hsa-miR-214-3p	-1.61
hsa-miR-30d-3p	-1.55
hsa-miR-186-5p	-1.54
hsa-miR-499a-5p	-1.41
hsa-miR-133a-3p	-1.38
hsa-miR-195-5p	-1.34
hsa-miR-99a-5p	-1.29
hsa-miR-125b-5p	-1.27
hsa-miR-378a-3p	-1.26
hsa-miR-136-5p	-1.25
hsa-miR-148a-3p	-1.13
hsa-miR-22-5p	-1.10
hsa-miR-145-5p	-0.93
hsa-miR-23b-3p	-0.93
hsa-miR-208a-5p	-0.92
hsa-miR-133b	-0.91
hsa-miR-210-3p	-0.73
hsa-miR-140-5p	-0.71
hsa-miR-25-3p	-0.70
hsa-miR-155-5p	-0.69
hsa-miR-675-3p	-0.69
hsa-miR-132-3p	-0.68
hsa-miR-30a-3p	-0.64
hsa-miR-204-5p	-0.62
hsa-miR-532-5p	-0.61
hsa-miR-18a-3p	-0.60
hsa-miR-342-3p	-0.59
hsa-miR-576-5p	-0.57

B

miR	Δ median CT
hsa-miR-199a-3p	0.55
hsa-miR-664a-3p	0.57
hsa-miR-197-3p	0.63
UniSp4 CP	0.64
hsa-let-7d-5p	0.69
hsa-miR-7-1-3p	0.69
hsa-miR-130b-3p	0.70
hsa-miR-103a-3p	0.71
hsa-miR-27a-5p	0.73
hsa-let-7a-5p	0.76
hsa-miR-665	0.83
hsa-miR-548c-5p	0.87
hsa-miR-208b-3p	0.92
hsa-miR-362-5p	0.95
hsa-miR-423-3p	0.97
hsa-miR-107	0.99
hsa-miR-335-3p	1.09
hsa-miR-128-3p	1.11
hsa-miR-193a-5p	1.14
hsa-let-7e-5p	1.18
hsa-miR-221-3p	1.21
hsa-miR-671-5p	1.23
hsa-miR-28-5p	1.49
hsa-miR-337-3p	2.25

Table 30: Change in miRs down the myocardial gradient.
Figures shown are calculated by taking the median CT value for a miR in the coronary sinus and subtracting this value from the median CT value in the coronary artery samples. All miRs increasing or decreasing a median ≥0.5 CT are shown. A negative value (panel A, coloured red) denotes a miR which is detected at increased concentration in the coronary sinus compared with the coronary artery; a positive value (panel B, coloured blue) denotes a decreased miR concentration in the coronary sinus. N=22.

A further analysis was carried out to identify which miRs were not detected in the coronary artery sample which could then be detected in the coronary sinus, which would likely reflect miRs released from the myocardial tissue (Table 31).

	# samples in which each miR detected		
miR	**Coronary artery**	**Coronary sinus**	**Δ CS-A**
hsa-miR-204-5p	10	18	8
hsa-miR-576-5p	6	13	7
hsa-miR-210-3p	10	17	7
hsa-miR-30d-3p	8	15	7
hsa-miR-208b-3p	11	17	6
hsa-miR-130b-3p	11	17	6
hsa-miR-652-3p	12	18	6
hsa-miR-132-3p	15	21	6
hsa-miR-99a-5p	14	20	6
hsa-miR-152-3p	15	20	5
hsa-miR-30a-3p	14	19	5
hsa-miR-195-5p	15	20	5
hsa-miR-222-3p	18	22	4
hsa-miR-199a-3p	20	23	3
hsa-miR-95-3p	11	14	3
hsa-miR-181b-5p	13	16	3
hsa-miR-421	16	19	3
hsa-miR-145-3p	10	13	3
hsa-miR-34a-5p	11	14	3
hsa-miR-342-3p	20	23	3
hsa-miR-133b	18	21	3
hsa-miR-378a-3p	16	19	3
hsa-miR-125b-5p	20	23	3
hsa-miR-499a-5p	15	18	3
hsa-miR-193b-3p	9	12	3
hsa-miR-664a-3p	17	19	2
hsa-miR-342-5p	10	12	2
hsa-miR-335-5p	15	17	2
hsa-miR-663a	16	18	2
hsa-miR-1	20	22	2
hsa-miR-532-5p	12	14	2
hsa-miR-22-5p	14	16	2
hsa-miR-133a-3p	18	20	2
hsa-miR-337-3p	6	4	-2
hsa-miR-885-5p	15	13	-2
hsa-miR-215-5p	22	20	-2
hsa-miR-155-5p	22	18	-4
hsa-miR-208a-5p	10	5	-5

Table 31: miRs detected in coronary artery versus coronary sinus samples.
Each column shows the number of samples (n=23) in which each miR was detected. The difference between the two sites was then calculated. A positive number (coloured red) indicates a miR is

detected in more coronary artery sinus samples and a negative number (coloured blue) indicates a miR is detected in more coronary artery samples. N=22.

Of the 33 miRs detected more frequently in the coronary sinus samples (all results indicated in red in Table 31), 12 had a strong correlation with troponin release (Table 32). Six of the miRs increased in the coronary sinus samples showed a strong correlation with MVO, *miR-95-3p, -193b, -1, -133a/b* and *-378a*.

A

miR
hsa-miR-1
hsa-miR-95-3p
hsa-miR-99a-5p
hsa-miR-125b-5p
hsa-miR-133a-3p
hsa-miR-133b
hsa-miR-152-3p
hsa-miR-193b-3p
hsa-miR-208b-3p
hsa-miR-30a-3p
hsa-miR-378a-3p
hsa-miR-499a-5p

B

miR
hsa-miR-99a-5p
hsa-miR-125b-5p
hsa-miR-133a-3p
hsa-miR-133b
hsa-miR-145-5p
hsa-miR-193b-3p
hsa-miR-30a-3p
hsa-miR-378a-3p
hsa-miR-499a-5p
hsa-miR-99a-5p
hsa-miR-125b-5p
hsa-miR-133a-3p

Table 32: Overlap between miRs myocardial miR detection and troponin release.
A: all miRs which are more frequently detected in the coronary sinus that also correlate strongly (r=≥0.4 and p≤0.05) with troponin release. **B:** shows all miRs which are detected at increased concentration in coronary sinus samples that also correlate strongly with troponin release strongly (r=≥0.4 and p≤0.05). Bold indicates miRs not previously linked with acute myocardial infarction.

The Endothelial Cell Culture Experiment identified which miRs are detected in cell supernatant, and therefore which are likely to be released from endothelial cells. Endothelial miRs and those released more frequently or at increased concentration in the coronary sinus are shown in Table 33, along with their potential roles in the published literature.

miR	Potential roles
hsa-miR-25-3p	Contractility in the failing heart[135]
hsa-miR-30a-3p	Regulates angiotensin II induced myocardial hypertrophy[141]
hsa-miR-99a-5p	Remodelling after acute myocardial infarction[142]
hsa-miR-125b-5p	Promotes myocardial fibrosis[143]
hsa-miR-132-3p	Regulates cardiac hypertrophy and autophagy[144]
hsa-miR-155-5p	Promotes cardiac hypertrophy and failure[145]
hsa-miR-214-3p	Myocardial protection from ischaemic injury[146]
hsa-miR-23b-3p	Induces left ventricular hypertrophy and failure[147]
hsa-miR-342-3p	Biomarker for heart failure[148]
hsa-miR-532-5p	Downregulated in ischaemia-reperfusion[149]

Table 33: miRs released from endothelial cells (identified in the Endothelial Cell Culture Experiment) that are also detected at increased concentration or frequency in coronary sinus samples.
Potential roles were identified with a literature search using the miR as a search term.

13.4 Discussion

Analysis of paired coronary artery and coronary sinus samples was carried out on a subset of the OxAMI cohort. MicroRNA analysis protocols developed for peripheral venous miR analysis were reliable and effective in these different sample types. The number of samples not achieving the pre-specified quality control criteria was increased in coronary sinus samples which may reflect the technical challenges of collecting these samples, namely the increased risk of haemolysis aspirating low-pressure blood through a long, narrow diameter catheter, and the high workload of the OxAMI fellow at this time point, processing up to six samples simultaneously.

More miRs were detected in the coronary sinus samples, which could reflect miRs being released from the myocardium into the circulation. The fact that the median raw CT value was comparable between venous, coronary artery and coronary sinus samples confirms this hypothesis, rather than this finding simply being related to increased experimental efficiency. Normalisation was carried out as before, using six reference miRs. The accumulated standard deviation was higher in the coronary artery and coronary sinus samples; despite this, the previously identified reference miRs were still the most stable of those detected in all samples, which was important to confirm prior to using them for normalisation.

This experiment has confirmed most known myocardial miRs increase in concentration down the myocardial gradient (Figure 54). As they all correlate with troponin release, itself released from damaged cardiomyocytes, it may be that the myocardial miRs are also released from damaged cardiomyocytes. This experiment supports this hypothesis. Many of the other miRs shown to increase down the myocardial gradient also strongly correlated with troponin release in the Validation Experiment. These miRs, shown in Table 32 (panel A) are likely to be released from myocardial tissue in acute myocardial infarction. Some (e.g. *miR-1, 133a/b, -208b, -499*) have been

previously shown to be increased in myocardial injury but this relationship has not previously been demonstrated in the remainder (shown in bold) and these are shown for the first time in this work.

The Cultured Endothelial Cell Experiment identified which miRs are released from endothelial cells. Of those that were endothelial, ten were also increased in coronary sinus samples, which may suggest that they were released from the myocardial endothelium. They have myriad potential roles, including in heart failure, ischaemia-reperfusion injury and left ventricular failure.

14 Conclusions

In this thesis, 102 patients with acute myocardial infarction were recruited for detailed clinical phenotyping including the measurement of blood biomarkers and ECG changes, quantification of microvascular obstruction and determination of final infarct size at six months. They then underwent comprehensive microRNA analysis with correlation of these findings with measures of clinical outcome.

The Discovery Experiment confirmed that the previously reported myocardial miRs increase in concentration in acute myocardial infarction, peaking earlier than troponin and showing a strong correlation with final infarct size. A broad, unbiased analysis confirmed which miRs are commonly detected in plasma after MI and a large number of miRs never detected, so they could reasonably not be measured in future analysis. This is an important finding: the analysis of a short list of candidate miRs is a highly biased approach, and is frequently seen in the miR literature; excluding specific miRs from routine analysis having determined them to be undetected in the majority of samples is a scientifically reasonable approach reducing cost and time taken for miR analysis.

The wide variation in methods for data pre-processing and normalisation is apparent on reviewing the miR literature. In this work, every stage of miR isolation, quantification and analysis have been optimised and validated. The different methods of normalisation were compared, and the variability of miR quantification with some methods, particularly spike-in normalisation, was striking. The importance of selecting appropriate, statistically determined, reference miRs for a particular sample type was shown and the performance of reference gene normalisation was shown to be close to that of global mean normalisation, but more appropriate for smaller miR analyses.

The Validation Experiment confirmed the findings from the Discovery Experiment and demonstrated the miR analysis protocol to be reliable. 16 miRs not previously linked with myocardial infarction were shown to strongly correlate with troponin release in both experiments. Separating the microvascular obstruction and myocardial necrosis signals was challenging, indeed all miRs correlating with MVO also correlate with troponin release and this work has proved that the two are inextricably linked. Analysing miR release in coronary sinus samples confirmed that most myocardial miRs increase down the myocardial gradient and may, like troponin, be released from damaged cardiomyocytes.

With such a large dataset, identifying the biological relevance of each miR can be challenging. The Endothelial Cell Culture Experiment identified which miRs are released from endothelial cells and, although 124 were reliably detected, none of these were the previously reported myocardial miRs which would suggest these are released from another cell type in the myocardial bed, perhaps cardiomyocytes. Principal Component Analysis was used to statistically identify and group miRs based on their correlation with clinical parameters. This approach allowed miRs to be identified for a regression model to predict outcome in patients after acute MI. Measurement of seven miRs six hours after MI provides more information on clinical outcome than ECG changes, cardiac MRI or existing blood biomarkers at the same time-point. While miR analysis currently takes longer than these contemporary clinical measures, the steps required for miR analysis can be readily automated and, as the technology improves, the time taken for miR analysis is likely to reduce.

Future work should build on the findings in this thesis, particularly in carrying out external validation of the regression model on a new group of patients. This model could be used to guide clinical decision making, including the targeting of treatment, determining length of stay on the coronary care unit and identifying patients who could be suitable for early discharge. While myocardial infarction is frequently a straightforward diagnosis it can also be a challenge, as illustrated by the

relatively low number of posterior myocardial infarctions recruited to this work. The use of miRs for diagnosis of myocardial infarction, with earlier detection than troponin, may be another area where miRs could contribute to clinical care.

15 Appendix 1: The OxAMI Plate

	1	2	3	4	5	6	7	8	9	10	11	12	13	14	15	16	17	18	19	20	21	22	23	24
A	hsa-miR-7-5p	hsa-miR-217	hsa-miR-337-5p	hsa-miR-328-3p	hsa-miR-143-3p	hsa-miR-218-5p	hsa-miR-136-5p	hsa-miR-127-5p	hsa-miR-140-5p	hsa-miR-210-3p	hsa-miR-199b-5p	hsa-miR-194-5p	hsa-let-7g-5p	hsa-miR-203a	hsa-miR-181a-5p	hsa-miR-137	hsa-miR-551b-3p	Blank (H2O)	UniSp2 CP	hsa-miR-486-5p	UniSp4 CP	UniSp5 CP	hsa-miR-329-3p	UniSp6 CP
B	hsa-miR-487b-3p	Cel-miR-39-3p CP	hsa-miR-191-5p	hsa-miR-378a-3p	hsa-miR-103a-3p	UniSp3 IPC	hsa-miR-423-5p	hsa-miR-221-3p	SNORD 38B	UniSp3 IPC	SNORD 49A	hsa-miR-532-5p	hsa-miR-99a-5p	hsa-miR-16-5p	miR-98-5p	hsa-miR-185-5p	hsa-miR-25-3p	hsa-miR-524-5p	hsa-miR-20a-5p	hsa-miR-765	hsa-miR-miR-24-3p	hsa-miR-369-5p	hsa-miR-425-5p	hsa-miR-590-5p
C	hsa-miR-760	hsa-miR-574-3p	hsa-miR-130b-3p	hsa-miR-30c-5p	hsa-miR-133b	hsa-miR-23a-3p	hsa-miR-193b-3p	hsa-miR-501-5p	hsa-miR-518c-3p	hsa-miR-130a-3p	hsa-miR-379-5p	hsa-miR-452-5p	hsa-miR-589-5p	hsa-miR-141-3p	hsa-miR-342-3p	hsa-miR-934	hsa-miR-101-3p	hsa-miR-539-5p	hsa-miR-331-3p	hsa-miR-499a-5p	hsa-miR-196a-5p	hsa-miR-330-3p	hsa-miR-570-3p
D	hsa-miR-200a-3p	hsa-miR-188-5p	hsa-miR-26a-5p	hsa-miR-99b-5p	hsa-miR-431-5p	hsa-miR-23b-3p	hsa-miR-505-3p	hsa-miR-18a-5p	hsa-miR-92a-3p	hsa-miR-500a-3p	hsa-miR-887-3p	hsa-miR-423-3p	hsa-miR-126-3p	hsa-miR-421	hsa-miR-376b-3p	hsa-miR-625-3p	hsa-miR-339-5p	hsa-miR-323a-3p	hsa-miR-1810-125a-5p	hsa-miR-374b-5p	hsa-miR-302d-3p	hsa-miR-346		
E	hsa-miR-151a-3p	hsa-miR-493-3p	hsa-miR-122-5p	hsa-miR-99a-3p	hsa-miR-361-5p	hsa-miR-125b-5p	hsa-miR-503-5p	hsa-miR-204-5p	hsa-miR-30d-5p	hsa-miR-301a-3p	hsa-miR-362-5p	hsa-miR-545-3p	hsa-miR-29b-2-5p	hsa-miR-491-5p	hsa-miR-92b-3p	hsa-miR-665	hsa-miR-363-3p	hsa-miR-132-3p	hsa-miR-651-5p	hsa-miR-628-3p	hsa-miR-432-5p	hsa-miR-154-5p	hsa-miR-27a-3p	hsa-miR-376c-3p
F	hsa-miR-940	hsa-miR-22-5p	hsa-miR-224-5p	hsa-miR-885-5p	hsa-miR-320a	hsa-miR-18b-5p	hsa-miR-187-3p	hsa-miR-186-5p	hsa-miR-199a-3p	hsa-miR-155-5p	hsa-miR-107	hsa-miR-662	hsa-miR-485-3p	hsa-miR-337-3p	hsa-miR-144-3p	hsa-miR-1-3p	hsa-miR-211-5p	hsa-miR-454-3p	hsa-let-7g-3p	hsa-miR-30e-5p	hsa-miR-34a-5p	hsa-miR-663a	hsa-miR-518e-3p	hsa-miR-29b-3p
G	nsa-miR-433-3p	hsa-miR-660-5p	hsa-let-7c-3p	miR-28-5p	hsa-miR-324-5p	hsa-miR-219a-1-3p	hsa-miR-19b-3p	hsa-miR-215-5p	hsa-miR-30b-5p	hsa-miR-199a-5p	hsa-miR-335-5p	miR-21-5p	hsa-miR-26b-5p	hsa-miR-214-3p	miR-32-5p	hsa-miR-324-3p	hsa-miR-371a-5p	hsa-miR-455-5p	hsa-miR-205-5p	hsa-miR-19a-3p	hsa-miR-150-5p	hsa-miR-15a-5p	hsa-let-7d-3p	hsa-miR-671-5p
H	hsa-miR-497-5p	hsa-miR-877-5p	hsa-miR-10b-5p	hsa-let-7i-5p	hsa-miR-202-5p	hsa-miR-652-3p	hsa-miR-126-5p	hsa-miR-30e-3p	hsa-miR-181c-5p	hsa-miR-152-3p	miR-93-5p	hsa-miR-365a-3p	hsa-miR-29c-3p	hsa-miR-133a-3p	hsa-miR-124-3p	hsa-miR-190a-5p	hsa-miR-302a-3p	hsa-miR-596	hsa-miR-602	hsa-miR-223-3p	hsa-miR-410-3p	hsa-miR-17-5p	hsa-miR-376a-3p	hsa-miR-148b-3p
I	hsa-miR-127-3p	hsa-miR-598-3p	miR-96-5p	hsa-let-7d-5p	hsa-miR-495-3p	hsa-miR-299-5p	hsa-miR-744-5p	hsa-miR-145-5p	hsa-let-7a-5p	hsa-miR-615-3p	hsa-let-7b-5p	hsa-miR-766-3p	hsa-miR-206	hsa-miR-193a-3p	hsa-miR-192-5p	hsa-miR-29a-3p	hsa-miR-18a-3p	hsa-miR-142-5p	hsa-miR-197-3p	hsa-miR-326	hsa-miR-15b-5p	hsa-miR-196b-5p	hsa-miR-296-5p	hsa-miR-20b-5p
J	hsa-miR-198	hsa-miR-375	hsa-miR-361-3p	miR-21-3p	hsa-miR-373-3p	hsa-miR-518f-3p	hsa-miR-222-3p	hsa-miR-154-5p	hsa-miR-708-5p	miR-95-3p	hsa-miR-517c-3p	hsa-miR-1511a-5p	hsa-miR-502-5p	hsa-miR-509-3p	hsa-miR-134-5p	hsa-miR-382-5p	hsa-miR-490-3p	hsa-miR-200c-3p	hsa-miR-30a-5p	hsa-miR-181b-3p	hsa-miR-33a-5p	hsa-miR-195-5p	hsa-miR-874-3p	
K	hsa-miR-135a-5p	hsa-miR-146b-5p	hsa-miR-412-3p	hsa-miR-miR-1	hsa-miR-299-3p	hsa-let-7e-5p	hsa-miR-338-3p	hsa-miR-584-5p	hsa-miR-216a-5p	hsa-miR-424-5p	hsa-miR-140-3p	hsa-miR-181a-3p	hsa-miR-10a-5p	hsa-miR-106a-5p	hsa-miR-370-3p	hsa-miR-576-5p	hsa-miR-425-3p	hsa-miR-411-5p	hsa-miR-216b-5p	hsa-miR-106b-3p	hsa-miR-miR-22-3p	hsa-miR-212-3p	hsa-miR-525-5p	hsa-miR-542-5p
L	hsa-miR-576-3p	hsa-miR-483-3p	hsa-miR-582-5p	hsa-miR-183-5p	hsa-miR-409-3p	hsa-miR-100-5p	hsa-miR-629-5p	hsa-miR-484	hsa-miR-381-3p	hsa-miR-148a-3p	hsa-miR-146a-5p	hsa-miR-139-5p	hsa-miR-149-5p	hsa-miR-642a-5p	hsa-let-7e-3p	hsa-miR-31-5p	hsa-miR-451a	hsa-miR-27b-3p	hsa-miR-523-3p	hsa-miR-374a-5p	hsa-miR-1913	hsa-miR-1245a	hsa-miR-1249	hsa-miR-502-3p
M	hsa-miR-490-5p	hsa-miR-125a-5p	hsa-miR-144-5p	hsa-miR-143-5p	hsa-miR-1207-5p	hsa-miR-675-3p	hsa-miR-942-5p	miR-24-2-5p	miR-28-3p	hsa-miR-548c-5p	hsa-miR-532-3p	hsa-miR-937-3p	hsa-miR-29c-5p	hsa-miR-499a-5p	hsa-let-7f-1-3p	hsa-miR-7e-3p	hsa-miR-643	hsa-miR-221-5p	hsa-miR-338-5p	hsa-miR-141-5p	hsa-miR-501-3p	hsa-miR-15b-3p	hsa-miR-29a-5p	hsa-miR-101-5p
N	hsa-miR-106b-5p	hsa-miR-208a-3p	hsa-miR-miR-17-5p	hsa-miR-224-3p	hsa-miR-130b-3p	hsa-miR-1271-5p	hsa-miR-520h	hsa-miR-769-5p	hsa-miR-1908-5p	hsa-miR-1260a	hsa-miR-365b-3p	hsa-miR-941	hsa-miR-23b-5p	hsa-miR-26b-3p	hsa-miR-30d-3p	hsa-miR-632	hsa-miR-181a-2-3p	hsa-miR-125b-1-3p	hsa-miR-708-3p	hsa-miR-20a-3p	hsa-miR-455-3p	hsa-miR-610	hsa-miR-511-5p	hsa-let-7a-3p
O	hsa-miR-1469-5p	hsa-miR-628-5p	hsa-miR-145-3p	hsa-miR-378a-3p	hsa-miR-miR-7-1-3p	hsa-miR-181c-5p	hsa-miR-505-5p	hsa-miR-450b-5p	hsa-miR-362-3p	hsa-miR-624-5p	hsa-miR-27a-5p	hsa-miR-744-3p	hsa-miR-139-3p	hsa-miR-99b-3p	hsa-miR-125b-2-3p	hsa-miR-miR-16-2-3p	hsa-miR-340-3p	hsa-miR-342-5p	hsa-let-7i-3p	hsa-miR-543	hsa-miR-664a-3p	hsa-miR-556-3p	hsa-miR-93-3p	hsa-miR-1972
P	hsa-miR-2110	hsa-miR-548a-3p	hsa-miR-320c	hsa-miR-636	hsa-miR-208b-3p	hsa-miR-223-5p	hsa-miR-424-3p	hsa-miR-339-3p	hsa-miR-551a	hsa-miR-24-1-5p	hsa-let-7b-3p	hsa-miR-193b-3p	hsa-miR-335-3p	hsa-miR-885-3p	hsa-miR-320d	hsa-miR-331-5p	hsa-miR-486-3p	hsa-miR-320b	hsa-miR-550a-3p	hsa-miR-30a-3p	hsa-let-7g-3p	hsa-miR-214-5p	hsa-miR-590-3p	hsa-miR-493-5p

16 Appendix 2: The OxAMI-Focused Plate

hsa-let-7a-5p	hsa-let-7c-3p	hsa-let-7d-3p	hsa-let-7d-5p	hsa-let-7e-5p	hsa-let-7g-5p	hsa-miR-1
hsa-miR-107	hsa-miR-122-5p	hsa-miR-125a-3p	hsa-miR-125b-5p	hsa-miR-126-3p	hsa-miR-126-5p	hsa-miR-128-3p
hsa-miR-132-3p	hsa-miR-133a-3p	hsa-miR-133b	hsa-miR-136-5p	hsa-miR-140-5p	hsa-miR-145-3p	hsa-miR-145-5p
hsa-miR-148a-3p	hsa-miR-150-5p	hsa-miR-151a-3p	hsa-miR-152-3p	hsa-miR-154-5p	hsa-miR-155-5p	hsa-miR-16-1-3p
hsa-miR-181b-5p	hsa-miR-181c-3p	hsa-miR-181c-5p	hsa-miR-186-5p	hsa-miR-18a-3p	hsa-miR-190a-5p	hsa-miR-193a-5p
hsa-miR-193b-5p	hsa-miR-195-5p	hsa-miR-1972	hsa-miR-197-3p	hsa-miR-199a-3p	hsa-miR-200a-3p	hsa-miR-203a
hsa-miR-208a-5p	hsa-miR-208b-3p	hsa-miR-210-3p	hsa-miR-211-5p	hsa-miR-214-3p	hsa-miR-214-5p	hsa-miR-215-5p
hsa-miR-221-3p	hsa-miR-222-3p	hsa-miR-22-3p	hsa-miR-224-3p	hsa-miR-22-5p	hsa-miR-23b-3p	hsa-miR-24-3p
hsa-miR-26a-5p	hsa-miR-27a-3p	hsa-miR-27a-5p	hsa-miR-28-5p	hsa-miR-299-5p	hsa-miR-302a-3p	hsa-miR-302d-3p
hsa-miR-30a-5p	hsa-miR-30d-3p	hsa-miR-30e-5p	hsa-miR-31-5p	hsa-miR-320a	hsa-miR-320b	hsa-miR-320d
hsa-miR-328-3p	hsa-miR-335-3p	hsa-miR-335-5p	hsa-miR-337-3p	hsa-miR-342-3p	hsa-miR-342-5p	hsa-miR-346
hsa-miR-361-5p	hsa-miR-362-5p	hsa-miR-365b-5p	hsa-miR-373-3p	hsa-miR-376c-3p	hsa-miR-378a-3p	hsa-miR-378a-5p
hsa-miR-421	hsa-miR-423-3p	hsa-miR-424-3p	hsa-miR-431-5p	hsa-miR-452-5p	hsa-miR-499a-5p	hsa-miR-501-3p
hsa-miR-548c-5p	hsa-miR-570-3p	hsa-miR-576-5p	hsa-miR-652-3p	hsa-miR-663a	hsa-miR-664a-3p	hsa-miR-665
hsa-miR-675-3p	hsa-miR-7-1-3p	hsa-miR-744-5p	hsa-miR-874-3p	hsa-miR-885-5p	hsa-miR-887-3p	hsa-miR-92a-3p
hsa-miR-95-3p	hsa-miR-99a-5p	hsa-miR-99b-5p	UniSp2 CP	UniSp4 CP	UniSp5 CP	

17 References

1. British Heart Foundation. *Cardiovascular disease statistics*. (2014).

2. Boersma, E., Maas, A. C., Deckers, J. W. & Simoons, M. L. Early thrombolytic treatment in acute myocardial infarction: reappraisal of the golden hour. *Lancet* **348,** 771–775 (1996).

3. Growth of Primary PCI for the treatment of heart attack patients in England 2008-2011: the role of NHS Improvement and the Cardiac Networks. *NHS Improv.* (2012).

4. Nielsen, P. H. *et al.* Primary angioplasty versus fibrinolysis in acute myocardial infarction: long-term follow-up in the Danish acute myocardial infarction 2 trial. *Circulation* **121,** 1484–1491 (2010).

5. De Rosa, S. *et al.* Transcoronary concentration gradients of circulating microRNAs. *Circulation* **124,** 1936–44 (2011).

6. Cuculi, F., De Caterina, A. R., Kharbanda, R. K. & Banning, A. P. Optimal reperfusion in ST-elevation myocardial infarction--the role of the coronary microcirculation. *Swiss Med. Wkly.* **141,** 2–10 (2011).

7. Stone, G. W. *et al.* Comparison of Angioplasty with Stenting, with or without Abciximab, in Acute Myocardial Infarction. *N Engl J Med* **346,** 957–66 (2002).

8. Grines, C. L. *et al.* A Comparison of Immediate Angioplasty with Thrombolytic Therapy for Acute Myocardial Infarction. *N Engl J Med* **328,** 673–679 (1993).

9. Gruppo Italiano per lo Studio della Streptochinasi nell'Infarto Miocardico (GISSI). Effectiveness of Intravenous Thrombolytic Treatment in Acute Myocardial Infarction. *Lancet* **8478,** 397–402 (1986).

10. Niccoli, G., Burzotta, F., Galiuto, L. & Crea, F. Myocardial no-reflow in humans. *J Am Coll Cardiol* **54,** 281–292 (2009).

11. Wu, K. C. *et al.* Prognostic Significance of Microvascular Obstruction by Magnetic Resonance Imaging in Patients With Acute Myocardial Infarction. *Circulation* **97,** 765–772 (1998).

12. Klug, G. *et al.* Prognostic value at 5 years of microvascular obstruction after acute myocardial infarction assessed by cardiovascular magnetic resonance. *J. Cardiovasc. Magn. Reson.* **14,** 46 (2012).

13. van de Hoef, T. P. *et al.* Impact of Coronary Microvascular Function on Long-Term Cardiac Mortality in Patients With Acute ST-Segment-Elevation Myocardial Infarction. *Circ. Cardiovasc. Interv.* **6,** 207–215 (2013).

14. Braunwald, E. Evolution of the management of acute myocardial infarction: a 20th century saga. *Lancet* **352,** 1771–1774 (1988).

15. Oppenheimer, B. S. & Rothschild, M. A. Electrocardiographic changes associated with

myocardial involvement with special reference to prognosis. *JAMA* **69,** 429–431 (1917).

16. Wearn, J. Thrombosis of the coronary arteries with infarction of the heart. *Am J Med Sci* **165,** 250–275 (1923).

17. Teixeira, R., Gonçalves, L. & Gersh, B. Acute myocardial infarction - Historical notes. *Int. J. Cardiol.* **167,** 1825–1834 (2013).

18. Levine, S. A. & Lown, B. Armchair treatment of acute coronary thrombosis. *JAMA* 1365–1369 (1952).

19. Killip, T. & Kimball, J. T. Treatment of myocardial infarction in a coronary care unit. *Am. J. Cardiol.* **20,** 457–464 (1967).

20. Tillett, W. S., Sherry, S. & Read, C. T. The use of streptokinase-streptodornase in the treatment of chronic empyema; with an interpretive discussion of enzymatic actions in the field of intrathoracic diseases. *J. Thorac. Surg.* **21,** 325–41 (1951).

21. Fletcher, A. P., Alkjaersig, N., Smyrniotis, F. E. & Sherry, S. The treatment of patients suffering from early myocardial infarction with massive and prolonged streptokinase therapy. *Trans. Assoc. Am. Physicians* **71,** 287–96 (1958).

22. ISIS study group. Randomized trial of intravenous streptokinase, oral aspirin, both, or neither among 17,187 cases of suspected acute myocardial infarction: ISIS-2.ISIS-2 (Second International Study of Infarct Survival) Collaborative Group. *J. Am. Coll. Cardiol.* **12,** 3A–13A (1988).

23. Baigent, C. *et al.* ISIS-2: 10 year survival among patients with suspected acute myocardial infarction in randomised comparison of intravenous streptokinase, oral aspirin, both, or neither. The ISIS-2 (Second International Study of Infarct Survival) Collaborative Group. *BMJ* **316,** 1337–43 (1998).

24. The GUSTO Investigators. An International Randomized Trial Comparing Four Thrombolytic Strategies for Acute Myocardial Infarction. *N Engl J Med* **329,** 673–682 (1981).

25. The GUSTO Angiographic Investigators. The Effects of Tissue Plasminogen Activator, Streptokinase, or Both on Coronary-Artery Patency, Ventricular Function, and Survival after Acute Myocardial Infarction. *N Engl J Med* **329,** 1615–1622 (1981).

26. Meyer, J. *et al.* Percutaneous transluminal coronary angioplasty immediately after intracoronary streptolysis of transmural myocardial infarction. *Circulation* **66,** 905–13 (1982).

27. Grines, C. L. *et al.* A Comparison of Immediate Angioplasty with Thrombolytic Therapy for Acute Myocardial Infarction. *N Engl J Med* **328,** 673–679 (1993).

28. Roguin, A. Stent: The Man and Word Behind the Coronary Metal Prosthesis. *Circ. Cardiovasc. Interv.* **4,** 206–209 (2011).

29. Grines, C. L., Cox, D. A., Stone, G. W. & et al. Coronary angioplasty with or without stent implantation for acute myocardial infarction. *N Engl J Med* **341,** 1949–1956 (1999).

30. McNamara, R. L. *et al.* Effect of door-to-balloon time on mortality in patients with ST-

segment elevation myocardial infarction. *J. Am. Coll. Cardiol.* **47,** 2180–2186 (2006).

31. MINAP. Myocardial Ischaemia National Audit Project (MINAP) Annual Report. (2014).

32. Chia, S. *et al.* Utility of cardiac biomarkers in predicting infarct size, left ventricular function, and clinical outcome after primary percutaneous coronary intervention for ST-segment elevation myocardial infarction. *JACC. Cardiovasc. Interv.* **1,** 415–423 (2008).

33. Burns, R. J. *et al.* The relationships of left ventricular ejection fraction, end-systolic volume index and infarct size to six-month mortality after hospital discharge following myocardial infarction treated by thrombolysis. *J. Am. Coll. Cardiol.* **39,** 30–6 (2002).

34. Lønborg, J. *et al.* Final infarct size measured by cardiovascular magnetic resonance in patients with ST elevation myocardial infarction predicts long-term clinical outcome: an observational study. *Eur. Hear. J. - Cardiovasc. Imaging* **14,** 387–395 (2013).

35. Liem, A. L. *et al.* Influence of treatment delay on infarct size and clinical outcome in patients with acute myocardial infarction treated with primary angioplasty. *J Am Coll Cardiol* **32,** 629–633 (1998).

36. Eitel, I. *et al.* Prognostic Significance and Determinants of Myocardial Salvage Assessed by Cardiovascular Magnetic Resonance in Acute Reperfused Myocardial Infarction. *J. Am. Coll. Cardiol.* **55,** 2470–2479 (2010).

37. Payne, A. R. *et al.* Microvascular Resistance Predicts Myocardial Salvage and Infarct Characteristics in ST-Elevation Myocardial Infarction. *J. Am. Heart Assoc.* **1,** e002246 (2012).

38. Kloner, R. A., Ganote, C. E. & Jennings, R. B. The 'no-reflow' phenomenon after temporary coronary occlusion in the dog. *J Clin Invest* **54,** 1496–1508 (1974).

39. Rochitte, C. E. *et al.* Magnitude and time course of microvascular obstruction and tissue injury after acute myocardial infarction. *Circulation* **98,** 1006–1014 (1998).

40. Gibson, C. M. *et al.* TIMI Frame Count : A Quantitative Method of Assessing Coronary Artery Flow. *Circulation* **93,** 879–888 (1996).

41. Van `t Hof, a. W. J. *et al.* Angiographic Assessment of Myocardial Reperfusion in Patients Treated With Primary Angioplasty for Acute Myocardial Infarction : Myocardial Blush Grade. *Circulation* **97,** 2302–2306 (1998).

42. Stone, G. W. *et al.* Impact of normalized myocardial perfusion after successful angioplasty in acute myocardial infarction. *J. Am. Coll. Cardiol.* **39,** 591–7 (2002).

43. Porto, I. *et al.* Angiographic assessment of microvascular perfusion--myocardial blush in clinical practice. *Am Hear. J* **160,** 1015–1022 (2010).

44. Pijls, N. H. & De Bruyne, B. Coronary pressure measurement and fractional flow reserve. *Heart* **80,** 539–42 (1998).

45. Tonino, P. P. A. L. *et al.* Fractional flow reserve versus angiography for guiding percutaneous coronary intervention. *N. Engl. J. Med.* **360,** 213–224 (2009).

46. Pijls, N. H. J. Coronary Thermodilution to Assess Flow Reserve: Validation in Humans. *Circulation* **105,** 2482–2486 (2002).

47. De Bruyne, B., Pijls, N. H. J., Smith, L., Wievegg, M. & Heyndrickx, G. R. Coronary Thermodilution to Assess Flow Reserve: Experimental Validation. *Circulation* **104,** 2003–2006 (2001).

48. Jaffe, R., Dick, A. & Strauss, B. H. Prevention and Treatment of Microvascular Obstruction-Related Myocardial Injury and Coronary No-Reflow Following Percutaneous Coronary Intervention A Systematic Approach. *JACC. Cardiovasc. Interv.* **3,** 695–704 (2010).

49. Ambros, V. A hierarchy of regulatory genes controls a larva-to-adult developmental switch in C. elegans. *Cell* **57,** 49–57 (1989).

50. Friedman, R. C., Farh, K. K.-H., Burge, C. B. & Bartel, D. P. Most mammalian mRNAs are conserved targets of microRNAs. *Genome Res.* **19,** 92–105 (2009).

51. Mitchell, P. S. *et al.* Circulating microRNAs as stable blood-based markers for cancer detection. *Proc. Natl. Acad. Sci. U. S. A.* **105,** 10513–8 (2008).

52. Janssen, H. L. a *et al.* Treatment of HCV infection by targeting microRNA. *N. Engl. J. Med.* **368,** 1685–94 (2013).

53. Lee, R. C., Feinbaum, R. L. & Ambros, V. The C. elegans heterochronic gene lin-4 encodes small RNAs with antisense complementarity to lin-14. *Cell* **75,** 843–54 (1993).

54. Ambros, V. *et al.* A uniform system for microRNA annotation. *RNA* **9,** 277–279 (2003).

55. Kiezun, A. *et al.* miRviewer: a multispecies microRNA homologous viewer. *BMC Res. Notes* **5,** 92 (2012).

56. Reinhart, B., Slack, F. & Basson, M. The 21-nucleotide let-7 RNA regulates developmental timing in Caenorhabditis elegans. *Nature* **403,** 901–906 (2000).

57. Calin, G. A. *et al.* Frequent deletions and down-regulation of micro- RNA genes miR15 and miR16 at 13q14 in chronic lymphocytic leukemia. *Proc. Natl. Acad. Sci. U. S. A.* **99,** 15524–9 (2002).

58. van Rooij, E. *et al.* A signature pattern of stress-responsive microRNAs that can evoke cardiac hypertrophy and heart failure. *Proc Natl Acad Sci U S A* **103,** 18255–18260 (2006).

59. Chen, X. *et al.* Characterization of microRNAs in serum: a novel class of biomarkers for diagnosis of cancer and other diseases. *Cell Res.* **18,** 997–1006 (2008).

60. Adachi, T. *et al.* Plasma MicroRNA 499 as a Biomarker of Acute Myocardial Infarction. *Clin. Chem.* **56,** 1183–1185 (2010).

61. Krützfeldt, J. *et al.* Silencing of microRNAs in vivo with 'antagomirs'. *Nature* **438,** 685–689 (2005).

62. Griffiths-Jones, S. The microRNA Registry. *Nucleic Acids Res.* **32,** 109D–111 (2004).

63. Kozomara, A. & Griffiths-Jones, S. miRBase: integrating microRNA annotation and deep-sequencing data. *Nucleic Acids Res.* **39,** D152–7 (2011).

64. Pritchard, C. C., Cheng, H. H. & Tewari, M. MicroRNA profiling: approaches and considerations. *Nat. Rev. Genet.* **13,** 358–69 (2012).

65. Turchinovich, A., Weiz, L., Langheinz, A. & Burwinkel, B. Characterization of extracellular circulating microRNA. *Nucleic Acids Res.* **39,** 7223–33 (2011).

66. Arroyo, J. D. *et al.* Argonaute2 complexes carry a population of circulating microRNAs independent of vesicles in human plasma. *Proc. Natl. Acad. Sci. U. S. A.* **108,** 5003–8 (2011).

67. Diehl, P. *et al.* Microparticles : major transport vehicles for distinct microRNAs in circulation. *Cardiovasc. Res.* **93,** 633–644 (2012).

68. Vickers, K. C., Palmisano, B. T., Shoucri, B. M., Shamburek, R. D. & Remaley, A. T. MicroRNAs are transported in plasma and delivered to recipient cells by high-density lipoproteins. *Nat. Cell Biol.* **13,** 423–33 (2011).

69. Park, C. Y., Choi, Y. S. & McManus, M. T. Analysis of microRNA knockouts in mice. *Hum. Mol. Genet.* **19,** R169–75 (2010).

70. Boon, R. a *et al.* MicroRNA-34a regulates cardiac ageing and function. *Nature* **495,** 107–10 (2013).

71. Bonauer, A. *et al.* MicroRNA-92a controls angiogenesis and functional recovery of ischemic tissues in mice. *Science (80-.).* **324,** 1710–1713 (2009).

72. Corsten, M. F. *et al.* Circulating MicroRNA-208b and MicroRNA-499 reflect myocardial damage in cardiovascular disease. *Circ. Cardiovasc. Genet.* **3,** 499–506 (2010).

73. Mccall, M. N. *et al.* MicroRNA profiling of diverse endothelial cell types. *BMC Med. Genomics* **4,** 78 (2011).

74. Wang, G.-K. K. *et al.* Circulating microRNA: a novel potential biomarker for early diagnosis of acute myocardial infarction in humans. *Eur. Heart J.* **31,** 659–666 (2010).

75. Widera, C. *et al.* Diagnostic and prognostic impact of six circulating microRNAs in acute coronary syndrome. *J Mol Cell Cardiol* **51,** 872–875 (2011).

76. Zampetaki, A. *et al.* Prospective study on circulating MicroRNAs and risk of myocardial infarction. *J. Am. Coll. Cardiol.* **60,** 290–299 (2012).

77. Wang, K. *et al.* Comparing the MicroRNA Spectrum between Serum and Plasma. *PLoS One* **7,** e41561 (2012).

78. Zampetaki, A. & Mayr, M. Analytical challenges and technical limitations in assessing circulating miRNAs. *Thromb. Haemost.* **108,** 592–8 (2012).

79. Blondal, T. *et al.* Assessing sample and miRNA profile quality in serum and plasma or other biofluids. *Methods* **59,** S1–6 (2013).

80. Boom, R. *et al.* Rapid and simple method for purification of nucleic acids. *J. Clin. Microbiol.* **28,** 495–503 (1990).

81. Kim, Y.-K., Yeo, J., Kim, B., Ha, M. & Kim, V. N. Short Structured RNAs with Low GC Content Are Selectively Lost during Extraction from a Small Number of Cells. *Mol. Cell* **46,** 893–895 (2012).

82. Mestdagh, P. *et al.* A novel and universal method for microRNA RT-qPCR data normalization. *Genome Biol.* **10,** R64 (2009).

83. D'haene, B., Mestdagh, P., Hellemans, J. & Vandesompele, J. miRNA expression profiling: from reference genes to global mean normalization. *Methods Mol. Biol.* **822,** 261–72 (2012).

84. Vandesompele, J. *et al.* Accurate normalization of real-time quantitative RT-PCR data by geometric averaging of multiple internal control genes. *Genome Biol.* **3,** RESEARCH0034 (2002).

85. Andersen, C. L., Jensen, J. L. & Ørntoft, T. F. Normalization of real-time quantitative reverse transcription-PCR data: a model-based variance estimation approach to identify genes suited for normalization, applied to bladder and colon cancer data sets. *Cancer Res.* **64,** 5245–50 (2004).

86. Edwards, P. *et al.* Final results of MRC CRASH, a randomised placebo-controlled trial of intravenous corticosteroid in adults with head injury-outcomes at 6 months. *Lancet* **365,** 1957–9 (2005).

87. Perkins, G. D. PARAMEDIC 2: The Adrenaline Trial. *ISRCTN 73485024* at <www.warwick.ac.uk/go/paramedic2>

88. Dizon, J. M. *et al.* Relationship between ST-segment resolution and anterior infarct size after primary percutaneous coronary intervention: analysis from the INFUSE-AMI trial. *Eur. Hear. journal. Acute Cardiovasc. care* **3,** 78–83 (2014).

89. McLaughlin, M. G. *et al.* Prognostic utility of comparative methods for assessment of ST-segment resolution after primary angioplasty for acute myocardial infarction: the Controlled Abciximab and Device Investigation to Lower Late Angioplasty Complications (CADILLAC) trial. *J. Am. Coll. Cardiol.* **44,** 1215–23 (2004).

90. Langer, a *et al.* Prognostic significance of ST segment shift early after resolution of ST elevation in patients with myocardial infarction treated with thrombolytic therapy: the GUSTO-I ST Segment Monitoring Substudy. *J. Am. Coll. Cardiol.* **31,** 783–9 (1998).

91. Cutlip, D. E. *et al.* Clinical End Points in Coronary Stent Trials: A Case for Standardized Definitions. *Circulation* **115,** 2344–2351 (2007).

92. Mestdagh, P. *et al.* Evaluation of quantitative miRNA expression platforms in the microRNA quality control (miRQC) study. *Nat. Methods* (2014). doi:10.1038/nmeth.3014

93. Meyer, S. U., Pfaffl, M. W. & Ulbrich, S. E. Normalization strategies for microRNA profiling experiments: a 'normal' way to a hidden layer of complexity? *Biotechnol. Lett.* **32,** 1777–88 (2010).

94. Kuwabara, Y. *et al.* Increased microRNA-1 and microRNA-133a levels in serum of patients with cardiovascular disease indicate myocardial damage. *Circ. Cardiovasc. Genet.* **4,** 446–454 (2011).

95. D'Alessandra, Y. *et al.* Circulating microRNAs are new and sensitive biomarkers of myocardial infarction. *Eur Hear. J* **31,** 2765–2773 (2010).

96. Olivieri, F. *et al.* Diagnostic potential of circulating miR-499-5p in elderly patients with acute non ST-elevation myocardial infarction. *Int. J. Cardiol.* **167,** 531–6 (2013).

97. Oerlemans, M. I. F. J. *et al.* Early assessment of acute coronary syndromes in the emergency department: the potential diagnostic value of circulating microRNAs. *EMBO Mol. Med.* **4,** 1176–85 (2012).

98. Wang, R., Li, N., Zhang, Y., Ran, Y. & Pu, J. Circulating MicroRNAs are promising novel biomarkers of acute myocardial infarction. *Intern Med* **50,** 1789–1795 (2011).

99. Eitel, I. *et al.* Relation of circulating MicroRNA-133a concentrations with myocardial damage and clinical prognosis in ST-elevation myocardial infarction. *American heart journal* **164,** 706–714 (2012).

100. Cheng, C., Wang, Q., You, W., Chen, M. & Xia, J. MiRNAs as biomarkers of myocardial infarction: a meta-analysis. *PLoS One* **9,** e88566 (2014).

101. Bostjancic, E., Zidar, N., Stajer, D. & Glavac, D. MicroRNAs miR-1, miR-133a, miR-133b and miR-208 are dysregulated in human myocardial infarction. *Cardiology* **115,** 163–9 (2010).

102. Fiedler, J. *et al.* MicroRNA-24 regulates vascularity after myocardial infarction. *Circulation* **124,** 720–730 (2011).

103. Hullinger, T. G. *et al.* Inhibition of miR-15 protects against cardiac ischemic injury. *Circ Res* **110,** 71–81 (2012).

104. Long, G. *et al.* Human circulating microRNA-1 and microRNA-126 as potential novel indicators for acute myocardial infarction. *Int. J. Biol. Sci.* **8,** 811–8 (2012).

105. Long, G. *et al.* Circulating miR-30a, miR-195 and let-7b associated with acute myocardial infarction. *PLoS One* **7,** e50926 (2012).

106. van Rooij, E. *et al.* Dysregulation of microRNAs after myocardial infarction reveals a role of miR-29 in cardiac fibrosis. *Proc Natl Acad Sci U S A* **105,** 13027–13032 (2008).

107. Wang, X. *et al.* MicroRNA-494 Targeting Both Proapoptotic and Antiapoptotic Proteins Protects Against Ischaemia/Reperfusion-Induced Cardiac Injury. *Circulation* **122,** 1308–1318 (2010).

108. Ren, X.-P. *et al.* MicroRNA-320 is involved in the regulation of cardiac ischemia/reperfusion injury by targeting heat-shock protein 20. *Circulation* **119,** 2357–66 (2009).

109. Cheng, Y. *et al.* Ischaemic preconditioning-regulated miR-21 protects heart against ischaemia/reperfusion injury via anti-apoptosis through its target PDCD4. *Cardiovascular research* **87,** 431–439 (2010).

110. Xiao, J. *et al.* Serum microRNA-499 and microRNA-208a as biomarkers of acute myocardial infarction. *Int. J. Clin. Exp. Med.* **7,** 136–41 (2014).

111. Nazari-Jahantigh, M. *et al.* MicroRNA-155 promotes atherosclerosis by repressing Bcl6 in macrophages. *J. Clin. Invest.* **122,** 4190–202 (2012).

112. Rotllan, N., Ramírez, C. M., Aryal, B., Esau, C. C. & Fernández-Hernando, C. Therapeutic silencing of microRNA-33 inhibits the progression of atherosclerosis in Ldlr-/- mice--brief report. *Arterioscler. Thromb. Vasc. Biol.* **33,** 1973–7 (2013).

113. Thum, T. *et al.* MicroRNA-21 contributes to myocardial disease by stimulating MAP kinase signalling in fibroblasts. *Nature* **456,** 980–984 (2008).

114. Wei, Y., Nazari-Jahantigh, M., Neth, P., Weber, C. & Schober, A. MicroRNA-126, -145, and -155: a therapeutic triad in atherosclerosis? *Arterioscler. Thromb. Vasc. Biol.* **33,** 449–54 (2013).

115. Livak, K. J. & Schmittgen, T. D. Analysis of relative gene expression data using real-time quantitative PCR and the DDCT Method. *Methods* **25,** 402–408 (2001).

116. Jolly, S. S. *et al.* Randomized Trial of Primary PCI with or without Routine Manual Thrombectomy. *N. Engl. J. Med.* **372,** 1389–1398 (2015).

117. Gershlick, A. H. *et al.* Randomized Trial of Complete Versus Lesion-Only Revascularization in Patients Undergoing Primary Percutaneous Coronary Intervention for STEMI and Multivessel Disease. *J. Am. Coll. Cardiol.* **65,** 963–972 (2015).

118. Ludman, P. BCIS Audit Return of Adult Interventional Procedures. in *British Cardiovascular Intervention Society* (2014).

119. Liebetrau, C. *et al.* Release kinetics of circulating muscle-enriched microRNAs in patients undergoing transcoronary ablation of septal hypertrophy. *J. Am. Coll. Cardiol.* **62,** 992–8 (2013).

120. Liang, Y., Ridzon, D., Wong, L. & Chen, C. Characterization of microRNA expression profiles in normal human tissues. *BMC Genomics* **8,** 166 (2007).

121. Shelke, G. V., Lässer, C., Gho, Y. S. & Lötvall, J. Importance of exosome depletion protocols to eliminate functional and RNA-containing extracellular vesicles from fetal bovine serum. *J. Extracell. vesicles* **3,** 1–8 (2014).

122. Riss, T. L. *et al.* Cell viability assays. *Assay Guid. Man.* (2013).

123. Oliveros, J. C. An interactive tool for comparing lists with Venn's diagrams. (2015). at <http://bioinfogp.cnb.csic.es/tools/venny/index.html>

124. Basile, D. P., Fredrich, K., Chelladurai, B., Leonard, E. C. & Parrish, A. R. Renal ischemia reperfusion inhibits VEGF expression and induces ADAMTS-1, a novel VEGF inhibitor. *Am. J. Physiol. Renal Physiol.* **294,** F928–F936 (2008).

125. Nagalingam, R. S. *et al.* A cardiac-enriched microRNA, miR-378, blocks cardiac hypertrophy by targeting Ras signaling. *J. Biol. Chem.* **288,** 11216–32 (2013).

126. Ganesan, J. *et al.* MiR-378 Controls Cardiac Hypertrophy by Combined Repression of Mitogen-Activated Protein Kinase Pathway Factors. *Circulation* **127,** 2097–2106 (2013).

127. Xing, Y. *et al.* microRNA-378 promotes mesenchymal stem cell survival and vascularization under hypoxic–ischemic conditions in vitro. *Stem Cell Res. Ther.* **5,** 130 (2014).

128. Rao, P. K. *et al.* Loss of cardiac microRNA-mediated regulation leads to dilated cardiomyopathy and heart failure. *Circ. Res.* **105,** 585–94 (2009).

129. Zhang, N. *et al.* MicroRNA-30a suppresses breast tumor growth and metastasis by targeting metadherin. *Oncogene* **33,** 3119–28 (2014).

130. Liu, N. & Bezprozvannaya, S. microRNA-133a regulates cardiomyocyte proliferation and suppresses smooth muscle gene expression in the heart. *Genes …* 3242–3254 (2008). doi:10.1101/gad.1738708.al.

131. Bostjancic, E., Zidar, N., Stajner, D. & Glavac, D. MicroRNA miR-1 is up-regulated in remote myocardium in patients with myocardial infarction. *Folia biologica* **56,** 27–31 (2010).

132. Landry, P., Benham, A., Coarfa, C., Gunaratne, P. H. & Provost, P. The Repertoire and Features of Human Platelet microRNAs. *PLoS One* **7,** 1–14 (2012).

133. Willeit, P. *et al.* Circulating MicroRNAs as Novel Biomarkers for Platelet Activation. *Circ. Res.* **112,** 595–600 (2013).

134. Fichtlscherer, S. *et al.* Circulating microRNAs in patients with coronary artery disease. *Circ Res* **107,** 677–684 (2010).

135. Wahlquist, C. *et al.* Inhibition of miR-25 improves cardiac contractility in the failing heart. *Nature* **508,** 531–5 (2014).

136. Huang, Z.-P. *et al.* MicroRNA-22 regulates cardiac hypertrophy and remodeling in response to stress. *Circ. Res.* **112,** 1234–43 (2013).

137. Neal, C. S. *et al.* Circulating microRNA expression is reduced in chronic kidney disease. *Nephrol. Dial. Transplant.* **26,** 3794–3802 (2011).

138. Faletra, F. F., Pandian, N. G. & Ho, S. Y. in *Anatomy of the Heart by Multislice Computed Tomography* 109–115 (2008).

139. Habib, A., Lachman, N., Christensen, K. N. & Asirvatham, S. J. The anatomy of the coronary sinus venous system for the cardiac electrophysiologist. *Europace* **11 Suppl 5,** v15–21 (2009).

140. Silver, M. A. & Rowley, N. E. The functional anatomy of the human coronary sinus. *Am. Heart J.* **115,** 1080–1084 (1988).

141. Pan, W. *et al.* MiR-30-regulated autophagy mediates angiotensin II-induced myocardial hypertrophy. *PLoS One* **8,** e53950 (2013).

142. Li, Q. *et al.* Overexpression of microRNA-99a attenuates heart remodelling and improves cardiac performance after myocardial infarction. *J. Cell. Mol. Med.* **18,** 919–28 (2014).

143. Nagpal, V. *et al.* MiR-125b Is Critical for Fibroblast-to-Myofibroblast Transition and Cardiac Fibrosis. *Circulation* **133,** 291–301 (2016).

144. Ucar, A. *et al.* The miRNA-212/132 family regulates both cardiac hypertrophy and cardiomyocyte autophagy. *Nat. Commun.* **3,** 1078 (2012).

145. Heymans, S. *et al.* Macrophage microRNA-155 promotes cardiac hypertrophy and failure. *Circulation* **128,** 1420–32 (2013).

146. Aurora, A. B. *et al.* MicroRNA-214 protects the mouse heart from ischemic injury by controlling Ca2+ overload and cell death. *J. Clin. Invest.* **122,** 1222–1232 (2012).

147. Wang, J. *et al.* Cardiomyocyte overexpression of miR-27b induces cardiac hypertrophy and dysfunction in mice. *Cell Res.* **22,** 516–27 (2012).

148. Ellis, K. L. *et al.* Circulating microRNAs as candidate markers to distinguish heart failure in breathless patients. *Eur. J. Heart Fail.* **15,** 1138–1147 (2013).

149. Zhou, L. *et al.* MicroRNA and mRNA Signatures in Ischemia Reperfusion Injury in Heart Transplantation. *PLoS One* **8,** e79805 (2013).